STUDY OF MINERAL AND MATRIX MATURATION IN DENTIN

Kostas Verdelis

A dissertation submitted to the faculty of North Carolina at Chapel Hill in partial fulfillment of the requirements for the degree of Doctor of Philosophy in the Department of Oral Biology

Chapel Hill
2005

Approved by
Advisor: J. Timothy Wright
Advisor: Adele L. Boskey
Reader: Patrick Flood
Reader: Roland Arnold
Reader: Wagner Duarte

ABSTRACT

KOSTAS VERDELIS: Study Of Mineral And Matrix Maturation In Dentin
(Under the direction of Adele L. Boskey and J. Timothy Wright)

Spectroscopic analysis was used to study the patterns of changes in the mineral and matrix properties of dentin during maturation of the tissue. Fourier Transform Infrared Imaging (FTIRI) analyses on undecalcified semi-thin sections from fetal bovine incisors and developing mouse molars were performed. In addition, fetal bovine microdissected mantle and circumpulpal dentin specimens of successive tissue age were analyzed by Fourier Transform Infrared (FTIR) analysis and by amino acid and matrix phosphate assays.

In the initial studies, the formation of mantle and circumpulpal dentin as two distinct dentin compartments in the developing fetal incisors was established through analysis of distribution of mineral:matrix and mineral crystallinity values. Changes in the mineral:matrix, mineral crystallinity, acidic phosphate substitution and carbonate substitution in the mineral of mantle and circumpulpal dentin during maturation were subsequently quantitatively analyzed from FTIRI results. In this study, separate patterns of changes in mineral properties were found for mantle and circumpulpal dentin, in terms of initial and final levels and rates of increase or decrease of mineral properties values. Spectroscopic analysis of different maturation stages

microdissected mantle and circumpulpal dentin specimens showed a great decrease in the dentin relative water content, affecting the dentin matrix conformation.

Chemical analyses of similar microdissected specimens showed a significant increase in the organic phosphate of dentin matrix occurring during maturation. This increase was associated with continuing phosphorylation of existing phosphoproteins without further changes in the protein density. Finally, the study of dentin maturation using 6 day-old mouse molars by FTIRI was validated. Reproducibility in the pattern of changes in the mineral properties examined was found to be highly dependent on the sectioning orienation of molars. It is likely that higher resolution analytical methods and/or slightly older animal age would enhance the analytical outcome in such studies.

ACKNOWLEDGEMENTS

To the memory of Dr Miles Crenshaw. To my wife Daphne, my mentors and the members of my thesis committee and Lyuda Lukashova. They provided me with a lot of support.

TABLE OF CONTENTS

LIST OF TABLES

LIST OF FIGURES

LIST OF ABBREVIATIONS AND SYMBOLS

Å	Angström
Asp	Aspartic acid
BaF_2	Barium fluoride
BSE	backscattered electron imaging
BSP	bone sialoprotein
C=O	Carbonyl
Ca^{2+}	Calcium
CO_3^{2-}	Carbonate
Da	Dalton
DEJ	Dentinoenamel junction
DMP1	dentin matrix protein 1
Dpp	Dentin phosphoprotein
Dsp	Dentin sialoprotein
DSPP	dentin sialophosphoprotein
ECMVs	Extracellular matrix vesicles
EDAX	Energy dispersive X-ray
FTIR	Fourier Transform Infrared
FTIRI	Fourier Transform Infrared Imaging
FTIRM	Fourier Transform Infrared Microscopy

GAG	Glycosaminoglycan
Gla	Glutamic acid
HPO_4^-	Acidic phosphate
Hyp	Hydroxyproline
MCT	Mercury-Cadmium-Telluride
MEPE	matrix phosphoglycoprotein
NCPs	Noncollagenous proteins
NCPs	Noncollagenous proteins
Nm	nanometers
NMR	nuclear magnetic resonance
OCP	Octacalcium phosphate
OH^-	Hydroxyl
OPN	osteopontin
PG	Proteoglycan
PMMA	Polymethylmethacrylate
PO_4^{3-}	Phosphate
Pse	Phosphoserine
SEM	Scanning electron microscopy
Ser	Serine
SIBLING	Small Integrin-Binding Ligand, N-Linked Glycoproteins
SLRPs	Small leucine-rich proteoglycans
TGF	Transforming growth factor
Thr	Threonine

CHAPTER I

INTRODUCTION

Mechanical strength is a characteristic of hard tissues in organs like teeth and bones. This strength is a requisite for their main function in the body (mastication for teeth and bearing the body weight for bones) and is imparted to these tissues by the mineral. The deposition of mineral crystals by living organisms (biomineralization) that occurs in dentin, cementum and bone is mediated by the organic matrix in a controlled manner, resulting in crystals with a well defined orientation relative to the matrix, narrow size ranges and a unique composition (Lowenstam, 1981; Lowenstam and Weiner, 1989). The organic matrix consists of collagen, noncollagenous proteins and also some non-protein components synthesized and secreted by the tissue-forming cells, such as odontoblasts, cementoblasts and osteoblasts. The first stage of mineral deposition is nucleation of mineral crystals which occurs after the secretion and organization of the matrix components, followed by crystal growth and proliferation (Veis, 1993; Boskey, 2001). Concurrently, changes occur in the organic matrix, including degradation of the matrix (Masters PM, 1985) or changes in the collagen cross-linking (Mechanic et al, 1987). These changes could be related to the mineralization process. The process of mineral formation coupled with concomitant changes in the matrix for a particular hard tissue is called maturation. The study of maturation can contribute to a better

understanding of hard tissue pathology mechanisms and to developing induction of mineralization as a therapeutic modality. Bone maturation has been described in a few studies (reviewed in Glimcher, 1998). While studies on an organogenesis and matrix formation level have been conducted on dentin (Suzuki et al, 1996; Fanchon et al, 2004; Hao et al, 2004; Yamamoto et al, 2004), there are fewer similar studies of dentin maturation (Magne et al, 2001) on a mineral formation and matrix changes after the initial mineralization stage level. Unfortunately, in the latter studies, important factors such as the selection of proper age group samples, the spatial resolution needed for analysis or the histological variation present in dentin were not adequately addressed.

Dentin presents an excellent model for the study of maturation of a hard tissue, as samples for experimental studies are abundant and remodeling does not take place, contrary to what happens in bone (Linde and Goldberg, 1994; Butler et al, 1997). At the same time, histology and composition of the matrix (especially the noncollagenous part of it) are known to vary substantially within dentin. As will be discussed in detail later, the main elements involved in dentinogenesis also appear to vary within dentin. It follows that for dentin maturation to be studied, a methodology should be established that enables the analysis and comparison of mineral and matrix properties between equivalent dentin regions, differing only in maturation stage, throughout development. A relatively high spatial resolution method is desirable, as zones of different histological, matrix/mineral properties and maturational stage in developing dentin are relatively narrow and close to each other.

In this thesis, a high spatial resolution method (Fourier Transform Infrared Spectroscopic Imaging-FTIRI) for analysis of mineral and matrix properties was employed using a fetal bovine dentin model to examine whether histologically and developmentally different dentin zones are represented by different spectroscopic properties throughout maturation (Chapter II). Such differences in mineral properties were next described for various maturational stages (Chapter III) on a quantitative basis, to compare these changes between mantle and circumpulpal dentin and establish a pattern in which they occur in normal dentin. Mineral changes were analyzed using FTIRI on fetal bovine incisor sections, while matrix changes were analyzed using microdissected dentin samples that represent discrete maturation stages localized on the fetal teeth, as defined in Chapter II. Similar microdissected dentin samples were analyzed for the profile of their matrix protein amino acid and matrix phosphorylation levels (Chapter IV), to investigate the changes in phosphorylated proteins of the matrix and in the phosphorylation of these proteins that occur during maturation. Finally, in Chapter V mouse molar dentin was examined by FTIRI to establish whether the maturation model derived from bovine teeth is applicable to normal mouse dentin and compare changes in the mineral properties during dentin maturation described in Chapter II to similar changes in mouse molar dentin.

HISTOLOGY OF DEVELOPING AND MATURE DENTIN

The structure of a fetal bovine incisor is presented from a microcomputed tomography analysis in Figure 1-1. Histology of dentin development has been

reviewed systematically elsewhere (Ten Cate, 1994). Dentin is formed by odontoblasts that differentiate from ectomesenchymal cells of the dental papilla (the formative organ of dentin that eventually becomes the pulp of the tooth) under the organizing influence of cells of the internal dental epithelium (from which the enamel-producing ameloblasts are derived). Dentin formation starts at the tip of the cusps of the tooth in molars, or at the incisal edge of incisors, and spreads down the cusp slope as far as the cervical loop of the dental organ. At the same time enamel starts forming outwards from the dentino-enamel junction (DEJ). The initial dentin thickens until all the dentin of the crown of the tooth is formed. The initial soft matrix in dentin and enamel hardens with the mineral apposition, the latter consisting of two discrete stages: formation of the initial mineral crystals and crystal growth by expansion of these crystals and formation of secondary nuclei. In the case of enamel this process occurs with a dramatic concurrent removal of the matrix. Formation of dentin and cementum (hard tissue layer at the periphery of the root, adjacent to dentin) starts at a later stage of development. Dentin and enamel formation continues (in humans at an average rate of 4μm a day) until the external form of the tooth is completed and dentin formed up to this point is called primary dentin. The dentin that is formed, at a reduced rate, after the tooth erupts and becomes functional is called secondary. Dentin that forms after full eruption of the tooth and as a response to external stimuli, such as chemicals, caries, restorative procedures or attrition is called tertiary dentin.

Initial dentin formation-mantle dentin: After the differentiation of odontoblasts from undifferentiated ectomesenchymal cells, large (0.1-0.2μm in diameter) collagen fibrils are produced that, together with the noncollagenous proteins, constitute the

organic matrix of the mantle dentin (first-formed dentin, Figure 1-2 a). The orientation of collagen fibrils is parallel to that of dentinal tubules in the mantle dentin. Membrane-bound vesicles called extracellular matrix vesicles (ECMVs) are the site of initial mineral deposition in mantle dentin. ECMVs bud off from the odontoblasts exclusively in mantle dentin, as in the rest of dentin (circumpulpal) initial mineral deposition occurs directly on collagen fibers. Hydroxyapatite first appears within matrix vesicles as individual crystals that grow rapidly, rupture the vesicle's membrane and spread as a cluster of crystallites fusing with adjacent clusters and aligning with the collagen fibrils to form the fully mineralized matrix.

The deposition of mineral always lags behind the formation of the organic matrix so that there is always a layer of organic matrix called predentin (10-40μm wide in human teeth, depending how active odontoblasts are) between the odontoblasts and the mineralization front. Odontoblasts later begin to move toward the center of the pulp, leaving the principal extension of the cell, the odontoblast process, inside the dentinal tubule.

Circumpulpal dentin: After mantle dentin, the rest of dentin, which is called circumpulpal dentin (Figure 1-2 a), is subsequently formed. Circumpulpal dentin exhibits different characteristics from mantle dentin (discussed also in section "Spatial variation in dentin properties"), such as: 1.collagen fibrils of smaller size, more closely packed and oriented at right angles to the dentinal tubules 2. absence of matrix vesicles and direct deposition of initial mineral on collagen fibrils 3. different synthesis of the organic matrix and especially the noncollagenous component of the matrix. Mineralization in circumpulpal dentin occurs directly on

collagen fibrils, unlike mantle dentin. Mineralization follows a globular (calcospheric) calcification pattern, in which continuously enlarging globular masses that finally fuse are formed. On occasion these globular masses fail to fuse fully, leaving small areas of uncalcified dentin matrix known as interglobular dentin.

Peritubular dentin formation: As new dentin is formed, the odontoblast shrinks by about a third of its length into the dentin and a collar or sheath of highly mineralized dentin, called peritubular dentin, is deposited in the dentinal tubule wall. The rest of the dentin, which is formed between dentinal tubules, is then called intertubular dentin. Figure 1-2 b presents empty dentinal tubules on a fetal bovine incisor examined by SEM with the peritubular dentin around the dentinal lumens and intertubular dentin between the tubules clearly appearing. Peritubular dentin is hypermineralized with respect to intertubular and, as will be discussed in detail later, these two kinds of dentin also present differences in their mineral composition, matrix properties and mechanical properties. With age, there is a progressive deposition of peritubular dentin and obliteration of the tubule is observed. Peritubular dentin that obliterates the tubule space is called sclerotic.

COMPOSITION OF DENTIN

On a weight basis, mature dentin is approximately 70% inorganic material (mineral phase), 20% organic material and 10% water (adsorbed on the surface of the mineral or in interstices between crystals). On a volume basis, the same fractions are 45%, 33% and 22%, respectively (ten Cate, 1994). The mineral and organic phases of dentin are going to be examined separately.

a)Mineral

The mineral phase in mature dentin represents the major part of its dry weight. The mineral in dentin is very similar to the bone mineral and it is an analog of the naturally occurring mineral hydroxyapatite, whose unit cell can be represented as $Ca_{10}(PO_4)_6(OH)_2$ (reviewed in Boskey, 2001 and Glimcher, 1998). The unit cell of the hydroxyapatite crystal constitutes the smallest building unit of the parallelepiped shape which includes the Ca^{++}, PO_4^{3-} and OH^- ions. The crystal belongs to the hexagonal system. The unit cell can generate a large crystal by an indefinite repetition in the direction of the 3 axis of the crystal. All the ions in the unit cell are arranged consistently, with OH groups located at the corner of the unit cell or along the c-axis and PO_4^{3-} groups surrounding the OH^- groups at the corners of the unit cell. Ca^{++} atoms are occupying the so called columnar Ca or the screw axis Ca position (Ca II position) forming triangles around the central OH- group located along the c-axis. Using electron diffraction on high magnification transmission electron microscopy, this arrangement has also been confirmed for dentin crystals located either within or between collagen fibers (Ichijo et al, 1993).

The first studies of the mineral crystal structure in hard tissues were performed on bone by DeJong (DeJong, 1926), where bone mineral was identified as hydroxyapatite based on x-ray diffraction data. Although the progress in identifying the exact chemical composition and specific spatial arrangements of its constituents during development has been slow mainly because of technical challenges (Glimcher MJ, 1998), some facts, such as the role of ionic substitutions, have been well established about mineral in biological systems. It is recognized that because

mineral crystals are so small (~20 x 40 x 200 Å) much of the unit cell is on the surface. This provides an opportunity for substitution by similarly sized cations (Mg^{2+}, Sr^{2+}, Fe^{2+}, Pb^{2+}, Na^{+}, K^{+}) and anions (CO_3^{2-} ,F^{-}, HPO_4^{2-} and $H_2PO_4^{-}$). Substitutions are found within the mineral lattice and on the surface of the apatite crystals. Dentin mineral (like bone) is a calcium-deficient apatite, with crystals slightly larger than the bone mineral crystals. The Ca deficiency is either due to a substitution of Na or Mg for Ca, or a true deficiency of Ca ions not substituted for by another cation, with electrical neutrality accomplished by the addition of protons to form $HPO_4^{=}$ groups accompanied by the creation of crystal vacancies. The bone and dentin crystals contain both HPO_4^{2-} and CO_3^{2-} in various lattice sites and on the surface of crystals. These substituents change as a function of time. Major sites in the lattice where carbonate ions can be introduced are the OH^{-} sites (type A carbonate apatite) and PO_4^{3-} sites (type B carbonate apatite). The type and extent of substitution varies for different mineralized tissues, e.g for mature dentin and bone apatite is predominantly type B, whereas in enamel it is almost entirely type A. The HPO_4^{2-} groups, present as substitutions in the apatite of mineralized tissues, were shown by ^{31}P NMR analysis to be unique and unlike those naturally present in other mineral phases such as octocalcium phosphate, amorphous calcium phosphate or synthetic apatites precipitated from solution.

It has long been recognized that collagen serves as the template for the mineral formation in bones and teeth. The ultrastructural interaction between collagen and mineral crystals was studied by high voltage electron microscopic tomography on bone or mineralizing tendon (Landis and Song, 1991; Landis et al, 1996). The

longest dimension of the apatite crystal, corresponding to the c-axis crystallographically, was found to be parallel to the collagen fibril long axis. Crystals were periodically (~67nm repeat distance) arranged along the fibrils and their location appeared to correspond to collagen hole and overlap zones. Platelet-shaped crystals were arranged in channels or grooves formed by collagen hole zones in register, while crystal sizes sometimes exceed the dimensions of the hole zones. It was concluded that crystals grow in part by removing water and ions present in the extracellular tissue volume and, possibly, at the expense of collagen, causing changes in its higher order organization. In addition, the organic structures may be enveloped by the growing crystals. In the same studies, mineral deposits were imaged and color-coded in back-scattered mode, a method which is based on intrinsic electron scattering power of the sample components, i.e. density in the case of the mineral. In the bone it was observed that: 1. there is a general correlation between density and mineral deposit size (increasing mineral density is indicative of more mature deposits) 2. high voxel density regions of many individual larger deposits appear to be surrounded by low voxel density ones (newly deposited crystal mass along and on the surfaces of pre-existing particles). Images from mineralizing fibrils in contact with a dense mineral phase showed distribution of mineral associated with the collagen tapered, narrow at locations along the fibril farther from the dense mineral, gradually thickening when approaching the large mineral mass. Crystals form generally in planar fashion and extend in the direction of the long axis of collagen. This longest dimension of individual mineral particles

corresponds to the crystallographic c-axis of the mineral, defined by electron diffraction.

In dentin, mineral has been reported to form ribbon-like crystallites (Arnold et al, 1999).By conventional electron microscopy, apatite crystals in other mineralized tissues have been described either platelet-shaped or needle-like; using a sensitive method, small angle x-ray scattering, it was suggested that bone had platelet-shaped crystals (Fratzl et al, 1992).

b)Matrix

There is presently some confusion surrounding the taxonomy and terminology of dentin extracellular matrix components, which partly arose from an earlier characterization of the matrix components based on biochemical purification from tissues and from the possible discrepancies in characterization of the matrix components between different species. Today, these components have been mainly identified based on odontoblastic cDNA libraries and are generally classified as follows:

1.Collagen: type I, typeIII&V (predentin and some species-not normally found in mature dentin)

2.Proteoglycans

3. SIBLING (Small Integrin-Binding Ligand, N-Linked Glycoprotein) proteins

4. Glutamic acid (Gla) proteins (Osteocalcin, MGP, S100)

5. Other components: (many not found in mature dentin)

Proteinases: -procollagen peptidases

-Cathepsin D

-Matrix metalloproteases

Other enzymes: -Alkaline phosphatase

-Lysyl oxidase

-PC-1

Lipids

It has to be noted that a great part of information about dentin ECM has come from studies on bone, as dentin and bone are thought to be similar in composition and mechanism of formation, in many respects. Organic matrices, predominantly collagenous, are formed in both tissues and eventually mineralize. Forming cells, osteoblasts and odontoblasts respectively, secrete type I collagen-rich unmineralized extracellular matrices, osteoid and predentin, which form the template for deposition of apatite crystals. Formation and mineralization of these matrices are highly regulated processes. Whereas the main (approx. 90%) constituent of dentin matrix is collagen, it is the noncollagenous macromolecules (noncollagenous proteins- NCPs) which are believed to promote both initial deposition of mineral on collagen fibers and crystal growth. Dentin matrix NCPs have diverse functions, such as cell attachment and collagen fibrillogenesis (Xu et al, 1998; Keen et al, 2000; Jadlowiec et al, 2004). Regarding dentin mineralization, they have been the centre of focus (Linde and Goldberg, 1993; Veis, 1993; Qin et al, 2004). This importance of noncollagenous proteins is supported by dramatic phenotypic abnormalities in the mineralization process of bone and dentin observed in animals with deficiency of these NCPs or mutation in their genes (Xu et al, 1998; Xiao et al, 2001; Feng et al,

2002; Sreenath et al, 2003). A short description of the major dentin matrix components, with emphasis on the SIBLING proteins follows:

1. Collagen: Dentin collagen is primarily type I. Evidence also exists for synthesis of small amounts of collagen type III and V in rodent dentin that appear to be present in predentin.

Collagen is secreted by odontoblasts as procollagen, converted by the action of peptidases to collagen in predentin, where it is gradually packed and organized (Linde and Goldberg, 1994). Collagen type I is a bio-polymer made up of three α chains, two of which are identical, giving the composition $[\alpha1(I)]_2\alpha2$. Each chain comprises approximately 1000 amino acid residues and the central portion (95% of the total molecule) is triple helical in structure. In the helix, the individual α chains have an amino acid sequence with glycine in every third position, which is a requisite for triple helix formation. The amino acids proline and hydroxyproline (proline hydroxylation predominantly takes place in collagen) together account for approximately one fourth of the residues. Collagen molecules in the dentinal tissue are longitudinally staggered in register to form fibrils. This arrangement creates alternating spatial areas of the fibril with overlapping molecules (overlap zones) and with gaps (hole zones), creating a cross-striation appearance under electron microscopy examination. It is in the hole zones of collagen fibrils that initial formation of mineral crystals has been shown to occur in mineralized tissues. Formed fibrils become stabilized by subsequent formation of covalent cross-links between the collagen molecules (reviewed in Eyre, 1987). It is collagen that provides the

template for the initial mineralization and subsequent mineral crystal growth (see previous section on mineral).

2. Proteoglycans: Proteoglycans (PGs) are macromolecules with a number of carbohydrate side chains, glycosaminoglycans (GAGs), covalently bound to a protein core. Side chains are made up of repeating disaccharide units, each consisting of one uronic acid and one N-acetyl-hexosamine, mainly of the chondroitin, dermatan or keratin sulfate type. The PG distribution in mineralized dentin was found to be very heterogeneous using histochemistry. An intense reaction for glycosaminoglycan within the dentinal tubules and in mantle dentin compared to circumpulpal dentin was seen (Embery et al, 2003). Some of the proteoglycans which are also found in dentin are involved in collagen fibrillation (Keene et al, 2000; Neame et al, 2000) and one possible function for PGs in dentinogenesis could be to affect or control the organization of the predentin collagenous matrix. The most important group of PGs in dentin, small leucine-rich proteoglycans (SLRPs) play other biological roles such as in binding of TGF β (a cytokine family very important in dentinogenesis and osteogenesis) members and acting as a ligand for Epidermal Growth Factor receptor. They are involved in cell migration and calcium binding, which may be related to both the development and mineralization processes (Hunter et al, 1992; Xu et al, 1998). They have also been suggested to be directly involved in biomineralization from *in vitro* experiments where they functioned as inhibitors of hydroxyapatite formation (Boskey et al, 1997).

3. Small Integrin-Binding Ligand, N-Linked Glycoprotein (SILINGs) family: this matrix group has been the focus of attention regarding regulation of

biomineralization in hard tissues (Fisher et al, 2001; Butler et al, 2004). It includes proteins that are abundant in the bone matrix, but scarce in dentin, such as osteopontin (OPN) and bone sialoprotein (BSP) and the characteristic for dentin matrix protein 1 (DMP1), dentin sialophosphoprotein (DSPP) and matrix phosphoglycoprotein (MEPE). The last three SIBLING proteins in dentin are highly phosphorylated and their relative content and phosphorylation in the dentin matrix during maturation is examined in Chapter IV.

The different members of the SIBLING family share some common features, such as hard tissues in which they are found, common cell attachment-mediating and signaling motif and localization on the same chromosome regions. They undergo similar post-translational modifications, mainly phosphorylation (which has been found to determine the function in many) and glycosylation. Characteristic properties and potential relation to biomineralization of the SIBLING proteins are discussed below:

Osteopontin: a 301 amino acids long protein (rat OPN). It is expressed in large quantities in bone, but is also expressed in many other tissues and cells, implying a multiplicity of functions (Sodek et al, 2000). OPN appears to be an effective inhibitor of apatite formation and growth by *in vitro* studies and studies of the OPN deficient mice skeletal phenotype (Hunter and Goldberg, 1993; Boskey et al, 1993; Boskey et al, 2002). Although the OPN deficient mice studies indicate that osteopontin is not necessary for normal bone development, they show an involvement of osteopontin in bone remodeling. Phoshorylation of OPN occurs on serine residues and the

phosphate groups are considered critical to the inhibitory role of OPN in mineralization (Pampena et al, 2004).

Bone Sialoprotein: 303 amino acids long (rat BSP). Found exclusively in mineralized tissues, with a much higher expression in bone than in dentin. Some data suggest that BSP acts as a nucleator of the initial apatite formation and later as a regulator for the direction of crystal growth (Hunter and Goldberg, 1994). Serine and threonine residues on BSP are phosphorylated by caseine kinases, although the role that phosphorylation plays in BSP is unclear. Tyrosine residues are sulfated (Chenu et al, 1994). Phosphate groups on BSP could affect the apatite crystal growth in dentin and bone (Hunter and Goldberg, 1994).

DMP-1: Dmp-1 and the protein products of dspp gene (dentin sialoprotein and dentin phosphoprotein) are the 2 most abundant SIBLING members in dentin. They present a very similar amino acid composition and after secretion both need to be processed into N-terminal and C-terminal fragments. DMP-1 is a 473 amino acid long protein with an unusually large number of acidic domains. Aspartic acid (Asp) and glutamic acid (Glu) residues and also the phosphorylated fraction of the more than 100 serine residues that are potential protein kinase substrates make this protein highly acidic. Although it has not been proven, the numerous phosphate groups on DMP1 have been speculated to function in sequestering Ca^{++} and DMP1 function is dependent on its phosphorylation status (Tartaix et al, 2003). Dmp-1 is highly expressed in odontoblasts and also transiently expressed in pre-ameloblasts (the enamel-forming cells in a predifferentiated state). Transgenic cells overexpressing DMP-1 show earlier onset, more extensive production and larger

mineralized nodules compared to the normal cells (Narayanan et al, 2001). Having been first assumed to be dentin-specific, DMP1 has also been found in bone, hypertrophic chondrocytes and kidney.

Dmp-1 null mice develop a severe tooth phenotype characterized by partial failure of predentin to mature into dentin and increased width of predentin zone (rate of formation of unmineralized precursor layer higher than that of mineralization). Peritubular structure is poorly organized, presenting a coarse and irregular surface. These studies suggest that DMP1 is directly related to biomineralization and its absence is associated with hypomineralization of dentin (Ye et al, 2004).

Other matrix proteins are affected by DMP-1 deficiency, such a DSPP (regulation of one SIBLING member expression by another) and biglycan (a principal dentin PG).

dspp: this gene expresses a precursor protein from which two important dentin matrix proteins are derived after proteolytic processing A. dentin sialoprotein (DSP) from the 5' end and B. dentin phosphoprotein (DPP) from the 3' end. Both proteins were earlier identified independently as components of the dentin ECM. Some authors (Hao et al, 2004) believe that expression of DSP and DPP as one protein by the same gene is not a universal effect and is species-dependent.

A**.** DPP: it is the most abundant noncollagenous protein in dentin with DSP being the second most abundant such protein (18:1 ratio). It contains large amounts of aspartic acid (Asp) and phopshoserine (Pse) in repeating sequences of $(Asp\text{-}Pse\text{-}Pse)_n$ and $(Asp\text{-}Pse)_n$. DPP has been shown to be an important initiator and modulator of dentin apatite crystal formation (Boskey et al, 1990; George et al, 1996;

Saito et al, 1997). It is subject to extensive degradation after expression and the molecular mass reported has varied according to species –and, apparently, age of animal- from 72kDa for mouse DPP to 90-95kDa for rat DPP or 155kDa for bovine DPP. Approximately 45% of the DPP sequence are serine residues and most of them are phosphorylated. From the 3 isoforms of DPP, the most highly phosphorylated (HP-DPP) is the major one in DPP with 209 phosphates/mol. The predicted structure of DPP contains long ridges of alternating carboxyl and phosphate groups on opposite sides of the polypeptide chain, a conformation that would permit calcium phosphate crystals to grow on this lattice (Butler et al, 2004). After removal of the phosphate groups DPP was shown to lose the ability to nucleate apatite onto collagen (Saito et al, 1997).

There is a body of evidence suggesting that DPP is involved in the initiation of apatite formation in the collagen fibrillar lattice of dentin. DPP is strongly associated with calcium by forming an insoluble aggregate with it (Kuboki et al, 1979), binding high levels of Ca^{2+} with relatively high affinity (Marsh, 1989) forming extended β-sheets in the presence of calcium. Localization of DPP also indicates a function in mineralization: after synthesis by odontoblasts, DPP reaches the mineralization front (bypassing unmineralized collagen forming in predentin) relatively quickly (Weinstock and Leblond, 1974). At the mineralization front, limited numbers of DPP molecules bind to collagen at the gap region, where initial formation of apatite is known to occur.

In addition to promoting initiation of mineralization, DPP could also be involved in the control of crystal growth (Boskey et al, 1990; Addadi et al, 1992). When it

binds to the (100) face of growing crystals in high concentration, phosphoseryl and aspartyl groups interact with calcium ions in the lattice, resulting in a reduced rate of apposition of additional calcium and phosphate ions, thus making its role in biomineralization diverse.

B. DSP: it is only moderately phosphorylated (6.2 phosphates/mol with half of the potential Ser/Thr casein kinase substrate sites phosphorylated). Phosphate groups of DSP seem to have a minor role in mineralization (Boskey AL-personal communication).

Experiments showing the association of mutations in the dSPP gene with dentinogenesis imperfecta in humans (Xiao et al, 2001) and with defective mineralization of dentin in DSPP deficient mice (Sreenath et al, 2003) support the role of the dspp gene in dentinogenesis. DSPP is also expressed in bone, but at a much lower level than that in teeth. DSPP deficient mice showed also a role for it in regulation of proteoglycan distribution. Increased biglycan levels (both protein and mRNA levels) are observed in dspp null mice, as in DMP-1 null mice. The dspp null mice also show an increased production and accumulation of decorin are increased.

4. Glutamic acid containing proteins: The most prominent protein in this group is osteocalcin, a small (apparent MW=14,000 Da) protein which is found at relatively low levels in dentin, although it constitutes up to 15% of the bone noncollagenous matrix. Osteocalcin is an established marker of osteoblastic function for cells and is involved in osteoclast recruitment in bone. The specific functions of osteocalcin in dentin are unknown. Studies in osteocalcin-null animals (Boskey et al, 1998) and

osteocalcin-depleted bone implants (Glowacki and Lian, 1987) suggest a role for osteocalcin in osteoclast recruitment and bone remodeling.

Role of dentin phosphoproteins in biomineralization: The NCPs described above were found to be common in many mineralized tissues with possibly different functions. In dentin, the matrix proteins believed to be most relevant to biomineralization are the phosphorylated SIBLINGs. In many of the relevant studies, a protein called phosphophoryn was used, which may be coinciding with dentin phosphoprotein in some species, while it has been called DMP2 by others.

There are several lines of evidence that implicate phosphoproteins in dentin in one of more of the proposed functions in mineralization, some of which were already discussed. These are: 1.Synthesis and localization of phosphoproteins: Numerous studies (Dimuzio and Veis, 1978 a,b; Maier et al, 1983; Weinstock and Leblond, 1973; Rabie and Veis, 1991) have indicated that phosphoproteins and collagen are secreted independently in the odontoblast, the collagen is released into the predentin, while phosphoprotein-containing vesicles move through the odontoblastic processes directly to the mineralization front. 2. Association of phosphoproteins with collagen: At the mineralization front, phosphoproteins are directly associated with the mineralizing collagen fibrils. Phosphophoryn has *in vitro* been shown to bind to type I collagen fibers, specifically at the e-band of the fibril (Stetler-Stevenson and Veis, 1986; Traub et al, 1992). This is a region near the middle of the collagen gap zone, which has been demonstrated to be the site of initial mineral deposition along collagen fibrils (White et al, 1977). 3. Interaction of phosphoproteins with Ca^{++}: Phosphoproteins are secreted onto the collagen surface could have a function, in

dentin, of sequestering calcium ions in the vicinity of the gap region of the collagen and help the nucleation of mineral. There is also proof for a phosphophoryn interaction with mineral components, as it changes conformation into a β-sheet-like one when associated with Ca^{++} ions (Veis, 1993). 4. Regulation of crystal growth: Adsorption of acidic matrix molecules onto the surface of growing calcium sulfate, calcium carbonate and apatite crystals has been described to regulate crystal growth, by recognition of a specific stereochemical motif on the interacting crystal plane (Moradian-Oldak et al, 1992). Other studies (Adadi et al, 1992) have also shown binding of native phoshpophoryn to specific faces of the hydroxyapatite or octacalcium phosphate (another mineral phase that is occurring in some mineralizing systems). 5. Phenotypic alterations of mice deficient in phosphoprotein in mineralized tissues: discussed above.

In a recent study (He et al, 2005), many of the properties of the phosphoproteins described were specifically compared between native phosphophoryn and the active domain from rat phosphophoryn cloned and expressed recombinantly in E. coli, where it is not phosphorylated. Contrary to the native phosphophoryn, the recombinant unphosphorylated phosphophoryn failed to exhibit all the basic properties of phosphophoryn described -calcium binding, change of conformation upon calcium binding, mediation in transformation of amorphous calcium phosphate to apatite in nucleation experiments and formation of collagen aggregates.

MINERAL AND MATRIX IN DEVELOPING MINERALIZED TISSUES- DENTIN MATURATION

Dentinogenesis starts with formation of non-mineralized mantle dentin matrix. The young newly differentiated odontoblasts secrete collagen and noncollagenous components and, as discussed, the rate of mineralization is slower than that of matrix formation, so that a layer of unmineralized matrix –predentin- is always present. Bundles of collagen fibers are grouped in globular structures and, with the addition of new fibers in predentin, collagen is packed more tightly. In predentin, drastic changes also occur in proteoglycans, as a concentration gradient (hypothesized to represent gradual removal of mineralization inhibitor groups) is present for the predentin matrix from next to the pulp to the mineralization front (Embery et al, 2003). As described, highly phosphorylated proteins are not secreted in predentin, but rather transported through the odontoblastic processes of odontoblasts directly on the mineralization front, where they are finally secreted (Weinstock and Leblond, 1973). There, they are hypothesized to play a major role in initial mineral formation. In mantle dentin initial formation of mineral takes place inside the membrane-bound matrix vesicles. No vesicles are seen later during circumpulpal dentin formation, and the site of the initial mineral deposition is the collagen hole zones.

In mineralized tissues the events associated with crystal formation are generally nucleation, crystal growth and crystal proliferation (reviewed in Boskey, 2001). In nucleation, the crystal formation starts with the collision of the component lattice ions (calcium, phosphate, hydroxide) or clusters of these ions and a crystal nucleus is

formed when the colliding ions or ion clusters remain together in the orientation they will have in the final crystal lattice. After a stable nucleus is formed, ions or ion clusters add to the existing nuclei during the crystal growth process. They proliferate by the formation of additional nuclei and often they aggregate, resulting in an apparent increase in crystal size. Calcification of the collagen fibrils occurs by the heterogeneous nucleation of apatite crystals within the collagen fibrils in selected, spatially and physicochemically independent nucleation sites.

Changes in the physicochemical properties of the mineral, as mineralized tissues mature, have been described –mainly for bone- in a number of studies (reviewed in Glimcher, 1998). The composition, short-range order, local environments of the crystals change significantly with the age of the crystals *in vitro* and *in vivo* and these changes are reflected in changes of the crystallinity of the mineral phase, as defined by x-ray diffraction. Crystallinity as an index depends on the size of the small crystals and the degree of order of the ions or atom constituents of the crystals, as many of these atoms are located on the surface of the crystals, in a labile environment. It has been established from bone studies that the earliest crystals formed have a high concentration of HPO_4^{2-} ions and a low concentration of CO_3^{2-} ions and a high proportion of each is located in very labile, highly reactive environments, mostly on the surface of the crystals. With tissue age, there is a progressive increase in the CO_3^{2-} concentration, occurring first on the surface as labile ions, later displacing labile HPO_4^{2-} ions. During later stages, CO_3^{2-} ions are further incorporated into stable positions in the apatite lattice, as HPO_4^{2-} groups in the lattice are displaced. Thus, the stable CO_3^{2-} groups in the crystal lattice increase

during maturation and those on the surface present as labile CO_3^{2-} ions decrease, while both the surface labile HPO_4^{2-} groups and the stable HPO_4^{2-} groups in the lattice decrease during maturation. Apatite crystals that contain only a few labile phosphate ions have little capacity to mature and incorporate CO_3^{2-} ions into lattice positions and undergo few of the normal maturational changes in the composition and environment of both the HPO_4^{2-} and CO_3^{2-} ions. This also includes failure of the CO_3^{2-} ions to incorporate into the interior of the crystals in stable CO_3^{2-} sites (substituting for OH^- /A type and $PO4^{3-}$ positions/B type substitution).

As was already stated above, whereas there have been studies on organogenesis and matrix protein gene expression during dentin development, few studies have described dentin mineral and matrix maturation. In one of the latter studies (Engel and Hilding, 1984), electron probe analysis was used on dentin from developing mouse molars from different age groups and a mapping of dentin for relative densities of Ca and P and for Ca/P (as a measure of apatite maturity) was performed. Results from this study are difficult to interpret, as the location of dentin examined was not specified and only elemental analysis results were provided for the maturing mineral. Another study was based on a FTIR microspectroscopic analysis of adult human premolars and young 3rd molars, (Magne et al, 2001). It was concluded that –in contrast to what had already been reported for bone mineral- the total amount or the type (A vs B) of carbonate substitution did not change during dentin maturation, whereas crystallinity increased and $HPO4^{2-}$ ion concentration in the mineral decreased. The same study also focused on dentin matrix maturation, where the main conclusion was that collagen is progressively dehydrated as a result

of being calcified. However, this study's conclusions are questionable as the teeth analyzed were mostly mature, the inherent significant histologic variation in dentin as examined from predentin to enamel was interpreted only as variation in tissue maturation and a mantle dentin area was not identified (also discussed in Chapter II). A few studies, using whole fetal bovine teeth or human dentin, have been published on aspects of matrix changes during dentin development (Lee et al, 1983; Masters, 1985; Walters and Eyre, 1983). Among the findings, breakdown of noncollagenous proteins (mainly highly phosphorylated proteins), a prominent loss of phosphorylated and non-phosphorylated amino acids and a significant change in the collagen cross-linking pattern, with mature trivalent cross-links increasing and immature divalent cross-links decreasing, were reported. It must be noted that a similar breakdown of matrix proteins that occurs with maturation of the tissue has been observed in bone (Nagata et al, 1991 a-b). Similar to the dentin mineral data discussed, results from these studies of dentin matrix maturation can only be seen as comparing wide tissue age spans for dentin and as results for mantle and circumpulpal dentin averaged together (discussed in Chapter II). Matrix degradation and the phosphorylation profile of dentin matrix merit further investigation using samples of distinct tissue ages and carrying out separate analyses for circumpulpal and mantle dentin. There is an equal need for mineral-matrix interaction studies as it has been shown, for instance, that phosphoprotein conformation is altered in the presence of apatite (Fujisawa and Kuboki, 1998). The current lack of relevant data based on a convenient maturation model makes an appropriately designed mineral and matrix maturation study important in understanding biomineralization in dentin.

SPATIAL VARIATION IN DENTIN PROPERTIES

Histology of dentin shows a high degree of variability. In mature dentin, most of this variability is due to the presence of mantle dentin on the periphery of circumpulpal dentin and the presence of peritubular dentin inside the dentinal tubules. The relative density ratio of these two kinds of dentin is not constant, as the diameter of the dentinal tubules and the relative tubule density in the dentin mass is much higher close to predentin than close to the DEJ (Figure 1-2 a). Additional sources of variability in dentin are the presence of interglobular dentin and the interfaces existing around the mineralization front and on the DEJ, due to progressive transition between the unmineralized and mineralized matrix in dentin and between dentin and enamel. (Goldberg et al, 1992; Marshall et al, 2001; White et al, 2000).

The presence of mantle and circumpulpal dentin as two morphologically and developmentally distinct zones is one reason why dentin presents variability in histology and properties. Mantle and circumpulpal dentin are different in density and composition of both mineral and matrix. Concerning mineral density, mantle dentin has traditionally been thought to be slightly hypomineralized with respect to circumpulpal dentin (Mjor, 1966; Herr et al, 1986). Some studies showed that the overall mineral content in mantle dentin is very similar to that of the rest of dentin in both rats and humans (Sanchez-Quevedo et al, 1989- Stratmann et al, 1997). At the same time, the Ca/P ratio (correlated to a certain extent to apatite stoichiometry) has been shown to be lowest (compared to other dentin areas) in mantle dentin of rat

molars by electron probe microanalysis (Tjarerhane et al, 1995). In at least the part of mantle dentin lying adjacent to enamel, highly phosphorylated proteins are absent, as shown in human, calf and rat teeth using either histochemical or immunohistochemical staining (Nakamura et al, 1985; Tagaki and Sasaki, 1986; Rahima et al, 1988). Collagen fibers are organized in a different direction than in the rest of dentin, seemingly packed more tightly than in circumpulpal dentin, as it is evident by the collagen content assayed on samples dissected from the dentin bulk (Levine, 1972). Collagen type V, known to regulate type I collagen fiber growth, appears at an early stage (Bronckers et al,1986). The orientation of the collagen fibrils is also distinct, with collagen bundles running parallel to the odontoblastic processes and giving the appearance of the so called von Korff fibers, the true nature of which has been disputed (Moss, 1974). Matrix constituents that are minor in circumpulpal dentin seem to be substantial in mantle dentin: bone sialoprotein, osteopontin, phospholipids and γ-carboxy glutamic acid (gla) proteins of the osteocalcin type are all prominent in the mantle dentin matrix (Mc Kee et al, 1996; de Vries, 1987; Camarda et al, 1987). As discussed already, a distinct characteristic of mineral formation in mantle dentin is the key role of extracellular matrix vesicles (ECMVs), where initial formation of mineral takes place. This was shown dramatically in a study (Takano et al, 1998) where the inhibitory effect of a bisphosphonate –HEBP- was examined on rodent incisors: HEBP interfered significantly with initial mineralization in circumpulpal dentin but not in mantle dentin, although it did interfere with crystal growth in the latter. Mantle dentin also shows a special affinity for cationic dyes -suggesting an increased concentration of

proteoglycans- and phospholipid staining reagents (Lormée et al, 1989). Glycosaminoglycan levels have been shown, instead, to be only significant in the peritubular part of the circumpulpal dentin (Takagi et al, 1990). Proteoglycans in high concentration in the mantle dentin zone could function as mineral inhibitors, comparable to their presumed function in predentin.

Another factor contributing to dentin variability is related to the presence of peritubular in addition to intertubular dentin. Peritubular dentin is hypermineralized with respect to intertubular dentin, with differences in the estimated mineral content reported ranging from 9% to 40% (Miller et al, 1971; Johnson and Boyde, 1984). In addition to the mineral density difference, peritubular dentin is apparently scarce in collagen and results from the mineralization of a noncollagenous extracellular matrix (Johnson and Boyde, 1984). In humans, peritubular dentin starts to develop inside dentinal tubules at some distance away from the dentin-predentin border, that is, at a different site than intertubular dentin starts developing. As already discussed, the peritubular dentin matrix is primarily noncollagenous in nature and, also, the concentration of the NCPs in it is different than in intertubular dentin. Osteonectin, bone sialoprotein, osteocalcin, α2Hsglycoprotein and lipids are more abundant, as opposed to the highly phosphorylated matrix proteins that are the most prominent matrix noncollagenous group in intertubular dentin (M Goldberg, 1995). The mineral phase of peritubular dentin also is different, as it is also rich in Mg and contains high amounts of carbonate, accounting for its high solubility. The diameter and relative density of dentinal tubules is not the same throughout the coronal dentin (Pashley, 1986). In human teeth dentinal tubules measuring approximately 2.5μm near the

pulp, 1.2μm in the middle of the distance between pulp and dentinoenamel junction (DEJ) and 900μm near DEJ with a concomitant increase in their density towards the pulp (59,000 to 76,000 tubules/mm2 at the pulpal surface decreasing to half that density close to the DEJ). This creates a respective increase of the peritubular/intertubular relative density ratio from the DEJ towards the pulp, reported for human teeth to range from 5 close to the predentin border to .03 close to DEJ. Given that, as discussed, the mineral and matrix composition of the peritubular and intertubular dentin differ, this relative density ratio change should be reflected in a parallel variability in mineral and matrix properties.

There are other factors as well that may be contributing to a spatial variability in dentin, such as the already discussed distinct spatial-temporal pattern of expression for major SIBLING matrix proteins. DMP1 expression has been shown to peak at the initial mineral nucleation and gradually decrease during subsequent mineralization of the organic matrix, whereas DSPP components are expressed later (D'Souza et al, 1997; George et al, 2004), with unknown effects on the mineral that is formed when these proteins are expressed. Another such factor is the globular (known also as calcospheric) mineralization pattern of dentin. With continued crystal growth, globular masses are formed, that continue to enlarge and eventually fuse to form a single calcified mass. This pattern is best seen in circumpulpal dentin just below mantle dentin. Failure of these globular masses fail to fuse leaves small areas of uncalcified matrix known as interglobular dentin, that have an altered distribution of elements, such as calcium and phosphorus at various ages within coronal dentin (Lefèvre et al, 1976).

In addition to the histologic variability present in dentin at the time of formation, dentin changes continuously with age. There is a progressive deposition of peritubular dentin and obliteration of the tubule is observed. This obliteration of the dentinal tubules in human teeth most frequently occurs at the apical (tip of the root) third of root dentin and in the crown halfway between the DEJ and the surface of the pulp. Secondary dentin also keeps forming with age, continuously obliterating the pulp space. Although these effects are very important for the pulp-dentin complex physiology –in aspects like sensory transduction to the pulp, caries progression and immunology of the pulp- they are not directly linked to primary dentin maturation and will not be examined here.

METHODS USED FOR ANALYSIS OF MINERAL AND MATRIX AND FOR TISSUE MATURATION STUDIES IN HARD TISSUES

Mineral can be determined using classic analytic techniques or more modern methods (reviewed in Boskey et al, 2001). Classic analytic techniques include gravimetry, calorimetry and atomic absorption spectrophotometry. As an example, gravimetric analyses have been used to measure the water content, mineral content and the carbonate content of bone. These analyses are based on the loss of water at 110°, the loss of organic matrix at 600° and the loss of carbonate at 900°. Gravimetric measures provide reproducible quantitative information, but no information on the quality of the mineral. Similar limitations hold for the rest of the classic analysis techniques, in addition to the need for homogenized samples and the resulting lack of data on spatial distribution.

More modern methods are spectroscopy-based and the most widely used among them have been energy dispersive X-ray microanalysis (EDAX), X-ray diffraction, nuclear magnetic resonance (NMR), backscattered electron imaging (BSE), tomographic methods, infrared and Raman spectroscopy. Some of these techniques look at site-to-site variations of the analyzed parameters: EDAX analysis of unmineralized osteoid and mineralized bone has provided information on geographic distribution of calcium to phosphorus (Ca:P) ratios and the presence of trace elements. BSE (in a similar way to microradiography) has provided detailed information on the distribution of mineral with a high spatial resolution. BSE provides a two-dimensional image, which is reported to be highly correlated with ash weight but independent of compositional and crystal size variations. Thus, neither of these techniques provides sufficient information on the mineral quality.

X-ray diffraction has been the most widely used method in characterization of the bone mineral and studies of mineral maturation in calcifying tissues, with relevant data has been provided by ^{31}P NMR (Burnell et al, 1980; Bonar et al, 1983; Wu et al, 1994). Through these techniques, it was shown that mineral phases such as amorphous tricalcium phosphate or octacalcium phosphate [OCP-$Ca_8(HPO_4)_2(PO_4)_4$], which were earlier postulated to be apatite precursors, are not present during mineral formation, or are transiently present. X-ray diffraction is based on characteristic X-ray patterns that crystalline materials produce, wherein the angular locations of the peaks are directly related to the spacing between planes of atoms. This method was used to identify bone mineral as an analogue of hydroxyapatite (DeJong, 1926). The peaks in the bone and dentin X-ray diffraction

are broadened, as is characteristic of poorly crystalline materials in which the lattice planes are not perfectly in register and where there are impurities (holes, substitutions, kinks) in the lattice positions. According to the Debye-Scherrer equation, the line broadening β, of any unique peak measured at half maximum, is inversely related to the size and crystal perfection in that lattice plane. The broadening associated with the plane that cuts halfway through the c-axis of the apatite structure (the 002 plane) is often used to calculate the approximate c-axis size/perfection in bone samples. Although X-ray diffraction is the method of choice for assessing mineral quality, it has major limitations for use in tissue maturation studies, for example there is no capability for spatial variation analysis and there is a need for a relatively large amount of sample. Despite the substantial amount of data from these techniques on developing bone, there have not been any similar studies on developing dentin.

Numerous studies have been published on matrix components in dentin of different species. Most of these studies have used immunolocalization (referenced in section “Spatial Variation in Dentin Properties”) to identify associations of particular matrix proteins with the different dentin compartments and structures or with particular mineral formation locations and stages. Some studies addressed similar questions about the dentin matrix employing histochemical staining or aminoacid analysis of whole crown and root dentin (Takagi and Sasaki 1986; Takagi et al, 1988; Mc Curdy et al, 1988). Although immunohistochemistry or histochemistry are powerful localization techniques, they suffer serious limitations regarding quantitative analysis, as the intrinsic density of hard tissues makes fixation and affinity of

proteins for stains or antibodies unstable and the alternative of prior mineral extraction may be removing many of the target proteins (Mc Kee and Nancy, 1994).

VIBRATIONAL SPECTROSCOPIC ANALYSIS IN MINERALIZED TISSUES

Vibrational spectroscopy (Raman and infrared) has been extensively used to study mineralized tissues. These tissues may have formed as a result of physiologic (Mendelsohn et al, 1989; Rey et al, 1991; Tarnowski et al, 2002; About et al, 2000; Atti et al, 2002) or pathologic processes (Boskey, 1990; Tomazic et al, 1994; Camacho et al, 1996; Paschalis et al, 1997; Miller et al, 2004). Examples of tissues formed by physiologic processes are bones, teeth, calcified cartilage and for tissues formed through pathologic processes are atherosclerotic plaques, kidney and salivary stones and other pathologic deposits. In the relevant studies, vibrational spectroscopy provided information on the nature of the mineral phases present, the changes in the mineral and matrix composition as mineralization occurs and the nature and amounts of substituents in the mineral (reviewed in Boskey et al, 2005). All the relevant analyses were based on studies of synthetic or purified similar compounds (Rey et al, 1991; Paschalis et al, 1996; Bohic et al, 1998).

Fourier Transform Infrared (FTIR) analysis is based on the interaction of chemical structural fragments within molecules, known as functional groups, with infrared radiation (Smith, 2001). Functional groups tend to absorb infrared radiation in the same wavenumber (a different unit system for radiation wavelength) range regardless of the structure of the rest of the molecule that the functional group is in. For instance, the C=O stretch of a carbonyl group occurs at ~1700 cm-1 in ketones,

aldehydes and carboxylic acids. This correlation between the wavenumbers at which a molecule absorbs infrared radiation and its structure allows the structure of unknown molecules to be identified from the molecule's infrared spectrum. Small shifts from the characteristic wavenumber at which a particular group vibrates occur depending on the chemical environment of this group in the molecule and this allows for identification of this environment. For instance, well crystalline hydroxyapatites absorb infrared radiation at slightly different wavenumbers than less crystalline hydroxyapatites (see also Chapter II-Methods and Materials). In this way, broad spectral envelopes can be created from the existence of one functional group in different chemical environments within a molecule (qualitative analysis). This spectral envelopes are prominent in spectra from tissues, as the environment of groups analyzed within the tissues molecules is always more complex than in pure chemical compounds. Infrared analysis can also be quantitative for an already identified functional group through the intensity of radiation absorbed at the spectral region where it is active. This happens because IR spectroscopy obeys Beer's Law, according to which the intensity of the absorbed radiation is also dependent and linearly related to concentrations of the analyte. Figure 1-3 presents a characteristic spectrum of dentin. The spectral regions of interest are marked on the spectrum. The bands marked are associated with vibrational modes of the mineral (v_1v_3 $PO4^{3-}$, v_2 carbonate) and the matrix (Amide I and II) of the tissue. The information that is provided from analysis of these bands is discussed in Chapters II and III.

FOURIER TRANSFORM INFRARED IMAGING

There is a need, in hard tissue studies, to investigate spatial variations of the mineral and extracellular matrix properties in quantitative and qualitative terms. Recently, Fourier transform infrared imaging (FTIRI) and microspectroscopy (FTIRM), techniques where an array detector (FTIRI) or a single detector (FTIRM) is coupled with an infrared spectrometer through an optical microscope, have been used to obtain this type of information. FTIRI and FTIRM have also been used to investigate the development of hard tissues. Through their use mineralization in the developing tooth (Magne et al, 2000; Verdelis et al, 2003), conversion of calcified cartilage into bone (Mendelsohn et al, 1989) and calcification of turkey tendon (Gadaleta et al, 1996) have been studied. FTIRI was the main method that was used for analysis of developing dentin throughout this thesis.

FTIRI has been used to obtain qualitative and quantitative information on both mineral and matrix of bone (Mendelsohn et al, 1999; Marcott et al, 1999; Boskey et al, 2002), calcifying cartilage cultures (Boskey et al, 2002), cartilage (Bhargava and Levin, 2001; Camacho et al, 2001) and dentin (Verdelis et al, 2003). Its main advantage lies in providing molecular information on a large sample of a tissue, while retaining a relatively high spatial resolution of ~ 7μm x 7μm. The principle of operation and the layout of the imaging system for the FTIRI analysis are shown in Figure 1-4 a and b.

SCOPE AND RATIONALE FOR THIS DISSERTATION

As already discussed, in a dentin maturation study it is desirable to analyze the whole of dentin, from predentin to dentinoenamel junction, in many stages of development and interpret results accordingly. Imaging analysis techniques applied on a suitable developing dentin model have the potential to gather important information on the subject. The objective of this dissertation is to validate a fetal bovine model for the study of changes in dentin mineral and matrix during maturation using spectroscopic imaging analysis, describe these changes in quantity and quality terms and apply the same approach to evaluate developing murine dentin. Four topics are presented: topographical representation of mantle and circumpulpal dentin mineral properties of the developing bovine incisor, studies of mineral changes during dentin maturation of the bovine incisor, studies of matrix changes during dentin maturation of the bovine incisor and studies of mineral properties changes of the developing mouse molar. The specific aims in this thesis and the chapters in which the relevant experiments are described are listed below:

Specific Aim I: To test the hypothesis that spatial variation in dentin mineral and matrix properties during maturation is a function of both tissue age and the tissue's histological variation and that a fetal bovine incisor incisor model can be used for the study of dentin maturation. This specific aim is addressed in Chapter II, which describes the evaluation of two mineral properties, mineral: matrix ratio and -on a semi- quantitative basis- crystallinity, through images of spatial distribution for the two properties. Analysis of the two main dentin compartments, mantle and circumpulpal dentin, from the cervical through the incisal end in fetal bovine incisors

and in control 1-1.5yr-old bovine incisors was conducted. Preparation of the samples, the FTIRI system, spectroscopic parameters and the imaging techniques used are described in the Methods section. Patterns of spatial variation that mineral properties present in this section are examined and whether they represent different tissue ages or an inherent variation in the dentin tissue properties is discussed.

Specific Aim II: To describe the changes in mineral properties during mantle and circumpulpal dentin maturation and compare them between the two dentin regions. This was accomplished in the study described in Chapter III, where quantitative results for dentin mineral during maturation in mantle and in circumpulpal dentin are presented. A different FTIRI system and processing techniques were used in this part and are described. Groups of spectra, from a particular development stage of mantle or circumpulpal dentin, were extracted from the imaging files and processed for analysis. Changes in the apatite crystallinity, the carbonate and the acid phosphate substitution in the dentin apatite are described for each maturation stage. The type of carbonate substitutions is also evaluated and the results from this part are compared to existing dentin data and similar data reported for developing bone. In the second part of Chapter III, localized by microdissection mantle and circumpulpal dentin samples of consecutive tissue ages were acquired for FTIR spectroscopical analysis of the maturing matrix.

Specific Aim III: To test the hypothesis that there is a substantial change in relative content of highly phosphorylated proteins or decrease in the level of phosphorylation of phosphorylated proteins in dentin matrix during maturation and that this change is different in mantle and circumpulpal dentin, as reflected in their

relative content of phosphoproteins. The experiment addressing this specific aim is described in Chapter IV. A whole matrix amino acid and matrix phosphorylation analysis was performed on, similar to the ones analyzed in Chapter III, microdissected dentin specimens. Phosphorylation was examined because, as discussed above, it is believed to be the most relevant to biomineralization post-translational modification of matrix proteins and because it has been reported to vary with dentin maturation. Amino acid analysis was performed to investigate possible changes in the relative noncollagenous protein concentration. As in Chapter III, these specimens came from either mantle or circumpulpal dentin, covering a range of tissue development stages.

Specific Aim IV: To test the hypothesis that the model of mineral maturation used holds within species. In Chapter V, the feasibility of analyzing developing mouse molars with a similar approach to that used on bovine teeth in Chapters II and III was investigated. The patterns of spatial variation in mineral properties that developing mouse molars exhibit were analyzed and association of these patterns with dentin maturation and histological variability within the crown dentin is discussed. This study was undertaken to establish a methodology for prospective studies of the effects of deletion or mutation of dentin matrix proteins on forming mineral at different developmental stages of dentin. These studies will be studies of dentin mineral from early formation phases through maturity on mice transgenic for one or more of the proteins postulated to have a function in dentin formation and mineralization.

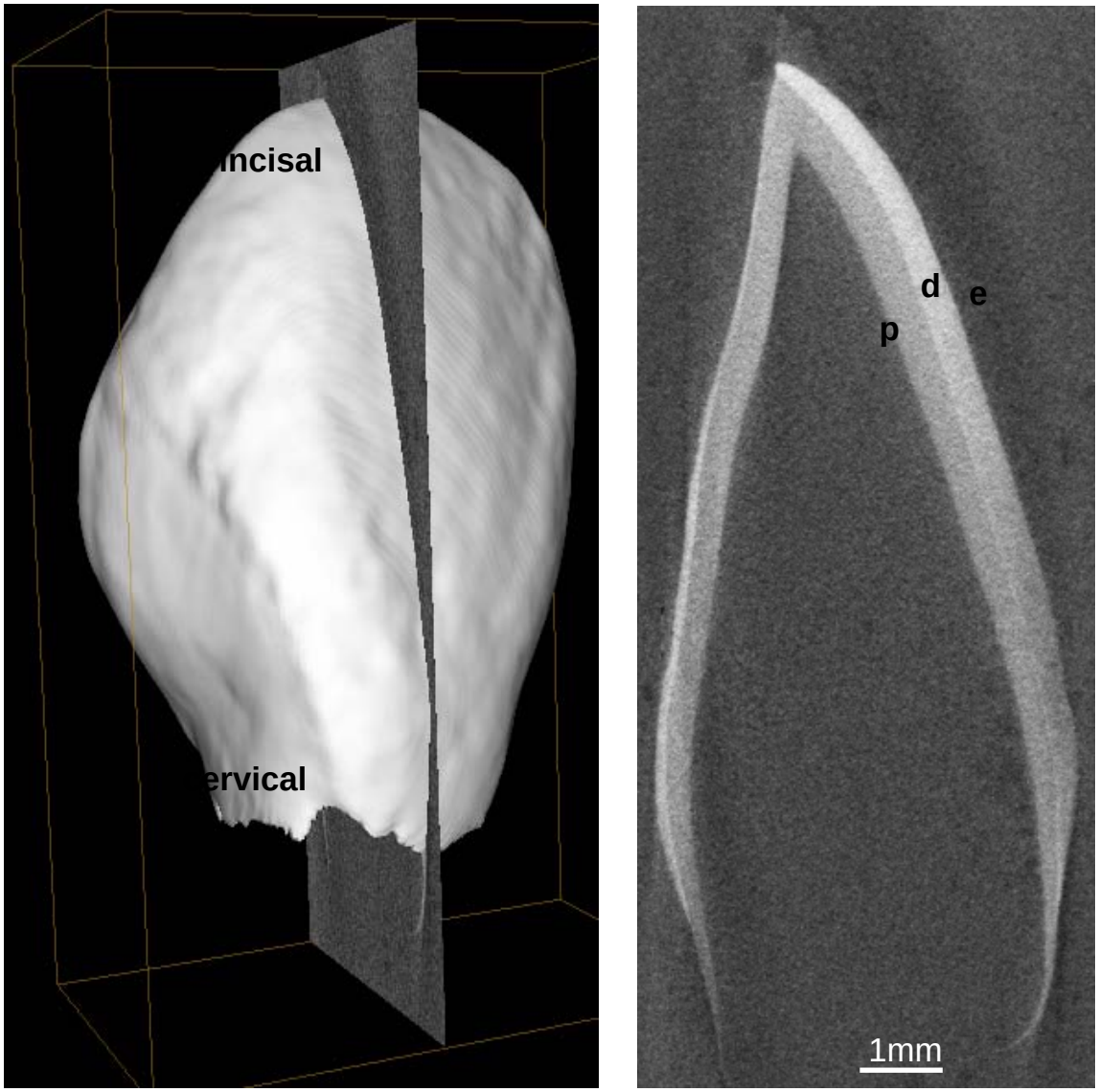

Fig. 1-1: Structure of a tooth. (a): 3D rendering of a microcomputed tomography analysis of a fetal bovine I4 incisor. Cervical and incisal parts are marked. (b): view on the sagittal plane as shown in a. p=pulp, d=dentin, e=enamel.

a.

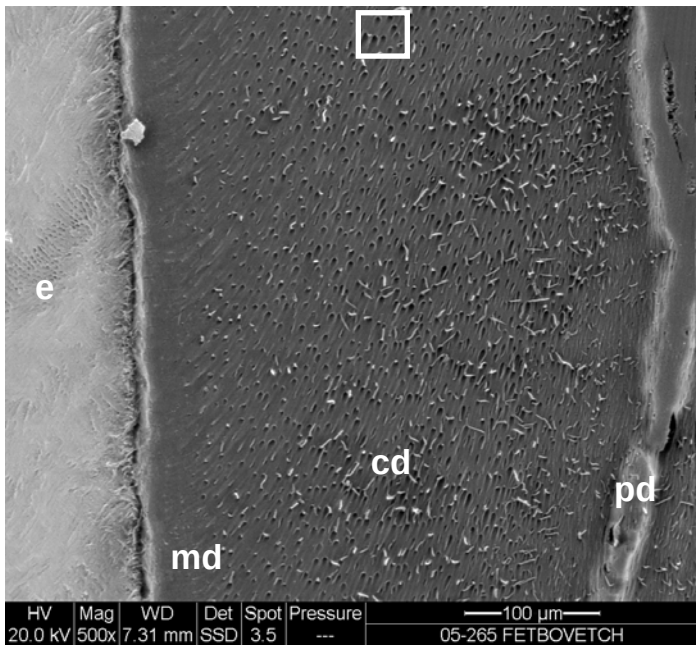

b.

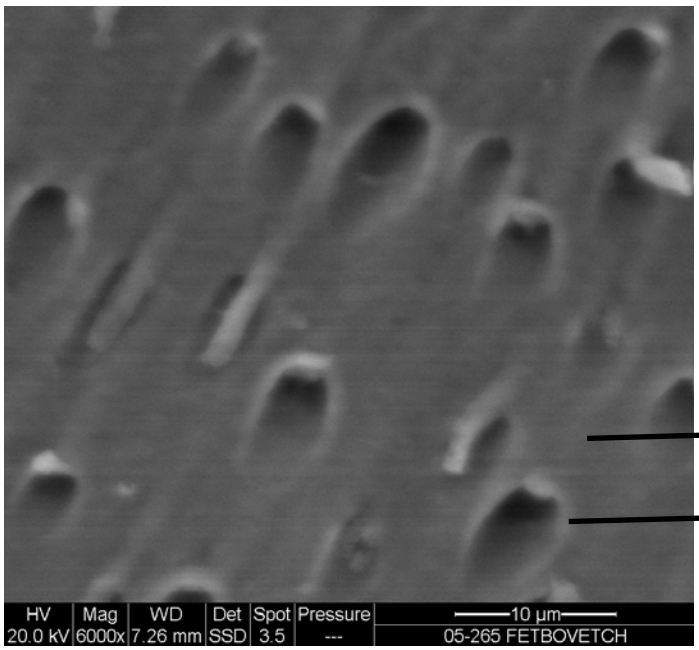

Fig. 1-2: Scanning electron image from a sectioned surface of a PMMA embedded fetal bovine incisor –backscattered electron imaging mode. The surface of the incisor was etched with .5N HCL to expose dentinal tubules. (a): lower magnification. e=enamel, md=mantle dentin, cd=circumpulpal dentin, pd=predentin. Note the decrease in density and diameter of the dentinal tubules from the predentin to the mantle dentin. (b): higher magnification of insert area in a. The peritubular dentin and intertubular dentin are marked.

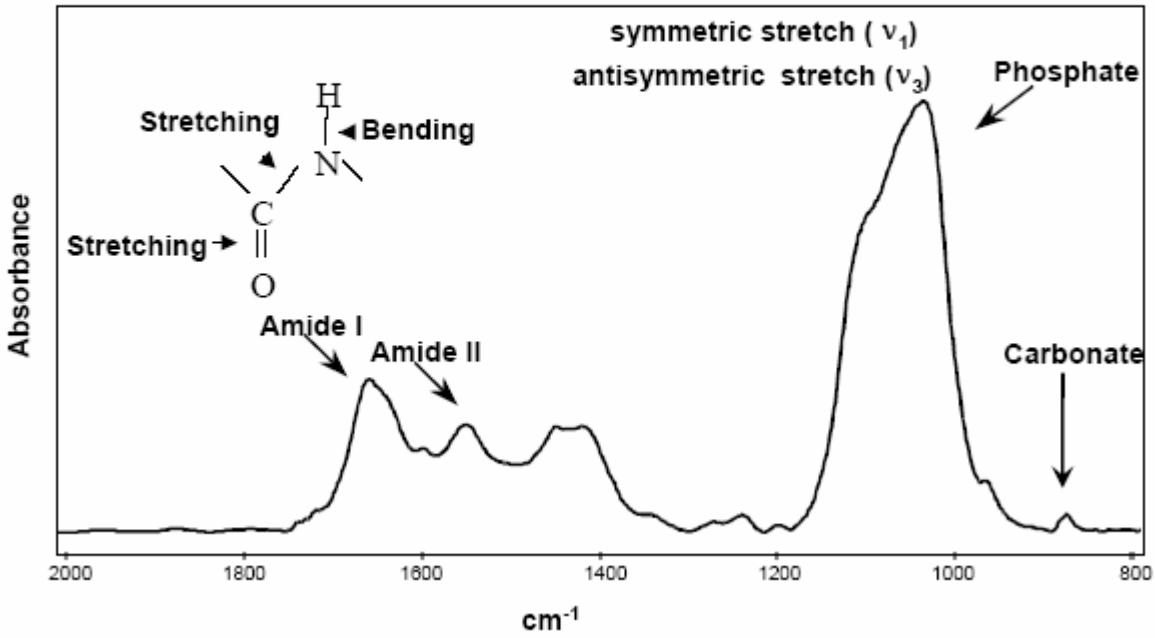

Fig. 1-3: Representative IR spectrum of dentin. The bands representing main vibrational modes of interest are marked.

a.

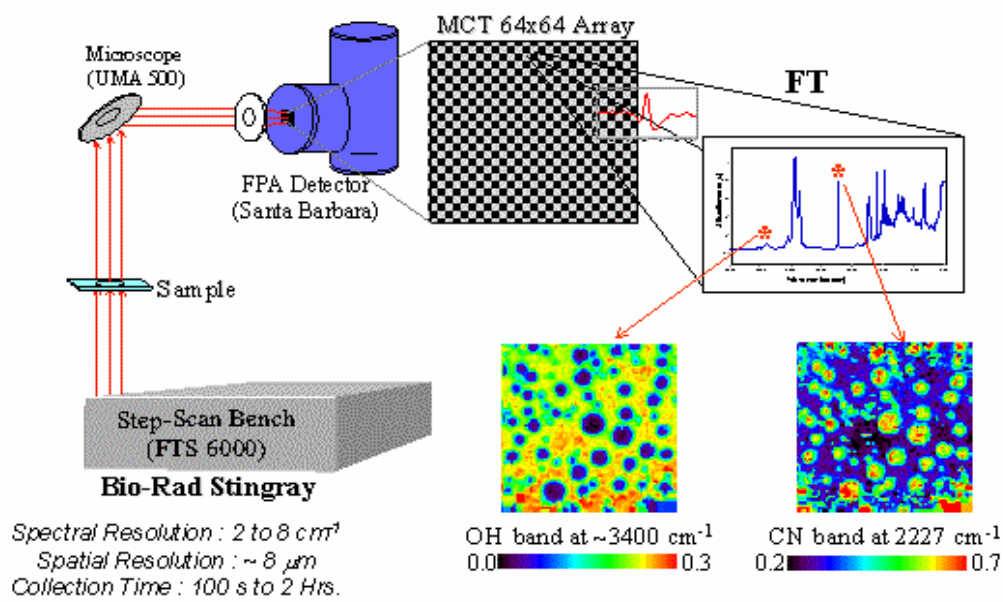

b.

Fig. 1-4: Fourier Transform Infrared Imaging analysis. (a):principle of operation (b):the imaging system.

CHAPTER II

CHARACTERIZATION OF MINERAL AND MATRIX CHANGES IN A BOVINE DEVELOPING DENTIN MODEL BY FOURIER TRANSFORM INFRARED IMAGING

INTRODUCTION

Dentin presents an excellent substrate for analysis in biomineralization studies, as samples for experimental studies are abundant, it has previously been characterized as homogenate (Butler, 1984; Linde, 1984) and it is not subject to remodeling (Veis, 1993; Rey et al, 1995). There are two distinct dentin tissue compartments: mantle dentin, which lies adjacent to the enamel and is the first of the two formed, and circumpulpal dentin, which is the remainder. These two compartments have distinct matrix composition, physical and biomechanical properties (Ten Cate, 1994) and would be expected to present different patterns of biomineralization and mineral maturation. The existing anatomical variation within dentin (Pashley, 1989) mandates a comprehensive analysis of both mantle and circumpulpal dentin throughout their width (mineralization front to DEJ) so that developmental variation can be differentiated from the inherent anatomical variations.

In this experiment, Fourier Transform Infrared Imaging (FTIRI), which is an infrared spectroscopic imaging method, was used to evaluate a fetal bovine model for the developmental investigation of mineral maturation. The distribution of mineral properties was examined for the whole width of dentin from early to late maturational stages, present in cervical and incisal regions, respectively, of bovine fetal incisors. The results of the imaging analysis in fetal incisors were compared with results from fully developed, mature 1 yr-old incisors.

MATERIALS AND METHODS

Specimen Preparation: Dentin samples from 6 developing unerupted incisors of third trimester calves and from 3 mature bovine incisors (1 year-old animals) were analyzed in this study. Bovine jaws were obtained from a commercial source (Aries Scientific, Dallas, TX) and stored at -70°C until they were used, at which time teeth were extracted from the jaws. The specimens were partially fixed in absolute methanol, dehydrated through a series of ethanol gradients and acetone and embedded in polymethylmethacrylate (PMMA). All teeth embedded in PMMA were bisected longitudinally with a diamond wafer wheel saw and nondecalcified 2μm-thick sections of the incisor crowns produced from one half using a Jung Polycut E microtome (Reichert-Jung, Heildeberg, Germany). The sections were mounted between two barium fluoride (BaF_2) windows for Fourier Transform Infrared Imaging (FTIRI).

The incisors from 1 year-old animals and not older were selected as the mature control because with age attrition of the incisors introduces pathology in the dental

tissues, making older samples impractical for the study, and also because primary teeth, as the bovine fetal teeth are, are subsequently replaced by the permanent dentition.

FTIRI analysis/ general methodology: In FTIRI spectra from the imaging files are processed for several spectroscopic parameters, calculated from different spectral areas. Each one of these parameters represents a property of the mineral or the matrix of the analyzed tissue. Calculated values all parameters can be shown as images, through the use of a color scale. The main spectral areas for dentin from which information is provided are shown in Figure 1-3 (Chapter I). All these areas are associated with a specific functional group (molecule or part of it) and some are wide spectral envelopes, consisting of underlying bands that are generated from different chemical environments of the functional group under analysis. Figure 2-1a shows the v_1v_3 PO_4^{3-} spectral area from a dentin spectrum. This is the major area that is associated with the mineral and represents vibrational modes of the mineral phosphate. Underlying bands (defined through a process called curve-fitting), which compose the final wide v_1v_3 PO_4^{3-} contour, are shown in that area. Integration of spectral areas and areas of sub-bands or calculation of relative peak heights of sub-bands provide the information for mineral and matrix components. Based on these integrated areas or on peak heights, spectroscopic parameters for the mineral and the matrix properties have been defined and validated by independent methods. The ratio of the area of the phosphate vibration (900-1200 cm^{-1}) to that of the Amide I vibration (1585-1720 cm^{-1}) is directly related to the chemically determined mineral content, based on ash weight (Pienkowski et al, 1997, Faibish et al, 2005). The

relative areas of sub-band at 1123 cm^{-1} (Rey et al, 1991; Paschalis et al, 1996) or the ratio of the 1030 and 1020 cm^{-1} sub-bands (Paschalis et al, 1996) correlate linearly with the relative content of HA in acid phosphate or HA crystal size and perfection in the c-axis direction as determined by X-ray diffraction analyses. Carbonate to phosphate ratios indicate the extent of carbonate incorporation into the hydroxyapatite lattice. Analysis of relative areas of sub-bands within the carbonate spectral area indicates whether the carbonate has replaced hydroxide (A-type) or phosphate (B-type) or is a labile, located on the periphery of the HA crystal form (Rey et al, 1989). This is shown on a v_2 carbonate spectral area from a dentin spectrum in Figure 2-2. In FTIRI relative areas of sub-bands are often expressed ratios of peak height intensities (Boskey et al, 2003), as will be done for calculation of parameters throughout this thesis (Figure 2-1 b). Analysis of carbonate substitution was not done in this experiment, as the high wavenumber cut off (900 cm^{-1}) of the system used did not permit collection of data for the carbonate band (855-890 cm^{-1}).

FTIRI analysis/ data collection and processing: FTIRI images were obtained from 20-40 fields (one 400μm x 400μm field was scanned at a time) per section, as described in detail elsewhere (Mendelsohn et al, 1999). This FTIR microscope is also coupled to an optical microscope for visually selecting the fields for analysis and acquisition of optical micrographs for reference. The average signal to noise ratio of the detector in the spectral region examined is approx. 50:1. All 4096 spectra from each field were processed for calculation of mineral and matrix parameters and creation of images using BioRad WinIR-Pro (BioRad Laboratories, Cambridge, MA)

program for processing of spectra as follows: Before parameter calculation the PMMA contribution was spectrally subtracted based on its 1729cm^{-1} component and the spectra in the file were baselined. In some cases individual spectra were extracted from selected areas for more detailed analysis. Parameters examined were: 1) mineral:matrix ratio (the ratio of the integrated areas of the phosphate ν_1,ν_3 contour (900-1200 cm^{-1}) to the Amide I band (1585-1700 cm^{-1}) 2) crystallinity determined as the 1030 cm^{-1} to 1020 cm^{-1} peak height ratio. Calculation was not performed for enamel pixels, as parameters were out of scale. A Microcal Origin (Microcal Software Inc., Northhampton, MA) program was used for plotting numerical results from the spectral processing program and create spectral images. Images were combined by superimposing overlapping regions of each 400μm x 400μm data set.

RESULTS

Typical sections of bovine teeth used for FTIR analyses are shown in Figure 2-3 a and b. FTIR images and spectroscopic information are shown from these specimens, but they are representative of all results obtained. The cervical (young tissue), mid-crown and incisal (mature tissue) areas that were analyzed are indicated in the Figure. Only cervical and incisal areas were analyzed for the 1 yr-old incisor to compare mineral and matrix properties and to validate the assumption that variation in dentin properties as a function of cervical/incisal location on the mature incisor is essentially negligible.

Figure 2-3c shows selected superimposed spectra acquired from the fetal incisor section of Figure 2-3a. These spectra were extracted from images of the mantle dentin area ~50μm from the DEJ at different distances from the cervix (as indicated). As tissue age progresses, a continuous increase in the total area of ν_1,ν_3 phosphate band of the successive in age tissue parts is obvious. Apart from the relative increase in area, a significant change of the ν_1,ν_3 phosphate band contour is also visible. This change is characteristic of a transition from an apatite with low crystallinity and high acidic phosphate content mineral to a more crystalline one with a lower acidic phosphate content (Bailey and Holt, 1989).

Results from FTIRI analysis of the indicated cervical, mid-crown and incisal areas of the fetal calf incisor are presented in Figure 2-4 as composites of micrographs and images from the 400μm x 400μm fields analyzed. Micrographs of fields are presented in 2-4a and respective color-coded images of mineral:matrix in 2-4b and crystallinity in 2-4c. Dentin (D), enamel (E) and pulp space (P) are noted on the micrograph from the cervical part. Similar composites of micrographs, mineral:matrix and crystallinity images are shown in Figure 2-5 from fields analyzed in control cervical and incisal areas of the 1 yr-old incisor. For the very young tissue (Figure 2-4-cervical region) both mineral:matrix and crystallinity values are higher adjacent to the DEJ, in the region that coincides with mantle dentin. At more mature stages mineral:matrix values in this area are lower while crystallinity values are not different for most of the circumpulpal dentin (Figure 2-4-middle and incisal regions). Mineral:matrix values reach a plateau for the narrow strip of mantle dentin tissue, while the rest of dentin matrix still shows increases in mineral:matrix (Figure2-4-

incisal and Figure 2-5). At later stages of development (Figure 2-4-incisal), mineral:matrix values and crystallinity values in circumpulpal dentin show a wide variability for locations at different distances from the mineralization front. This variability remains through late maturity (Figure 2-5-incisal). Overall values for the parameters examined are almost equal in cervical and incisal areas of the mature incisor. Crystallinity values are still increasing after complete mineralization (evidenced by the constant mineral:matrix ratio) of both mantle and circumpulpal dentin.

Figure 2-6 shows the distribution of values for mineral:matrix ratio and crystallinity along the predentin-enamel line represented by the white arrows on the cervical field from the fetal bovine incisor (2-6a) and the adjacent to the pulp cervical field of the 1 yr-old incisor (2-6b) that are noted with an asterisk in Figures 2-4a and 2-5a, respectively. The whole range of dentin (predentin through enamel) is covered in the distribution shown in 2-6a, whereas only the mineralization front and part of circumpulpal dentin is covered in 2-6b. In the mineralization front region for the fetal and 1 yr-old incisor, there is no sharp line demarcating the soft (predentin) from the mineralized matrix, but rather a zone of transition between the two (taking place within approximately 30 μm in young teeth). This transition is obvious in the mineral:matrix value distributions and partly evidenced in the crystallinity values distribution along the line analyzed. Adjacent to the DEJ in the fetal incisor, another transition from dentin mineral:matrix values to values characteristic for enamel occurs. Enamel crystallinity is not shown as the parameter cannot be calculated, as there is no “non-stoichiometric apatite” component and crystallinity values for these

pixels have been omitted. In mature teeth, the same distributions cannot be analyzed for the DEJ area, as enamel fractures away during sectioning.

DISCUSSION

Results from this experiment demonstrate the usefulness of the fetal bovine tooth model for characterizing changes in mineral properties of dentin during tooth development through the use of molecular spectroscopy imaging analysis. They also form the basis for acquisition of data in the Chapters III and IV. In the present section, age and site dependent changes in relative mineral content and relative crystal maturity in the mineral are analyzed on whole incisors. Quantitative information on these and additional mineral properties –such as acidic phosphate presence in the mineral, relative amount of carbonate and type of carbonate substitution in the apatite- were obtained from another set of data –using a newer FTIRI system for analysis- in Chapter III. In the latter section, localization on the incisors of mantle or circumpulpal dentin areas of distinct tissue age, but histologically equivalent, is performed and the resulting groups of spectra, each representing one dentin type and one time point in tissue maturation, were analyzed. Localization of samples acquired for the analysis of the fetal bovine developing dentin matrix properties in Chapter IV was also based on this experiment (Chapter II).

The spectroscopic parameters used here, mineral:matrix and crystallinity of the mineral, were selected for dentin analysis because they are independent of sectioning artifacts (being ratios) and they represent important properties for any

mineralized tissue. Control-fully formed incisors were also analyzed and results compared. Similar tooth groups ,namely lateral incisors II, III and IV (I2, I3 and I4), were used throughout Chapters III-V in order to have a relatively homogeneous crown anatomy, stage of eruption and formation between samples. These incisors from fetal 3rd trimester bovine animals were also a convenient tooth group to use for the present studies' purposes as teeth are still unerupted, while the cervical part of the crown has started forming, thus providing very early and relatively late stages of dentin formation within the same tooth. A notable point from the results shown is that enamel of the 3rd trimester incisors used in many cases could be sectioned intact, precluding study of the DEJ and developing enamel in the same sections.

The presence of the two distinct dentin compartments is obvious from the FTIRI data. The spectroscopic results demonstrate an earlier initiation of mineralization and crystal growth in mantle dentin and a more prolonged crystal growth period in circumpulpal dentin that finally reaches overall higher mineral:matrix values. Finally, mantle dentin evolves as a separate entity from the rest of dentin. The extent of mantle dentin (whether it's hypo- or hypermineralized with respect to the rest of dentin), as well as relative matrix content have been a subject of controversy (Moss, 1974; Herr et al, 1986). The distribution of mineral content and crystallinity, with respect to that in the circumpulpal dentin, seems to be clearly defined using FTIRI analysis. The distinct pattern of mineral maturation that appears in mantle dentin (final mineral:matrix and crystallinity levels, faster rate of changes in mantle dentin) may be part of a separate mechanism of biomineralization in this area. In mantle dentin mineralization is believed to be initiated in matrix vesicles

(Katchburian, 1973). The highly phosphorylated proteins, which are generally thought to regulate biomineralization in circumpulpal dentin (Butler, 1998), are less abundant here (Rahima et al, 1988) and minor circumpulpal dentin constituents, such as osteopontin and osteocalcin, are prominent (Mc Kee et al, 1996). It is also interesting to note that crystallinity values continue to increase after complete mineralization (evidenced by the constant mineral:matrix) of both mantle and circumpulpal dentin. As crystal growth would also increase the mineral:matrix, that increase in crystallinity can rather signify a decrease in ionic substitutions (mainly, acid phosphate and carbonate substitution) in the hydroxyapatite crystal. A continuing increase in mineral crystallinity after the relative mineral density has stopped increasing has also been observed in bone maturation (Bonnar et al, 1983). Spatial variation in mineral properties is caused both by the presence of mantle and circumpulpal dentin, and by the other factors discussed in Chapter I. This is more evident in the distribution of mineral:matrix values within circumpulpal dentin of the 1 yr-old incisor. While the mineralization is essentially completed (no difference between cervical and incisal region), the mineral:matrix is highly variable, with a maximum occurring around the middle of circumpulpal dentin. Previous studies have also shown mineral variation as a function of location in mature teeth (Kinney et al, 2001; Kinney et al, 1996). The study of Tesch et al, 2001, also showed variations in the structural and mechanical properties of the mineral as a function of location in the mature human tooth by various methods, including FTIR microspectroscopy. This variation is in part due to the decrease of the dentinal tubule density and a respective decrease in the peritubular dentin density in areas

farther away from the mineralization front (Pashley, 1989). As the mineral concentration and most likely the nature of the organic matrix in peritubular dentin differ from that in intertubular dentin (Weiner et al, 1999) a spatial variation is anticipated.

In the present results, linear gradients of increasing mineral:matrix at the mineralization front and the DEJ and an increasing crystallinity at the mineralization front for fetal and 1 yr-old bovine incisors were shown. These results agree with observations made by other techniques. The extensive predentin to dentin transition was observed in the rat both morphologically and by histochemical methods (Goldberg et al, 1992). The existence of a DEJ mineral gradient was hypothesized based on observations of biomechanical properties (Marshall et al, 2001; White et al, 2000). An important function of the DEJ gradient, such as being a barrier to crack propagation, was speculated in these studies. Moreover, as a conclusion from a similar observed continuum in mineral crystal properties of the DEJ (Cuisinier et al, 2001) a protein continuum was also hypothesized for DEJ. In our study, a compatible to this hypothesis progressive decrease in the Amide I (total matrix protein content) area was present in the DEJ. Although thickness is not always uniform within sections and relative integrated areas of bands (not area ratios) are therefore not entirely reliable, these findings most likely hold true as they came from a few adjacent pixels, between which section thickness would not vary substantially.

The fetal bovine model presented covers a maturation span for the tissue from very early stages to near full maturity. With tissue maturation, mineral proliferates through secondary nucleation, growth and perfection of individual

crystals and crystal agglomeration (Boskey et al, 1990; Heywood et al, 1990), while there is no further apposition of matrix proteins in the tissue after they are laid down either in the predentin or at the mineralization front. In this way, each mineral:matrix value within dentin represents a single time point in the development of the particular tissue. As the results from the 1-yr-old bovine incisor show, in the mature incisors values for mineral content and mineral maturation from cervical dentin are at comparable levels with these of the incisal area and the two areas are most likely eventually equivalent in properties. This validates the assumption that in the 3rd trimester fetal incisors differences in tissue properties between cervical and incisal areas for comparable locations with respect to the pulp or the DEJ are solely due to tissue age difference.

The fetal bovine model analyzed by FTIRI, as presented here, provides the ability for temporal and spatial analysis of tissue maturation, with ~7μm spatial resolution. Discrete stages of formation can be isolated and analysis can be conducted separately for mantle and circumpulpal dentin. The temporal resolution that the methodology used here provides is also a critical issue in order to understand how tissue matrices regulate the physicochemical mechanism of apatite formation, as different proteins may function at different tissue development stages (D'Souza et al, 1997; Papagerakis et al, 2002). Maturation of the mineral in hard tissues has been the subject of many studies (Roberts et al, 1992; Sodek et al, 2000; Bonnar et al, 1991; Aoba et al, 1990; Sydney-Zax et al, 1991). Changes in mineral properties reported in these studies can be compared to those observed during *in vitro* maturation of synthetically produced apatite (Rey et al, 1995). In

tissue studies, samples of various tissue ages have been analyzed, following isolation through the use of methods such as density fractionation (Grynpas and Hunter, 1988; Roberts et al, 1992; Sodek et al, 2000; Bonnar et al, 1991) or microdissection (Aoba and Moreno, 1990; Sydney-Zax et al, 1991). Although these isolation methods provide separation of tissue parts with dissimilar properties, they may introduce a certain range in the tissue age of the samples examined, depending on the efficiency of the separation method used, and the need for isolating discrete tissue age specimens for analysis has been stressed (Rey et al, 1995). For developing dentin, there has been a reports from a study (Magne et al, 2001) in which FTIR microspectroscopy was used to study mineral and matrix maturation as a function of tissue location on the crown of fully formed human molar dentin. Spectroscopic parameters for the mineral and the matrix similar to the ones examined here, in this and the next chapter, was examined in this study. Anatomical variation, as already explained however, is a concern in the interpretation of the results of this study, since the mineral and matrix properties distribution between the mineralization front and DEJ was assumed to only represent variation due to tissue maturation. This concern is even bigger for analysis on teeth from other species, such as human, where the intertubular to peritubular dentin relative density ratio varies significantly from the mineralization front to the DEJ.

In situ studies of dentin mineral and matrix maturation provide the opportunity to analyze the complex interactions between mineral and matrix of tissues during the biomineralization process. The fetal bovine model and FTIRI as a technique evaluated here show the development of mantle and circumpulpal dentin as

separate entities, the contribution of histological variation in the properties of each and the creation of histological structures with characteristic properties such as tissue interfaces in the mineralization front and DEJ area. Based on this model and FTIRI as a technique, analysis of the sequence of events that define dentin biomineralization can be made.

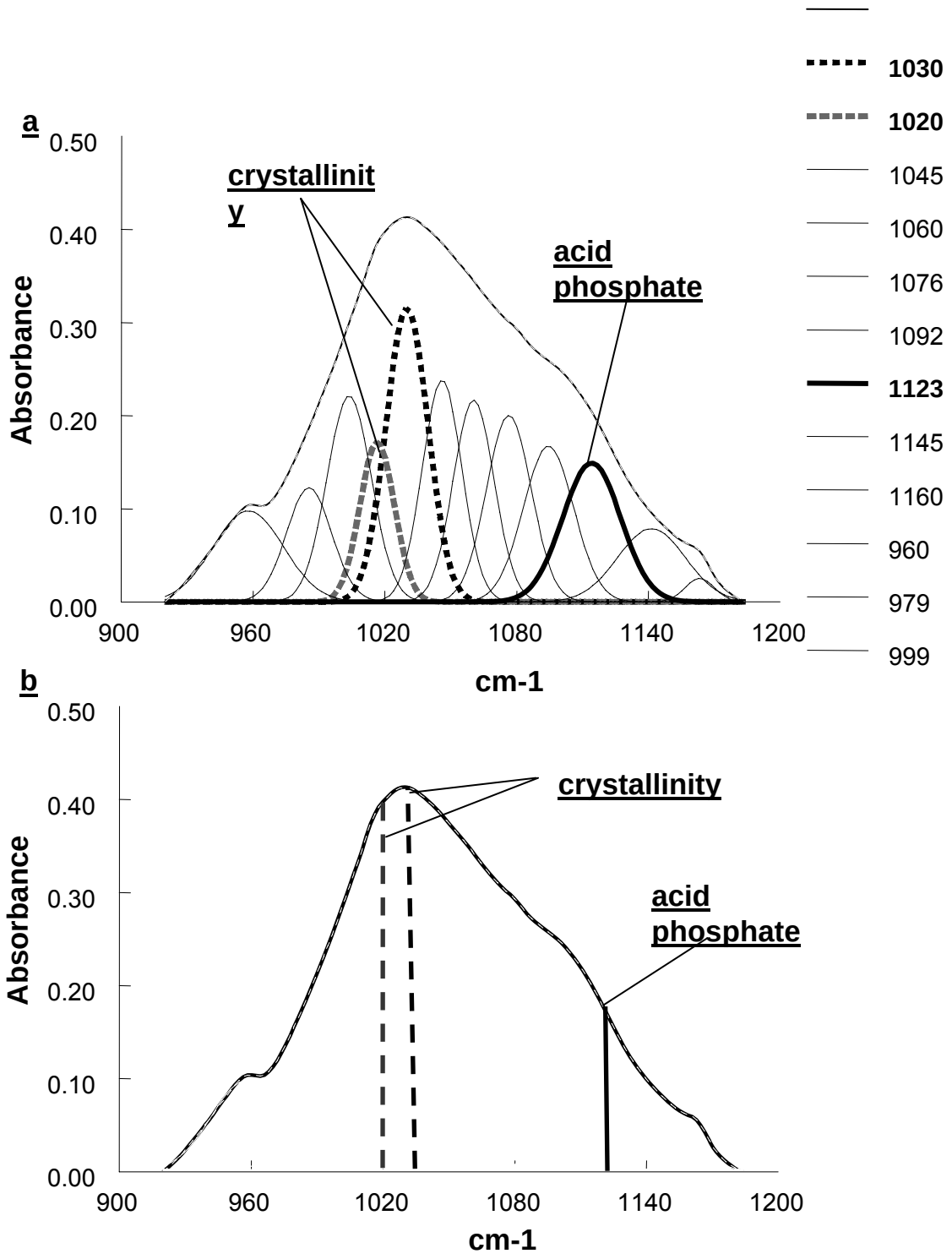

Fig. 2-1 : Representative v_1v_3 phosphate band from dentin spectrum. (a):underlying sub-bands superimposed. 1020, 1030 and 1123 cm^{-1} bands in bold (b): 1020, 1030 and 1023 cm^{-1}as relative peak heights.

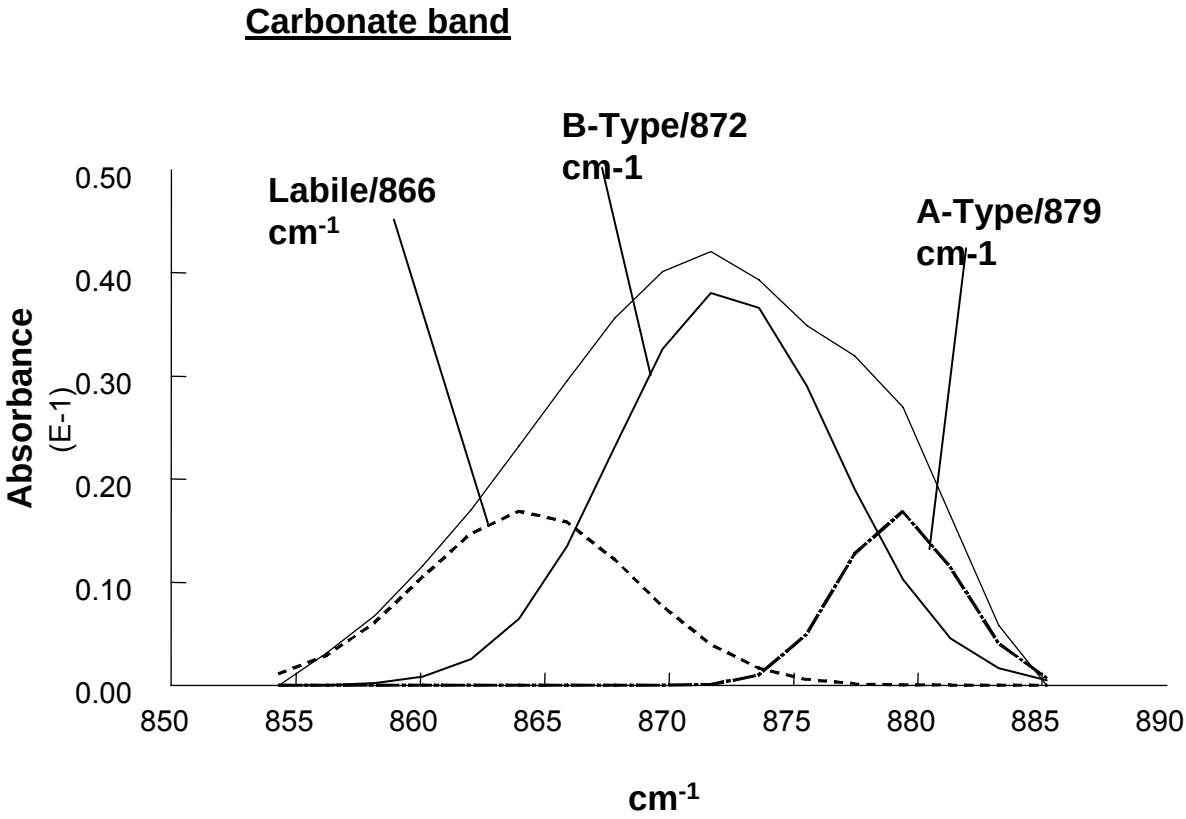

Fig. 2-2 : Representative v_2 carbonate band from dentin spectrum. Labile carbonate, B-type (substituting for PO_4^{3-}) and A-type carbonate (substituting for OH^-) sub-bands as they result from a curve-fitting process are drawn.

(Next page) **Fig.2-3**: Areas analyzed by FTIRI in fetal and mature bovine incisors and superimposed spectra extracted from fetal bovine incisor. (a): Areas analyzed from 3rd trimester I2 developing incisor (b): Areas analyzed from 1 yr-old I4 incisor Young dentin –cervical- and older dentin –mid-crown and incisal- areas are noted. Rectangles indicate areas analyzed. Cervical and incisal areas analyzed as controls also indicated on 1yr-old incisor. (c) Spectra extracted from mantle dentin area of fields analyzed in incisor 1a at various distances from cervix of the tooth (as indicated in 1a). $\nu 1, \nu 3$ PO43+ and Amide I bands noted.

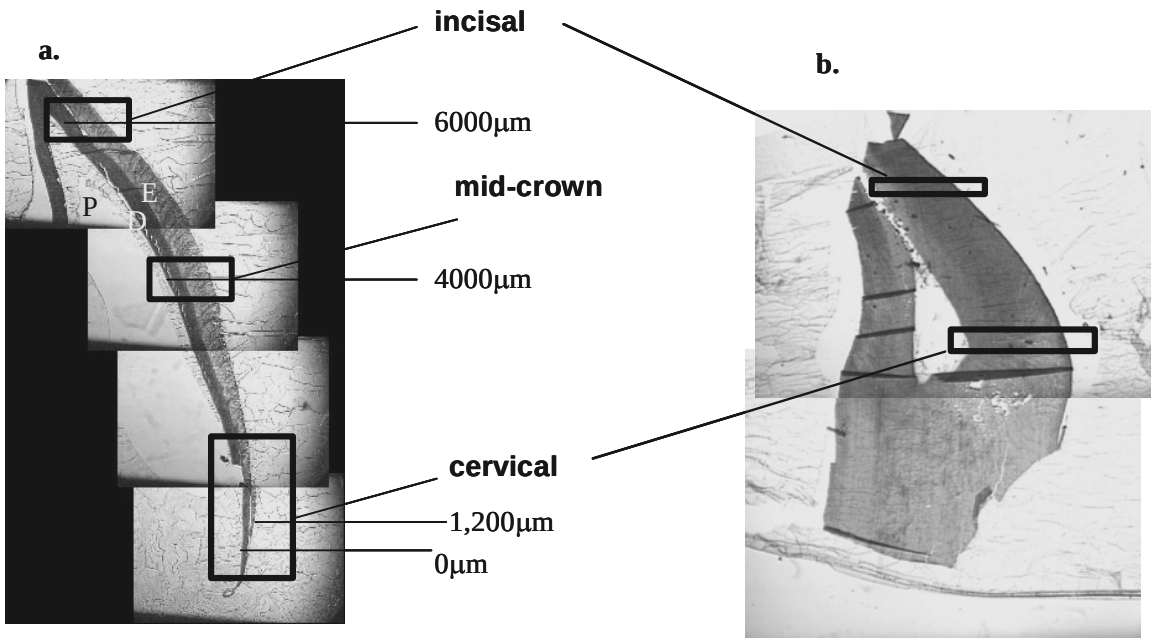
a.
incisal
6000μm
mid-crown
4000μm
cervical
1,200μm
0μm
P
E
D
b.

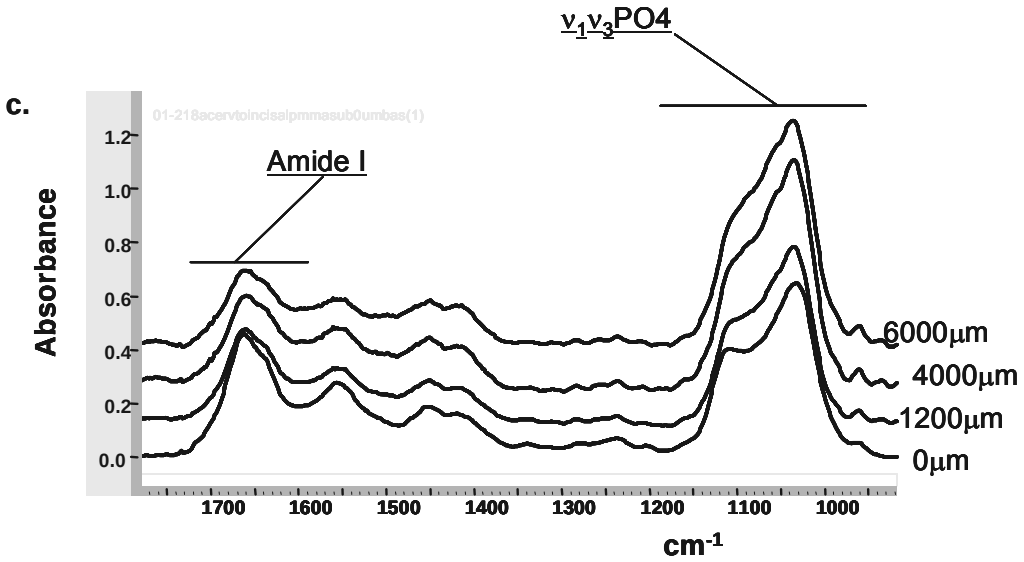
c.
ν1ν3PO4
Amide I
Absorbance
1.2
1.0
0.8
0.6
0.4
0.2
0.0
1700
1600
1500
1400
1300
1200
1100
1000
cm-1
6000μm
4000μm
1200μm
0μm

(Next page) **Fig. 2-4**: FTIR Imaging analysis of 400x400 μm consecutive fields from cervical, mid-crown and incisal parts of fetal calf incisor in Figure 2-3. Composites of (a) actual field optical micrographs (b) mineral:matrix ratio FTIR images (c) crystallinity FTIR images. Distribution of mineral:matrix and crystallinity values along a predentin to enamel line for the field marked with an asterisk is shown in fig. 2-6 a. P=Pulp, D=Dentin, E=Enamel. Bar=1mm.

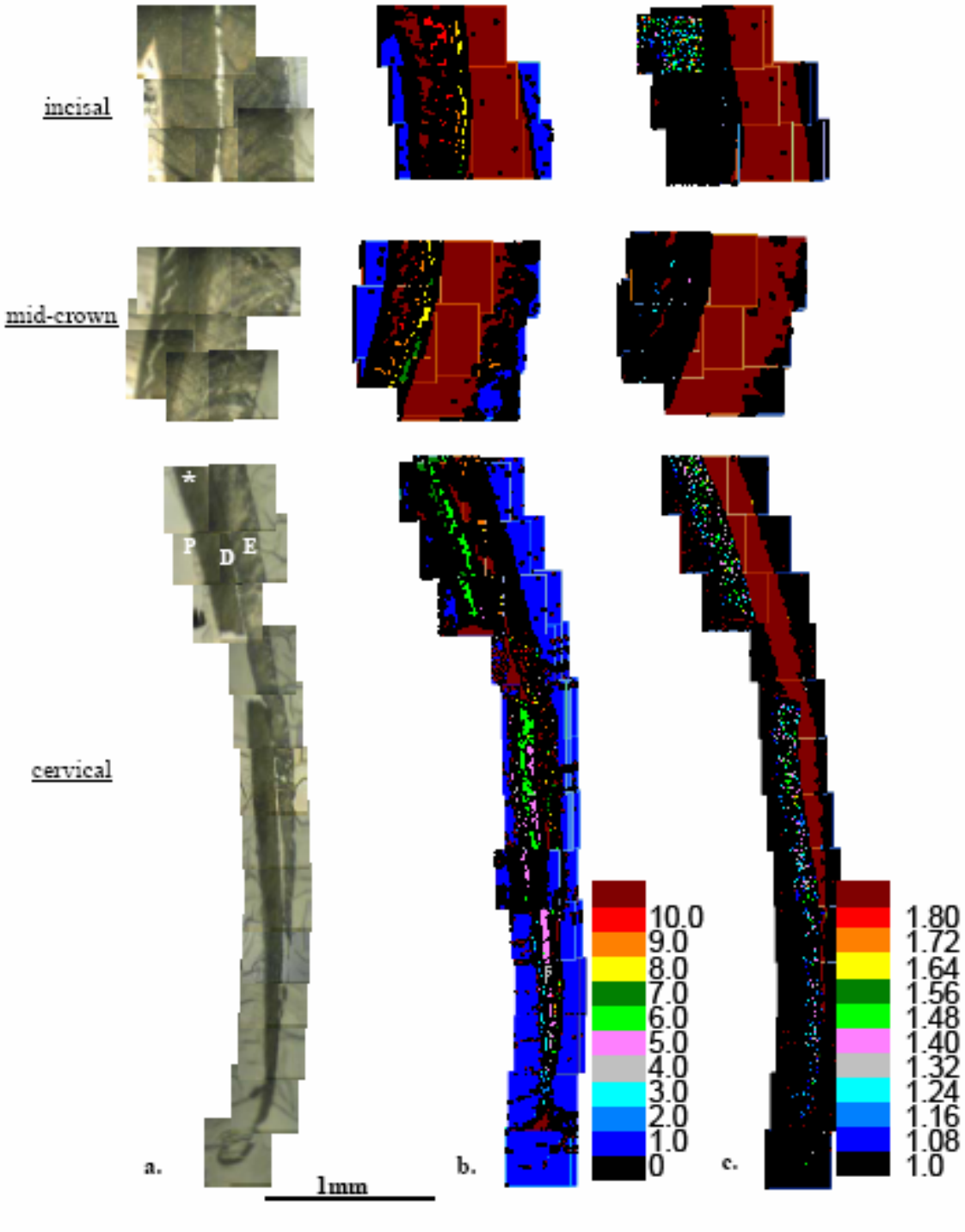
incisal
mid-crown
cervical
*
P
D
E
a.
1mm
b.
10.0
9.0
8.0
7.0
6.0
5.0
4.0
3.0
2.0
1.0
0
c.
1.80
1.72
1.64
1.56
1.48
1.40
1.32
1.24
1.16
1.08
1.0

(Next page) **Fig. 2-5**: FTIR Imaging analysis of 400x400 μm consecutive fields from cervical and incisal parts of 1 year-old bovine incisor in Figure 2-3. (a) optical micrographs (b) mineral:matrix ratio FTIR images (c) crystallinity FTIR images. Distribution of mineral:matrix and crystallinity values along a predentin to dentin line for the field marked with an asterisk is shown in fig. 2-6 b. P=Pulp, D=Dentin. Bar=1mm.

Fig.2-5

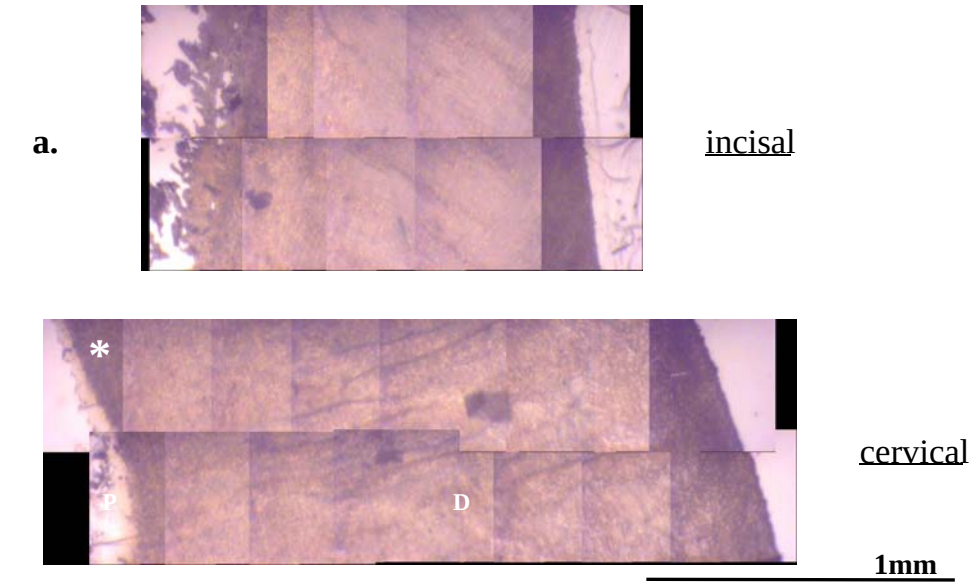
a.
incisal
*
P
D
cervical
1mm

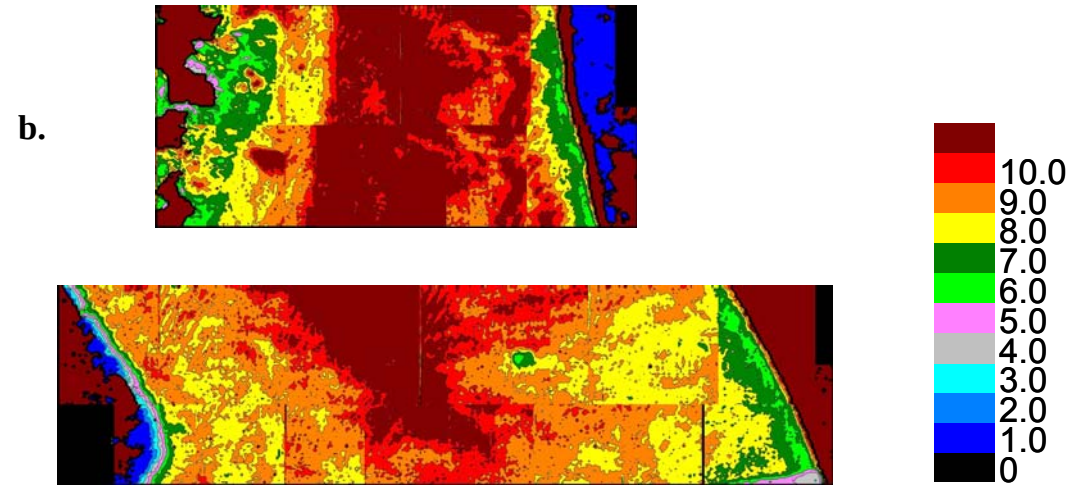
b.
10.0
9.0
8.0
7.0
6.0
5.0
4.0
3.0
2.0
1.0
0

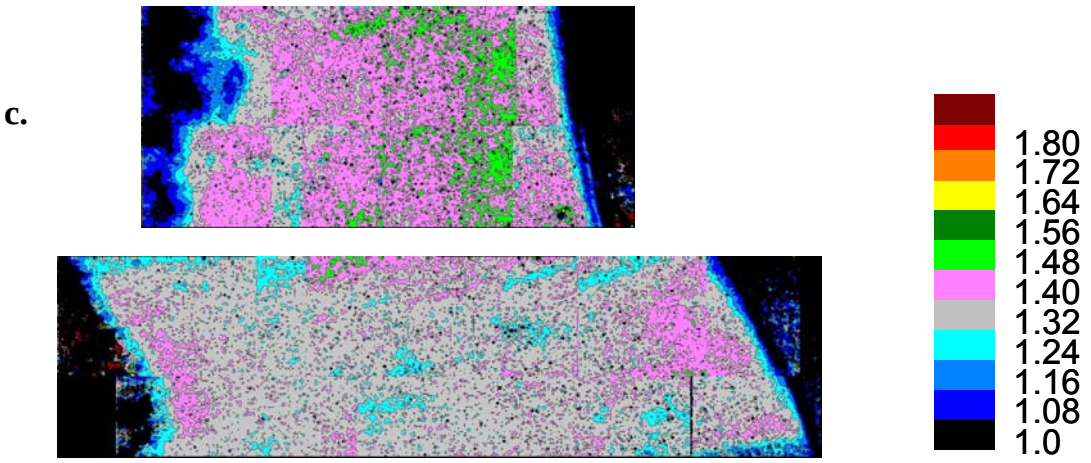
c.
1.80
1.72
1.64
1.56
1.48
1.40
1.32
1.24
1.16
1.08
1.0

(Next page) **Fig. 2-6**: Micrographs of the fields marked with an asterisk in Figures 2-4 a (fetal incisor) and 2-5 a(1 yr-old incisor). Graphs of mineral:matrix and crystallinity values taken from along the lines indicated by the white arrows on these fields are presented next to the respective micrographs.

Fig.2-6

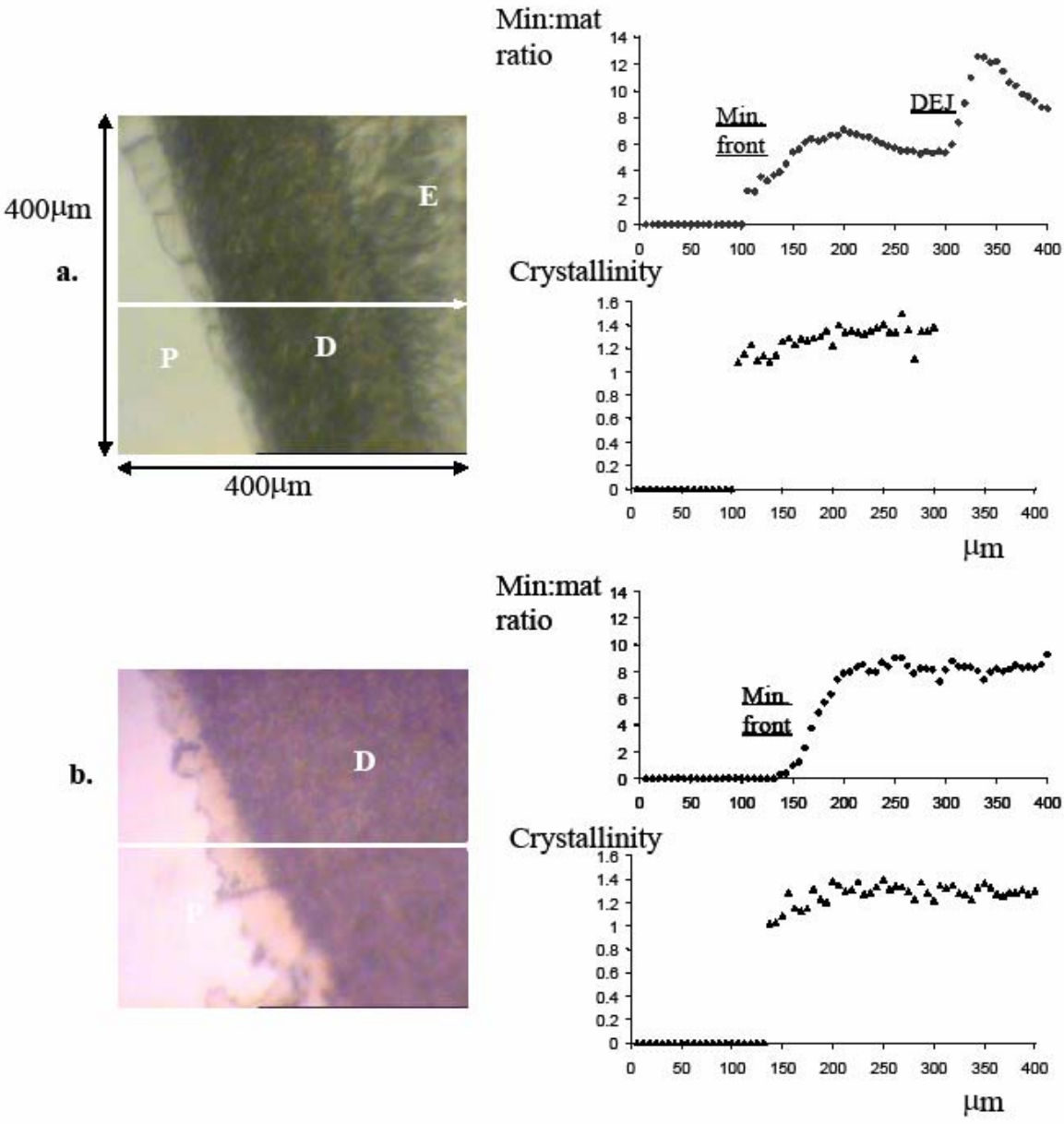
400µm
a.
E
P
D
400µm
Min:mat ratio
Min. front
DEJ
Crystallinity
µm
b.
D
P
Min:mat ratio
Min. front
Crystallinity
µm

Fig.2-6

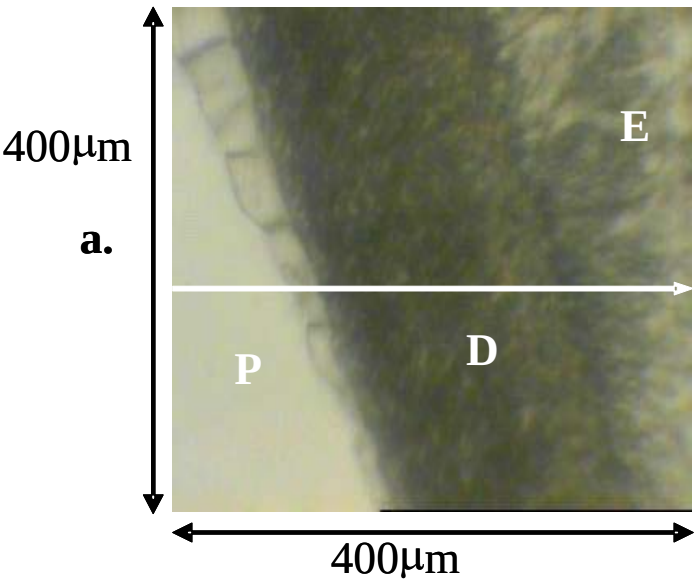
400µm
a.
E
P
D
400µm

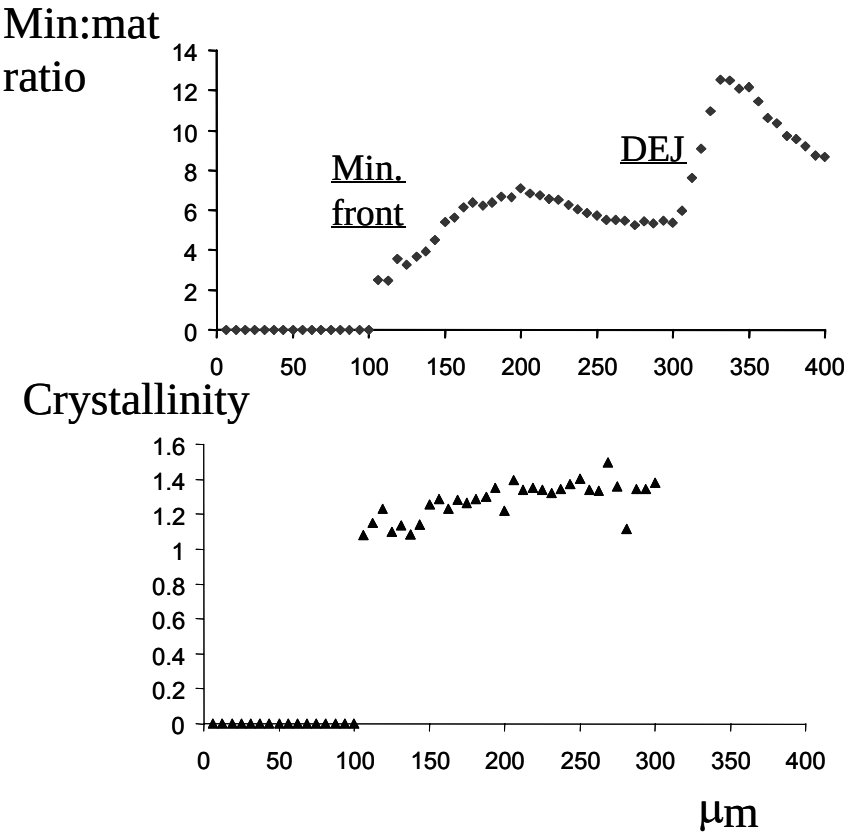
Min:mat ratio
Min. front
DEJ
Crystallinity
µm

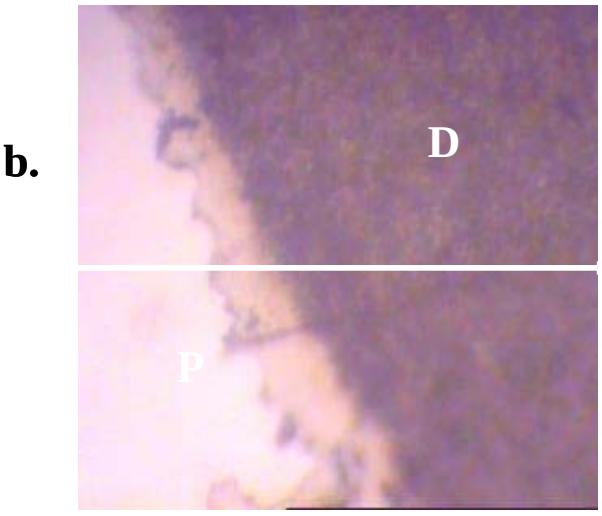
b.
D
P

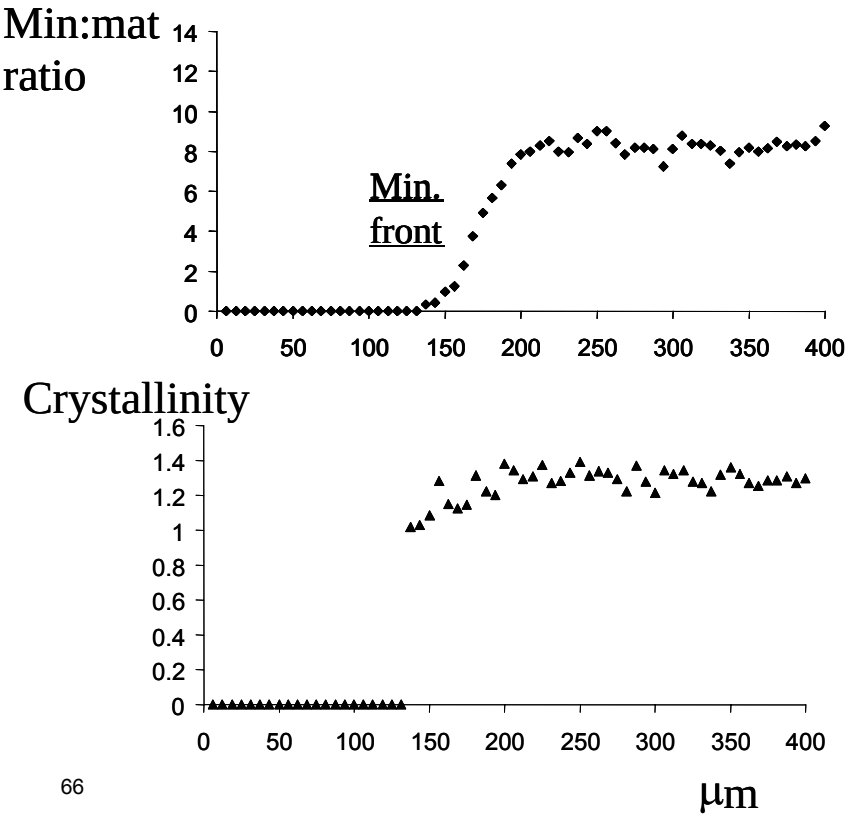
Min:mat ratio
Min. front
Crystallinity
µm

CHAPTER III

CHARACTERIZATION OF MINERAL AND MATRIX CHANGES IN DENTIN : SPECTRAL ANALYSIS

INTRODUCTION

In this chapter, changes in the properties of mantle and circumpulpal dentin compartments are examined in the mineral, through FTIRI results on developing incisor sections, and in the matrix, through FTIR analysis of microdissected mantle and circumpulpal dentin specimens. The basis for use of the developing calf incisors as a model for studying the dentin mineral and matrix maturation was established in Chapter II. In that study, it was shown that dentin mineral properties present a large spatial variability, mostly as a result of a respective histological variability at all developmental stages, when examined from the mineralization front through the DEJ. Mantle and circumpulpal dentin, on the other hand, present distinct mineral, at least, properties at any developmental stage, from the newly laid tissue through final maturation. Also presented was the extensive transition in mineral properties present at the dentinoenamel junction (DEJ), which calls for precise localization of dentin adjacent to DEJ. The results from Chapter II were used for reproducible localization of mantle and circumpulpal dentin immediately adjacent to mantle dentin, to make dentin areas of successive tissue age compared as histologically equivalent as possible.

The purpose of this study was to examine and compare the change in the mineral and matrix properties within the developing mantle and circumpulpal bovine dentin. Mineral density (expressed as mineral:matrix), overall mineral maturity (expressed as crystallinity) , the two major ionic substitutions in the apatite, acidic phosphate and carbonate substitution, and type of carbonate substitution are examined. In the part of spectral analysis of microdissected dentin samples, the relative water content of the developing tissue and conformation of the dentin matrix are also examined.

METHODS AND MATERIALS

Specimen preparation: In this study, twelve (left and right) lateral incisors 3 (I3) from six 3rd trimester fetal calves were used for FTIRI analysis. The samples were processed for histology, embedded in PMMA and 2μm sections cut as described in Chapter II.

FTIRI-data analysis: FTIRI analysis data were obtained using a different FTIR Imaging system (Spectrum Spotlight Imaging System, Perkin-Elmer Instruments, Shelton, CT) than that described previously, with capability for scanning of continuous areas and shorter scanning times. A different from the one used in Chapter II data processing software, with capability of spatial and spectral masking, was also used here. The FTIRI instrument consists of a continuous scan interferometer interfaced to a MCT (Mercury-Cadmium-Telluride) focal plane 2x8 array detector, yielding 16 spectra at a time. There is a one-to-one optical mapping correspondence between each detector element and

a ~ 7 x 7μm spot within the tissue which is located at the focal plane of an IR microscope. Cervical, middle-crown and incisal areas (see below) were analyzed with a 4cm^{-1} spectral resolution. A continuous segment of dentin from the cervical 4,000μm of the crown was analyzed and the rest of the crowns were scanned in non-continuous segments (middle and incisal). At all locations, the whole DEJ and at least 300μm of dentin adjacent to DEJ were scanned. Spectra were transferred to yield images corresponding to infrared band areas, peak height ratios and integrated area ratios by a combination of instrument software and ISYS chemical imaging software (v 3.1, Spectral Dimensions Inc., Olney, MD, USA). Background spectra were collected under identical conditions from the same BaF_2 windows. After acquisition, spectra were truncated to allow analysis of the region of interest (2000-700 cm^{-1}), zero-corrected for the baseline and the spectral contribution of PMMA embedding media was subtracted using ISYS software.

FTIRI- data processing: The FTIRI data processing general methodology has been described in Chapter II. Successive maturation stage areas for mantle and circumpulpal dentin were identified, from each one of which pooled spectra were extracted (shown schematically on an analyzed incisor micrograph in figure 3-2). Identification of these areas was done as follows: after processing of the FTIRI files as described in Chapter II, the DEJ was defined as the point of transition to progressively higher mineral: matrix values based on the mineral:matrix images already masked (non-tissue pixels in each analyzed field excluded from the image). The DEJ in the mineral: matrix images was typically

represented by a ~35μm, or ~5 pixels (see also discussion in Chapter II,) wide transition from the low mineral:matrix values characteristic for the developing and mature mantle dentin to the very high values characteristic for enamel. For analysis of mantle dentin, spectra were pooled and extracted in the selected maturation stages from the approximately 30μm of mantle dentin closest to the beginning of the DEJ. For circumpulpal dentin analysis, the equivalent area was dentin located from 100μm to135μm (35μm wide areas) from the beginning of DEJ in the same maturation stages (cervical to incisal locations). The length of these mantle and circumpulpal areas for analysis was approximately 130μm in a cervical to incisal direction for each maturation point, thus making a total of ~100 pixels at each mantle or circumpulpal dentin observation. The selection of the above analyzed dentin locations for every maturation stage was based on the imaging results from all the incisors. These results indicated an average approximately 100μm width for mantle dentin in lateral incisors I3, based on distribution of values in mineral: matrix and mineral crystallinity with respect to the rest of dentin and that was approximately the same width found for mantle dentin from the results of Chapter II. The area analyzed for circumpulpal dentin was that immediately adjacent to mantle dentin. This area was selected so that it histologically corresponded to the mantle dentin analyzed as close as possible, while including many maturation time points (starting the analysis as close to the cervix of the crown as possible). Twelve to fifteen points in a cervical to incisal direction on the crown were typically chosen for each incisor, starting at the most cervical point where enamel was present and proceeding to the incisal end,

collecting data every 200-400μm for the 1,000μm of the cervical end of the crown, then every 500-1,000μm towards the incisal edge for the rest of the analyzed cervical field. Relatively more areas were selected for spectral analysis in the cervical region, as in a pilot study it was found that the biggest changes in mineral properties occur during the initial stages in maturation. If the predetermined locations were not available, the closest locations for which data was available were used. In case of local section defects, the closest intact areas also substituted for designated mantle and circumpulpal areas. The final results for each analyzed parameter were grouped at 200μm regular intervals for the cervical 1,000μm and at 500μm after that and were plotted as means and standard deviations of values for every parameter at the designated distances from the cervix of the tooth.

In most of the sections, on the cervical ends of the crown mineralization had just started for dentin and enamel was still in the secretory or early maturation stage, where matrix produced is substantial and has not been yet degraded and mineral density is low. As a result, the DEJ was not readily identifiable on the mineral: matrix images in these areas and, to address this, a different spectroscopic parameter was developed from the ratio of the 1650 and 1660cm^{-1} relative peak heights in the Amide I band for locating the DEJ. That parameter is based on the fact that the 1660cm^{-1} represents a collagen triple helix peak, while amelogenins, a main group (90% of the matrix) of similar proteins formed during enamel development, form a characteristic α-helix (Krishnaraju and Scheyer, 2003) which generate a different peak occurring at 1650cm^{-1}. Identification of

early enamel using the 1650:1660 cm^{-1} spectroscopic ratio was validated by SEM backscattered imaging on blocks from analyzed sections in a pilot part. For the SEM analysis, the PMMA blocks were platinum-coated and a Quanta 6000 SEM unit (FEI, Peabody, MA) was used. Images of this ratio and mineral: matrix images from cervical areas of one incisor section were compared to scanning electron microscopy images of the selected incisors embedded in PMMA. After they were identified, an outline of dentin areas to be analyzed was generated on the mineral: matrix and 1650:1660 cm^{-1} images through a spatial masking function. A single spectrum was then produced as a product of addition of all the spectra from the ~100 pixels in the area and was exported for processing into a second spectroscopic analysis software (Win IR-Pro 3.1, Digilab, MA). The spectroscopic parameters examined were: mineral:matrix ratios, crystallinity (acquired as described in Chapter II) and relative acidic phosphate content of the mineral defined as relative peak height at 1123cm^{-1}: peak height of v_1v_3 PO_4^{3-} band at ~1040cm^{-1} (Paschalis et al, 1996; Rey et al, 1991). A separate set of thicker (5μm) sections from the same left incisors were used for analysis of the carbonate band, as the latter is relatively weaker than the v_1v_3 PO_4^{3-} band and the S/N had to be enhanced in the young parts of the mineral. The v_2 carbonate band consists of 3 sub-bands, corresponding to different types of carbonate substitution. These sub-bands within the broader carbonate spectral envelope were shown in Figure 2-2. Analysis of carbonate data was conducted as described by Rey et al (Rey et al, 1989). Parameters analyzed were as follows: relative carbonate mineral content defined as integrated area of $v_2CO_3^{2-}$:

integrated v_1v_3 PO_4^{3-} area ratio, relative type A carbonate substitution defined as the 879/871cm^{-1} relative peak heights ratio, relative labile carbonate substitution defined as the 866/871cm^{-1} relative peak height ratio, where the 871 cm-1 band corresponds to B type carbonate substitution.

Results for each parameter analyzed as described above were transferred into a Microsoft Excel datasheet and expressed as means and standard deviations from all left or right incisors of the animals analyzed. One of the right incisor samples was lost during processing, as a result of which a left incisor analyzed was unpaired. Results from a second right incisor were also discarded, after analysis indicated contamination with organic matter probably during processing. Results are shown only for left incisors analyzed and the correlation of those to the results from their right counterparts is discussed.

Microdissected dentin specimens/ spectral analysis: In a second part of this study, nondecalcified mantle and circumpulpal dentin samples of progressive tissue age were microdissected from four left and right I3 incisors from 2 fetal (3rd trimester of gestation) calves. The microdissected specimens were analyzed by diffuse reflectance (single transmission spectrum of the sample ground made into a pellet with infrared inactive KBr) FTIR. Each one of the animals provided the samples for either mantle or circumpulpal dentin. The incisors were again kept at -80°C until dissected. The microdissected dentin pieces of either mantle or circumpulpal dentin from a right incisor were combined with the respective microdissected pieces from the left incisor of the same animal, again to provide adequate S/N levels in young dentin specimens, where mineral was less dense.

Dissection was performed as follows: Incisors were mounted to a holder using a dental thermoplastic materialand sectioned by a diamond wafer disc on an automated sectioning device (Isomet 5000, Buehler, Germany), under copious irrigation with water. Approximately 800μm thick sections were acquired by serial sectioning of incisors perpendicularly to the long axis of the crown (shown on a 3D reconstruction of a microcomputing tomography analysis of an incisor in Figure 3-9 a), starting by the most cervical part of the crown and proceeding to the incisal. A total of 9 sections were acquired per incisor. The microdissection of dentin specimens was subsequently performed on the sections under the dissection microscope using scalpel blades. After removal of the enamel layer on every section, the borders of dentin to be dissected were marked by pencil on the section surface. Mantle dentin specimens were acquired from the ~ 80μm next to the DEJ, while circumpulpal specimens came from a ~80μm zone located 20-40μm away from mantle dentin (Figure 3-9 b). These locations for mantle and circumpulpal dentin on I3 incisors were defined by the FTIRI results in the present study and Chapter II. Every microdissected specimen provided 0.2-0.7 mgs of tissue. Immediately after dissection, the dentin specimens were homogenized with 200mg of KBr in a Spex-Mill microchamber cooled by liquid N_2 and pressed into pellets which were analyzed by FTIR. A Nicolet FT-IR 4700 (Thermo Corporation, Madison, WI) spectrometer was used for analysis in the 4000 cm^{-1} to 400 cm^{-1} region, with a 4 cm^{-1} resolution and 256 co-additions. The pellets containing the specimens were subsequently stored in a dessicator at 4°C overnight, after which spectra were acquired again. A third FTIR analysis of the

same specimen pellets was performed after overnight heating at 105°C for complete dehydration of the samples. The spectra were analyzed using spectroscopic software (Win IR-Pro 3.1, Digilab, MA), after spectral subtraction of water vapor and baselining. The integrated area and spectral contour for a broad band in the 2500-3500 cm^{-1} region and the spectral contour of the amide I band (1580-1725cm^{-1}) were compared after normalization for the amide I band, which represents the total amount of matrix.

RESULTS

Figure 3-1 shows one of the incisors used in a pilot part for validation of the 1650:1660 cm^{-1} relative peak heights ratio to differentiate between young enamel and dentin in the cervical area. The mineral:matrix images are shown (a), as image of the whole cervical area and of the most cervical part (insert) that was also analyzed by SEM (in c). While enamel in the rest of the crown presents characteristically high mineral:matrix values, young enamel (the approximately 500μm most cervical part) cannot be differentiated well from the adjacent dentin. On the 1650:1660 cm^{-1} ratio image (b) enamel is readily identifiable, extending down to the cervical loop. Higher magnification of the small area pointed by the arrow on c is shown on d, with dentin and enamel marked.

The distribution of mineral: matrix values in the developing crown of the left incisors, from mantle and circumpulpal dentin data points, is shown in Figure 3-3. Means and standard deviations are shown for respective distances from the incisor cervix of areas (where standard deviation values are not visible, they are

smaller than the data points plotted). The total number of observations was n=221 for the 6 left incisors analyzed and n=109 for the 4 right incisors analyzed. Similar distributions are shown for crystallinity (Figure 3-4), relative acidic phosphate content (Figure 3-5), relative carbonate in apatite content (Figure 3-6), type A/type B carbonate substitution (Figure 3-7) and relative amount of labile carbonate (Figure 3-8). All the results are reported as ratios.

The pattern of spectral changes observed from the microdissected dentin specimens analysis did not present a difference between mantle and circumpulpal dentin, at least from the one series of specimens, which was examined for each. Spectral results from only mantle dentin specimens is shown here. Representative spectra from microdissected mantle dentin specimens located at the distances from the cervix noted are shown in Figure 3-10a. The scale for each spectrum is adjusted so that the Amide I areas in all 3 spectra are equal. The mineral:matrix ratio increases from dentin located at the tooth cervix to the most incisally located (7200 μm) dentin, in a way parallel to that observed in the FTIRI analysis described above. The broad band between 2500 and 3500 cm^{-1} area decreases in area from the dentin dissected at 0μm to dentin dissected after 3600 μm, after which it remains constant. The scale of the spectra has been adjusted so that all 3 spectra present a similar peak height, to facilitate comparison. Amide I areas from the spectra shown in Figure 3-10 a are superimposed and shown in Figure 3-10 b. In the spectra from dentin located close to the cervix, in addition to the 1660 cm^{-1} characteristic peak of carbonyl groups in a collagen triple helical structure, there is a prominent peak around

1640 cm^{-1}, which forms an overall less sharp contour to the Amide I band. This 1640m cm^{-1} peak is gradually eliminated in spectra from the more incisally located dentin specimens, until the Amide I peak becomes very well defined around 1660 cm^{-1} in the most incisally located specimens. Spectra from the dentin specimen dissected at 800μm (most cervical section) before and after heating at 105° C are shown in Figure 3-11. The area of the 2,500-3,500 cm^{-1} band greatly decreases after dehydration, indicating that the difference observed in this band between cervical and more mature dentin spectra is due mainly to a decrease in water content.

DISCUSSION

The results for all the mineral properties studied here were examined separately as obtained from the left I3 incisors and from their right counterparts. Similar patterns in the distribution of the respective values (as means and standard deviations) were found between left and right incisors as a group for each one of these spectroscopic parameters corresponding to the mineral properties. On the other hand, comparative analysis of the mineral:matrix distribution in left and right incisors of the same animal did not show a high correlation in the respective patterns between counterparts. In most cases, the correlation in distribution of any spectroscopic parameter between a left and a right incisor of the same animal was not higher than the correlation between two random samples. This suggests that factors other than developmental variability between animals are equally responsible for variability observed in the results

from different samples. Differences in orientation of the sectioning plane on the developing crown can be expected to be a factor contributing to variability in distribution within dentin for the spectroscopic parameters examined. Sectioning orientation-related variability would affect similar analyses equally on mature teeth. In mature mouse molars, it has been observed by microcomputed tomography (unpublished results) that very different levels and patterns of distribution of mineral density could be acquired at different planes of analysis. Another reason for variability in the results is also the lack of precise formation and eruption stage of the crown among the different animals examined. Although all the animals analyzed were from the early third trimester of gestation, selected according to their crowns being formed to the same extent and one tooth type was analyzed, the developmental stage of dentin on their crown or their final crown length could not be exactly standardized. The length of teeth of the same type differs between animals and distance from cervix was selected by convention to represent tissue age in this study, although it cannot be exactly reproducible from one incisor to the other. Representation of dentin tissue age by mineral:matrix value within mantle or circumpulpal dentin of the same tooth, as was attempted in a pilot study, showed a poorer correlation with changes in the properties examined. This was possibly due to the fact that overall ranges of mineral density between different teeth can be different and/or the ambiguity involved in selection of image pixels next to the DEJ that make up mantle dentin.

The results for mineral:matrix show that while mineral density values in mantle dentin are initially similar to, or even a little greater than, those in the

circumpulpal dentin that is immediately adjacent to it, they steadily become 15-20% lower. These mineral density values in mantle and circumpulpal dentin continue increasing always on parallel levels, presenting at the same time some fluctuation along the crown, that seems to affect both dentin compartments the same. Finally these values reach a plateau where there is very little or no increase close to the incisal edge. As shown on the graphs, data points for circumpulpal dentin start higher up from the cervix of the incisor, at approximately 800μm, as in the very young dentin areas a strip of circumpulpal dentin wide enough for analysis has not been yet formed. As discussed already in Chapter II, it is possible that close to the DEJ a terminal branching of the dentinal tubules creates a higher relative amount of matrix, further adding to the lower mineral:matrix due to the inherent lower extent of mineralization in mantle dentin. Also contributing to the lower mineral density observed in mantle dentin may be a decrease in the relative density of the hypermineralized peritubular dentin, although the mineral density decrease observed is much steeper than could be explained by the difference in the relative density of peritubular dentin alone. The fluctuations in the increase in mineral density along the crown may be explained by the wavy distribution of dentinal tubules within the crown, which in a single sectioning plane might create alternating areas of higher and lower density of dentinal tubules and consequently peritubular:intertubular dentin ratio, as just discussed. Alternatively, masses of hypomineralized interglobular dentin presenting periodically on the analyzed plane within the crown could also contribute to these fluctuations observed. To the best of the author's knowledge,

no similar mineral density data in dentin to which the results of the present study could be compared exists in the literature. Similar quantitative reports on mineral density changes have been published on human cortical, trabecular and osteonal bone mineral maturation using FTIR microspectroscopy (Paschalis et al, 1996; Paschalis et al, 1997). For the osteonal bone, a much lower range of changes in the mineral:matrix values (approximately 25%)was described from the center of the osteon (youngest bone) to its periphery (most mature part), probably as a result of bone remodeling that does not allow for a tissue age range as wide as in dentin. Data from lamellar cortical and trabecular bone cannot be directly compared to the present data, due to its anatomical complexity.

Whereas mineral density expressed as mineral:matrix is analyzed from the integrated areas of the and the Amide I bands of the FTIRI results, crystallinity of the mineral and relative acidic phosphate content of the hydroxyapatite are spectral parameters represented by subbands within the broad v_1,v_3 PO_4^{3-} band. For quantitative determination of variations in the broad contour of poorly crystalline hydroxyapatite (as dentin hydroxyapatite is) data reduction techniques have been used, such as Fourier self-deconvolution (Rey et al, 1991; Rey et al, 1990) and curve fitting (Pleshko et al, 1991). Nevertheless, there is a certain amount of subjectivity involved with each one. Fourier self deconvolution requires a subjective choice of line narrowing parameters such as the full width at half height of the underlying bands. Curve fitting is tedious and requires the input of several parameters subjective such as the position, number and shape of the underlying bands. In this study, crystallinity was calculated as the ratio of the

relative peak heights at 1030 and 1020 cm^{-1}, which arise from stoichiometric and non-stoichiometric, HPO_4^{2-} and CO_3^{2-} containing apatite environments, respectively (Rey et al, 1991; Paschalis et al, 1996; Paschalis et al, 1997). This relative peak height ratio has also been shown to be correlated with results using a curve fitting process in bone (Boskey et al, 2003). In a similar way, the relative HPO_4^{2-} content in hydroxyapatite was calculated as the ratio of relative peak heights at 1123 cm^{-1} (Rey et al, 1991; Gadaleta et al, 1996; Paschalis et al, 1996) and the overall v_1,v_3 PO_4^{3-} band peak height. It has to be noted that the relative peak heights analysis is semi-quantitative. During maturation there is an increase in crystallinity up to some point (approximately 5,000 μm from the cervix in our samples), after which the crystallinity values decrease again (Figure 3-4). A very similar to that described for mineral:matrix pattern of changes was observed between mantle and circumpulpal dentin, with circumpulpal dentin values being initially lower than the respective in mantle dentin, but soon becoming steadily higher. The final decrease in the crystallinity values can be explained by a great amount of peritubular dentin forming late in dentin maturation, if indeed peritubular dentin mineral is less stoichiometric than intertubular dentin mineral. While these changes in the semi-quantitative 1030/1020 cm^{-1} ratio analysis are relatively small (approximately 10%), the real changes in crystallinity values may be much greater. A consistent trend of decrease in acidic phosphate content during maturation was noted, although in this case the difference between mantle and circumpulpal dentin levels was much smaller (Figure 3-5). As with crystallinity, these changes in the relative

acidic phosphate content happen over a wide time span (a long distance from the cervix) and after a plateau the acidic phosphate values slightly raise again towards the incisal edge, probably because of late formation of peritubular dentin, as just discussed. In the Magne et al FTIR microscopy study of dentin maturation (Magne et al, 2001), crystallinity was analyzed using the same 1030/1020 relative peak heights ratio that was used here. It was reported that dentin at the mineralization front, which was considered to constitute the earliest formed dentin, is poorly crystalline but very soon mineral crystals reach their final crystallinity values and do not evolve more. The present results did not corrobate those observations, as crystallinity seems to be increasing during a wide tissue age span. There are a number of differences in methodology between the present and the Magne et al study, as no distinction between mantle and circumpulpal dentin was made in the latter, the dentin areas compared were not histologically equivalent and no numerical data was given. Additionally, the observations in the Magne et al study were made on mature samples, in which hydroxyapatite crystals even adjacent to the mineralization front had probably matured enough to present crystallinity levels similar to those of dentin that had been laid down earlier. The same study reported decrease of the HPO_4^{2-} during maturation in dentin, although the rate at which this decrease occurs was not defined. Several studies of maturation in synthetic apatites (Gadaleta et al, 1996) or bone (Bonar et al, 1983; Rey et al, 1991; Paschalis et al 1996; Paschalis et al, 1997) also showed mineral crystallinity analyzed by either X-ray diffraction or spectroscopically increasing with tissue age. The existing quantitative data in

osteonal and lamellar bone (Paschalis at al, 1996; Paschalis et al, 1997) suggest that the overall increase in mineral crystallinity is much higher than the one observed here. The decrease in HPO_4^{2-} relative content has also been reported in bone (Bonar et al 1983; Roufosse et al, 1984; Rey et al, 1995). Ionic substitutions, such as the HPO_4^{2-}, are very important in determining the reactivity and physical properties of hydroxyapatite. In a study where infrared spectroscopy and X-ray diffraction were used to analyze hydroxyapatite heated at different temperatures (Young and Holcomb, 1984) it was concluded that HPO_4^{2-} expands the a axis at a rate of ~0.0015Å/ wt%, along with structural H_2O. Carbonate substitution for phosphate, which is the other major ionic substitution in biological apatites, has been shown to induce crystal disorder, even in well-crystallized hydroxyapatites (Le Geros et al, 1968). Findings of the present study on carbonate substitution are discussed below.

Because the main carbonate band ($v_2CO_3^{2-}$) is relatively weak in the early mineral, study of the carbonate substitution was conducted on thick (5μm) sections, which are unsuitable for study of the v_1v_3 PO_4^{3-} band, the main band from which results for mineral were acquired. While the spectral contour of the v_1v_3 PO_4^{3-} band on the thick sections is disrupted in the mature parts of the dentin sections, because the high intensities supersaturate the detector, the integrated area of the band can be still used for normalization of the carbonate content results, as found in a pilot study. From our findings, no significant change was found in the relative carbonate amount (carbonate:mineral) in either mantle or circumpulpal dentin during maturation of the tissue. The levels of carbonate

substitution between mantle and circumpulpal dentin are very similar, showing a slight trend for higher carbonate substitution during later stages of maturation in mantle dentin (Figure 3-6). Type of substitution also does not show to change between A and B types during dentin maturation (Figure 3-7). A type substitution was, nevertheless, somewhat higher in circumpulpal dentin compared to mantle dentin. No significant changes were observed, as well, in the relative presence of labile carbonate (Figure 3-8). The spectral assignments previously described (Rey et al, 1989) were used for study of the type of substitution: a band at 871cm-1 has been assigned to carbonate ions located in PO_4^{3-} sites (type A substitution), at 878cm^{-1} in OH^- sites (type B) and a component at 866 cm^{-1} has been assigned to a labile carbonate environment. The relative peak height ratios 879cm^{-1}/871cm^{-1} and 866cm^{-1}/871cm^{-1} were used here for analysis of relative changes in type of substitution. Changes in the relative amount of carbonate and the type of carbonate substitution in the nonstoichiometric apatite during maturation has been a controversial issue. The average content for carbonate in dentin has been estimated by gravimetry (expressed as carbonate) to be on very similar levels to that of bone, of the order of 3-4% (Posner AS and Tannenbaum PJ, 1984). In a study of mineral properties in density fractionated dentin (Coklica V et al, 1969), a slight increase of CO_2 (ranging from 2.99% to 3.21%), which was produced by the existing mineral carbonate and measured by microdiffusion as percent of dentin dry weight was reported. In the one existing study on dentin maturation, Magne et al (Magne et al, 2001) reported no change in the relative amount of carbonate and no indications of rearrangement of carbonate ions in A

or B sites, from spectral analysis. For the reasons discussed above, these results cannot be directly compared to the present results**.** More relevant studies have been conducted on bone. Paschalis et al, using FTIR microspectroscopy, reported a decrease of carbonate relative mineral content with maturation of human osteonal bone from the center to the periphery of the osteon, which represented a similar change with tissue maturation. The overall drop in the CO_3^{2-}/PO_4^{3-} ratio was estimated to be 20-30% from the youngest to the most mature mineral in the osteon. In the same study, changes of the carbonate environment with advancing tissue age were shown to be a decrease of the labile carbonate, slight decrease in Type A and slight increase in Type B carbonate. In contrast to those results, in another study of bone mineral maturation (Rey et al, 1991), an increase of the total carbonate content with increasing bone age was found. In this last study, bones samples of different tissue age were acquired by density fractionation of embryonic bone and were analyzed by spectroscopy.

In the second part of this study, spectral analysis of microdissected dentin specimens was undertaken in an effort to characterize matrix proteins in a native state and other than proteins matrix groups that are likely to be partially or completely lost during processing for embedding and sectioning of the tissue. It has been previously observed that chemical processing of tissues for microscopy incurs the risk of artifacts, such as extraction, displacement, condensation or denaturation of matrix components (reviewed in McKee and Nanci, 1995). The organic solvents applied and the dehydration that has to occur in order for the specimens to be infiltrated by the resin result in loss of chemical groups, such as

water and lipids, that are part of the analysis. Also, because only partial fixation of tissues was used here in order to avoid spectral artifacts from standard methods of fixation (Aparicio et al, 2002), the native state of matrix proteins under analysis might have been compromised. While determination of the relative matrix content, as performed in the last and the present chapters, is not likely to be affected by tissue processing, spectral analysis of microdissected mantle and circumpulpal dentin specimens was needed for analysis of proteins and the non-proteinaceous matrix components of dentin. Water was analyzed from the broad band between 2500 cm^{-1} and 3500cm^{-1}. The OH- stretching in water is a major component of this band, centered at 3420cm-1, while two other components of the same broad band are amide A and B (at 3325 and 3095 cm^{-1}, respectively), 2 bands that arise from molecular vibrations within the matrix proteins (Doyle et al, 1975). The latter bands are thought to originate in a, so called, Fermi resonance between the NH-stretching frequency and an overtone of the amide II (see below) band. As it can be seen in Figure 3-10 a, the 2500–3500cm^{-1} area decreases with the progress of maturation, mainly within the first ~3 of total 9 sections. This agrees with the hypothesis that water is being lost with the apposition of mineral crystals onto the collagen gap zones and, later, between the collagen fibrils. This decrease can be interpreted to loss of water mainly, as the great decrease in area of the same band is observed after dehydration of the matrix. The water associated with proteins is generally thought to be consisting of a structural (cannot be removed without destruction of the protein), strongly bound and free fraction. On an average, water has been

calculated to account for 8% to 16% of dentin, on an air-dried basis, and can be removed by heating to 120ºC (Wetherell and Robinson, 1973). Under the present conditions, with acquisition of spectra from freshly dissected specimens all the structural and strongly bound and part of the free water must have been preserved. In the Magne et al study on dentin maturation (Magne et al, 2001), the same conclusion was reached, although the dentin analyzed had previously been dehydrated and the total amount of water may have been underestimated. The main protein bands that are used for conformational analysis of the matrix are amide I (mainly C=O stretching, 1580-1725 cm-1) and amide II (mixed C-N stretching and N-H bending, 1500-1600cm-1) (Doyle et al, 1975). In the amide I region, which is most useful for peptide structural analysis (Haris and Chapman, 1995), collagen, as well as synthetic triple helical polypeptides, has a characteristic peak around 1660cm^{-1}. Collagen, as discussed in Chapter I, makes up approx. 90% of the matrix weight on an average and can be expected to be predominantly represented in the C=O stretch vibrational mode. Hydrogen bonding and the coupling between transition dipoles are the most important factors in conformational sensitivity of the amide I band (Haris and Chapman, 1995). In our results, the amide I peak from early dentin (up to the 2nd or 3rd section out of 9) presents a pronounced broadening towards much lower wavelengths, to 1635-1640cm^{-1} region. This is an area characteristic for a non-collagen secondary structure, namely the β-sheet structure (Haris and Chapman, 1995). That must mean that either a non-collagen matrix group is present early in mineralization, that is degraded later or the collagen itself has a very different

conformation at different stages of dentin maturity. A part of this significant conformational change might be due to elevated hydration of collagen during the initial maturation stages, as it has been shown to happen with synthetic collagen-like polypeptides (Doyle et al, 1975). From our study, indeed, the broadening of Amide I areas from cervical dentin spectra in question was partly eliminated after heat-dehydration of the matrix (not shown here). Still, it is debatable whether this was not a result of the intense denaturation of matrix proteins through prolonged heating at 110°C. There is not much available information existing on conformational changes of the mineralized tissue matrices during maturation. The major (at least in some species) dentin noncollagenous protein phosphophoryn (discussed more extensively in Chapter IV) has been shown to present an extensive β-sheet structure in the presence of apatite (Fujisawa and Kuboki, 1998). However, as it will be shown in Chapter IV, data in the relevant study of this dissertation did not support the possibility of significant changes in phosphophoryn concentration during dentin maturation. No other report exists, in our knowledge, on matrix conformational changes during maturation of mineralized tissues.

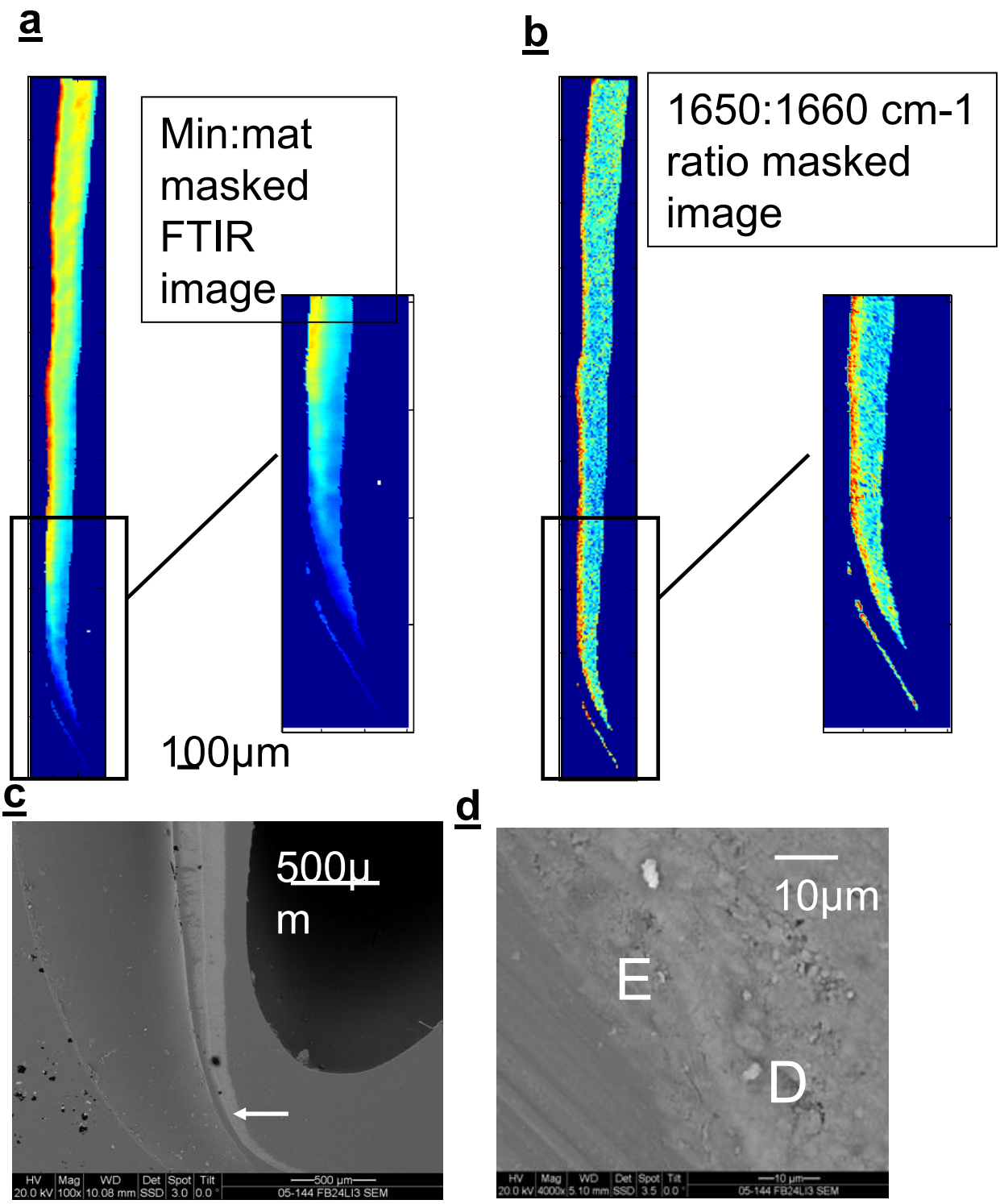

Fig.3-1 : Validation of the 1650:1660 cm^{-1} (noncollagenous:collagen relative peak heights ratio) spectroscopic ratio for identification of enamel in early stages of maturation on the cervical part of an analyzed incisor. (a) mineral: matrix FTIRI image (b)1650:1660cm^{-1} FTIRI images (c) : SEM image of area indicated in a and b (SEM analysis performed on the embedded incisor block). Arrow points at area shown in higher magnification in d. E=enamel, D=dentin.

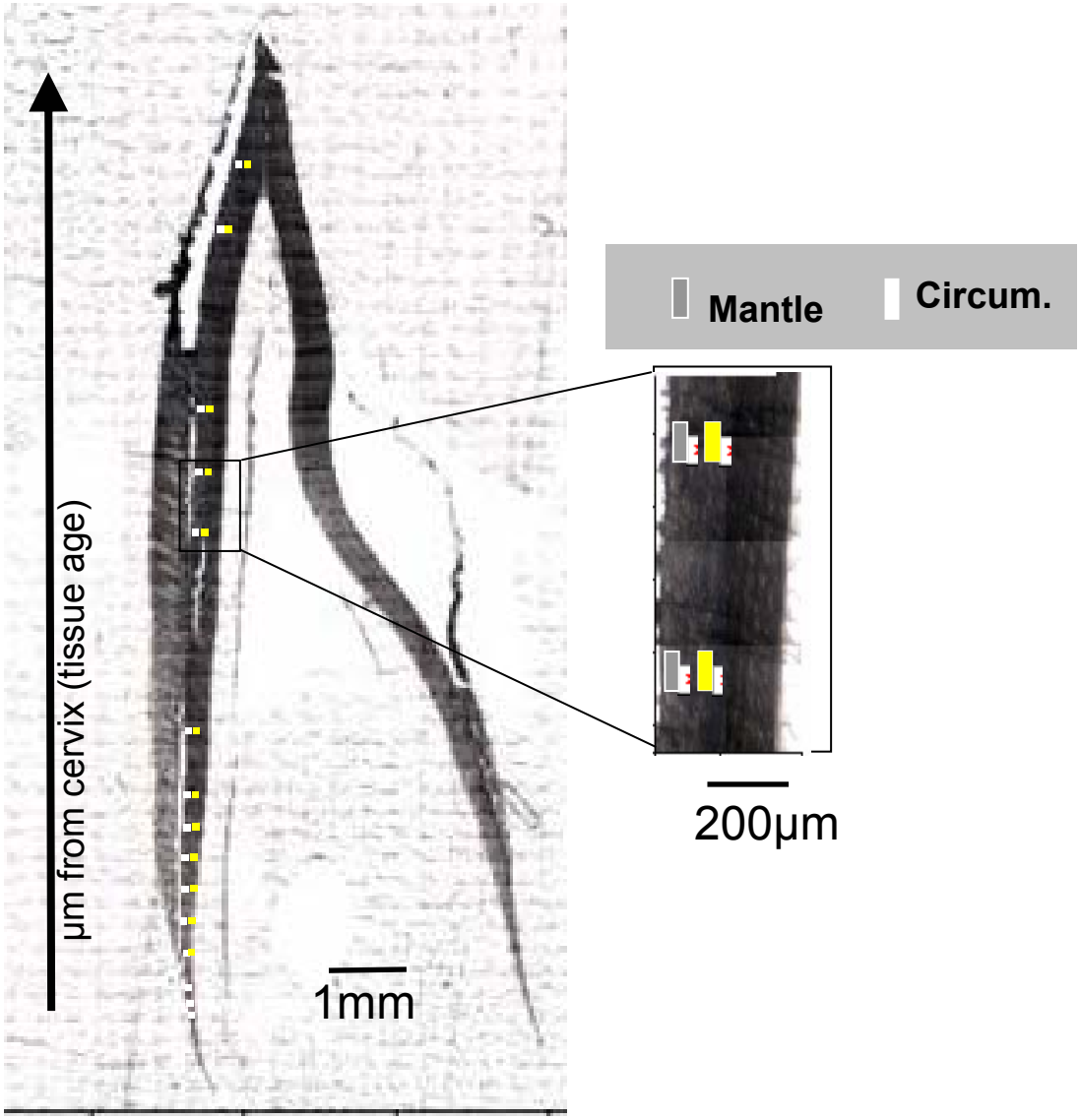

Fig. 3-2 : Schematic on identification of mantle and circumpulpal dentin areas for acquisition of spectral results from analyzed incisor sections. Increasing in distance from cervix mantle and circumpulpal dentin areas from which co-added spectra (to one spectrum for the total area) were extracted are shown. These areas were based on mineral:matrix images, here shown on an optical micrograph of an analyzed I3 incisor.

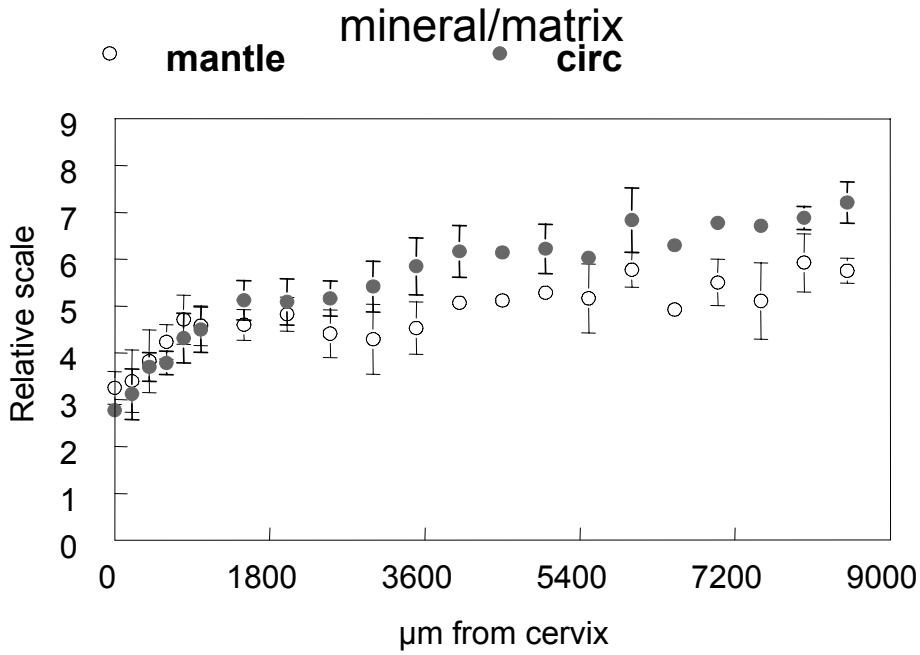

Fig. 3-3: Distribution of mineral:matrix values of mantle and circumpulpal dentin as a function of distance from the cervix of the incisor. Means and standard deviations of data points from all animals at same distance from cervix. Where bar is missing, standard deviation is too small to be shown.

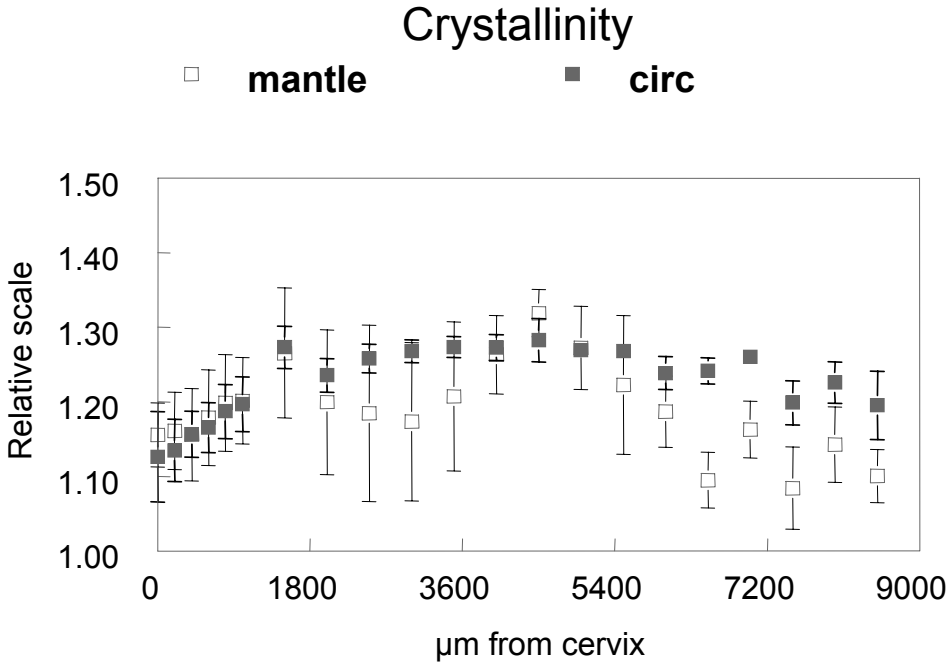

Fig. 3-4: Distribution of mineral crystallinity in the incisors crown as a function of distance from the cervix of the incisor. Means and standard deviations as in fig. 3-2.

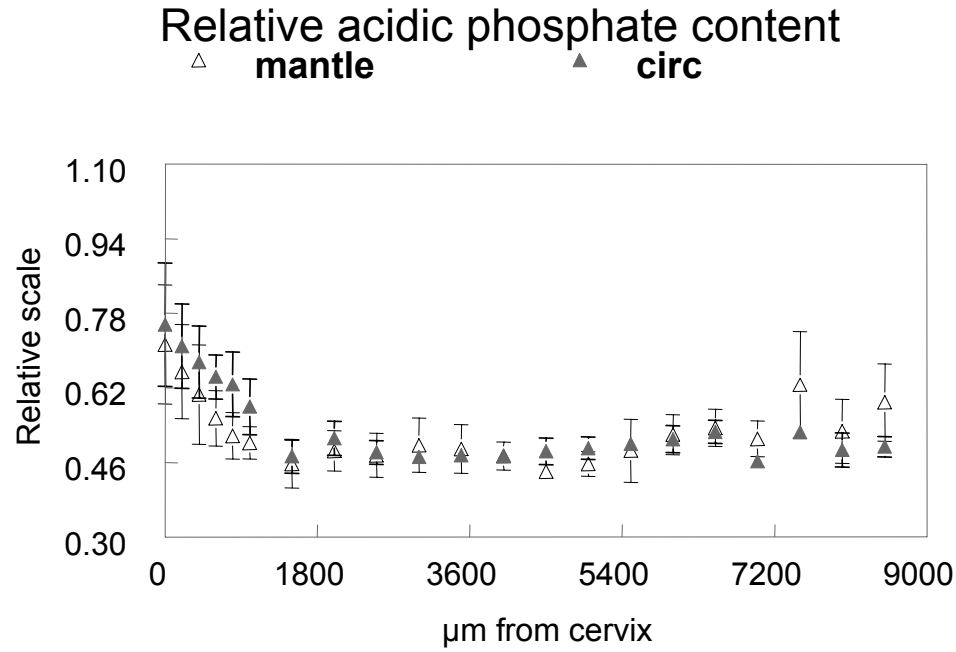

Fig. 3-5: Distribution of relative amount of acidic phosphate in the mineral as a function of distance from the cervix of the incisor. Means and standard deviations as in fig. 3-3.

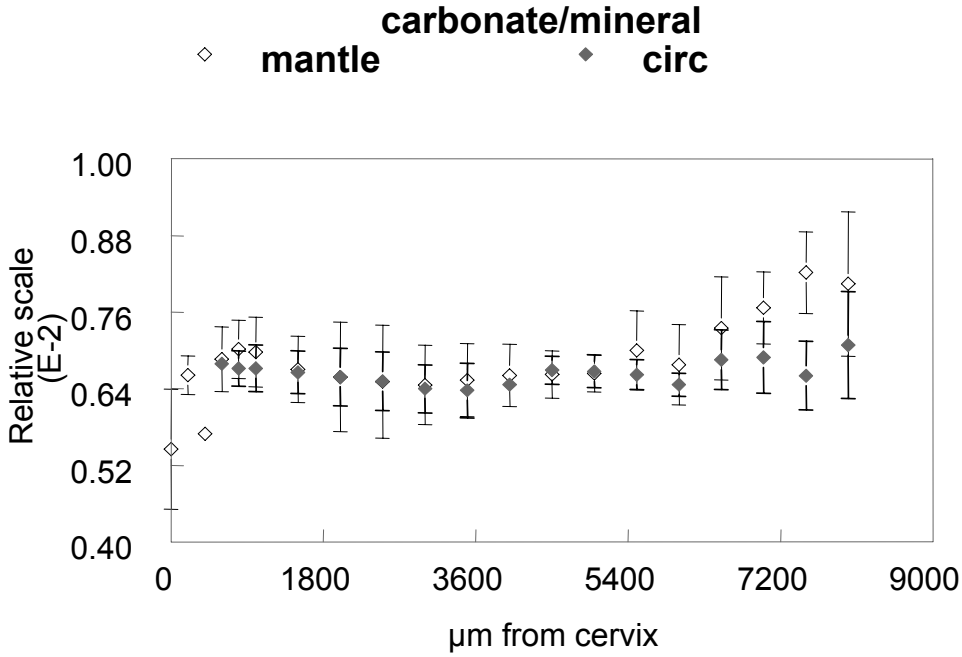

Fig. 3-6: Distribution of relative amount of carbonate in mineral as a function of distance from the cervix of the incisor. Data from the 5µm sections. Means and standard deviations of data points from all animals at same distance from cervix. Where bar is missing, data point comes from a single observation.

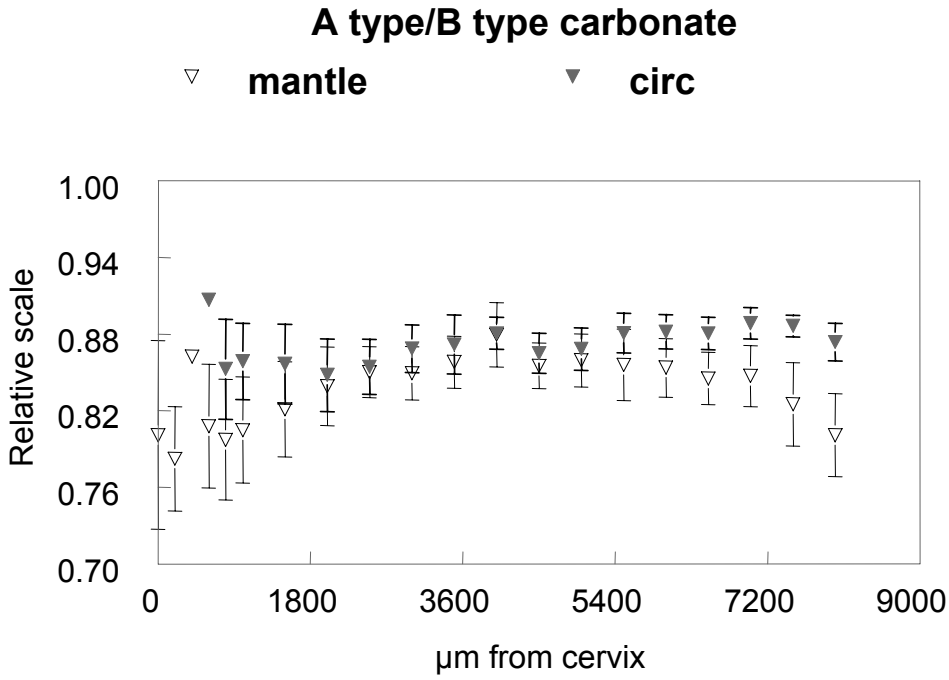

Fig. 3-7: A:B type of carbonate substitution in the mineral as a function of distance from the incisor cervix. Data from the 5µm sections. Means and standard deviations as in fig. 3-6.

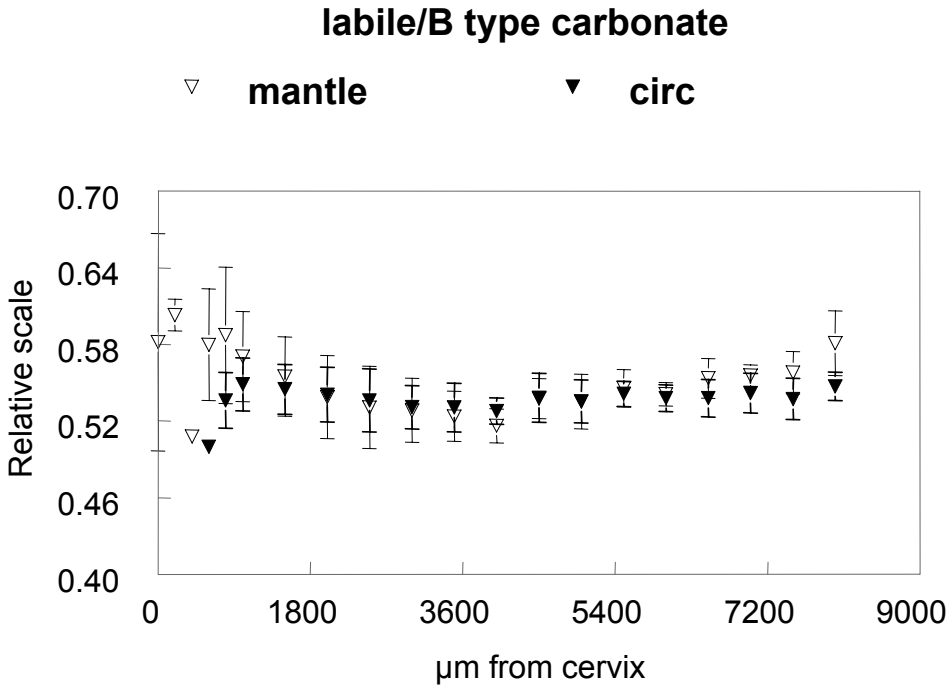

Fig. 3-8: Relative labile carbonate amount in the mineral as a function of distance from the incisor cervix. Data from the 5µm sections. Means and standard deviations as in fig. 3-6.

a.

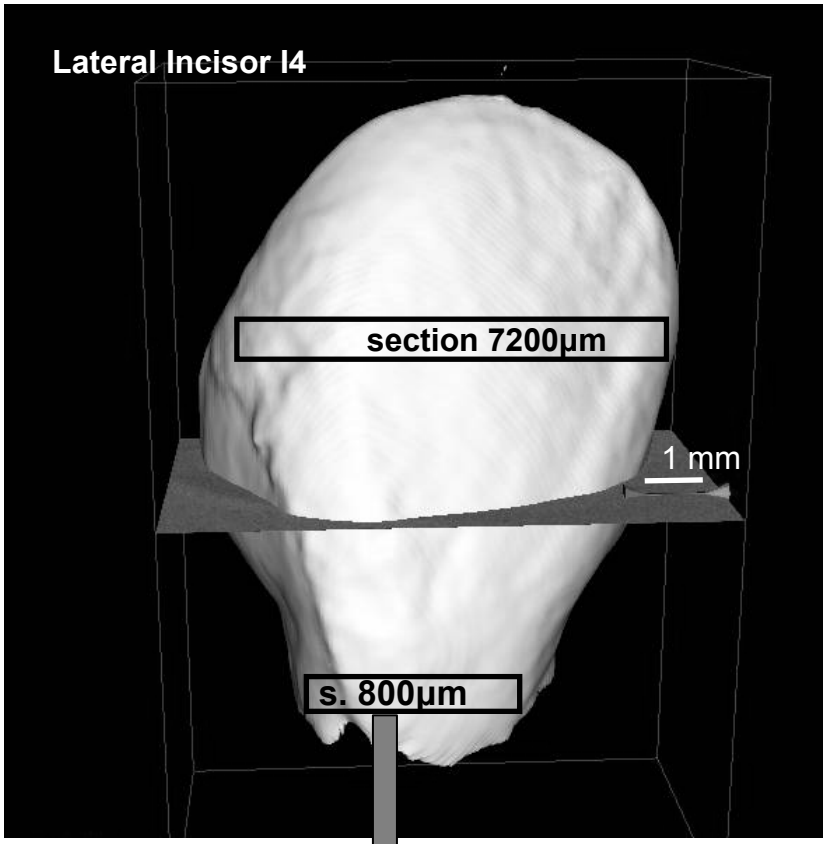

b.

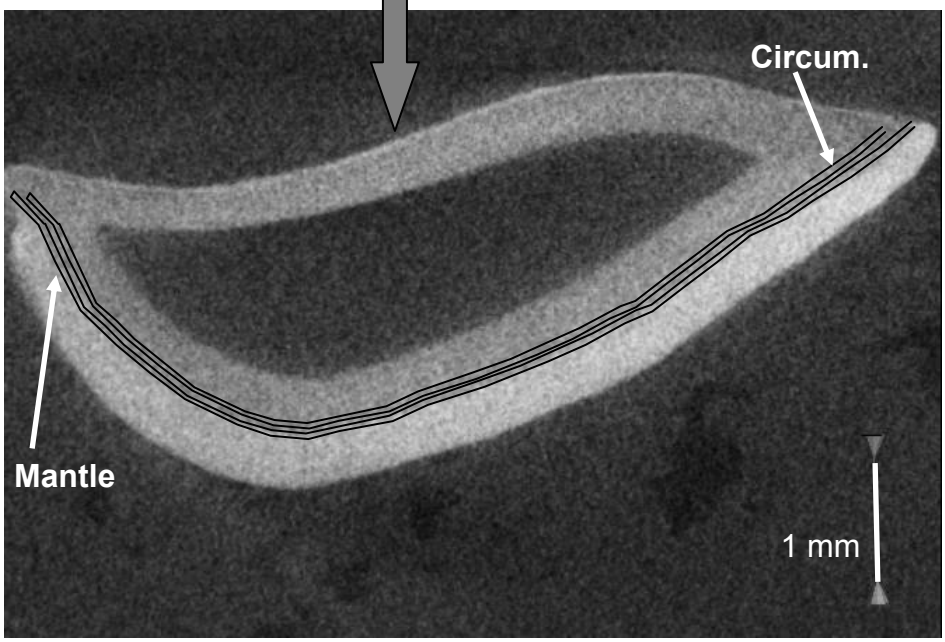

Fig. 3-9 : Schematic of method used for dentin specimens microdissection on a microCT image of an I4 lateral incisor. (a): Plane of vertical sectioning indicated on 3D image of the incisor. 800 µm vertical crown sections obtained sequentially (b): Location of dentin specimens microdissected in mantle (80 µm strip adjacent to DEJ) and circumpulpal dentin (80 µm strip 80-100µm away from DEJ) regions.

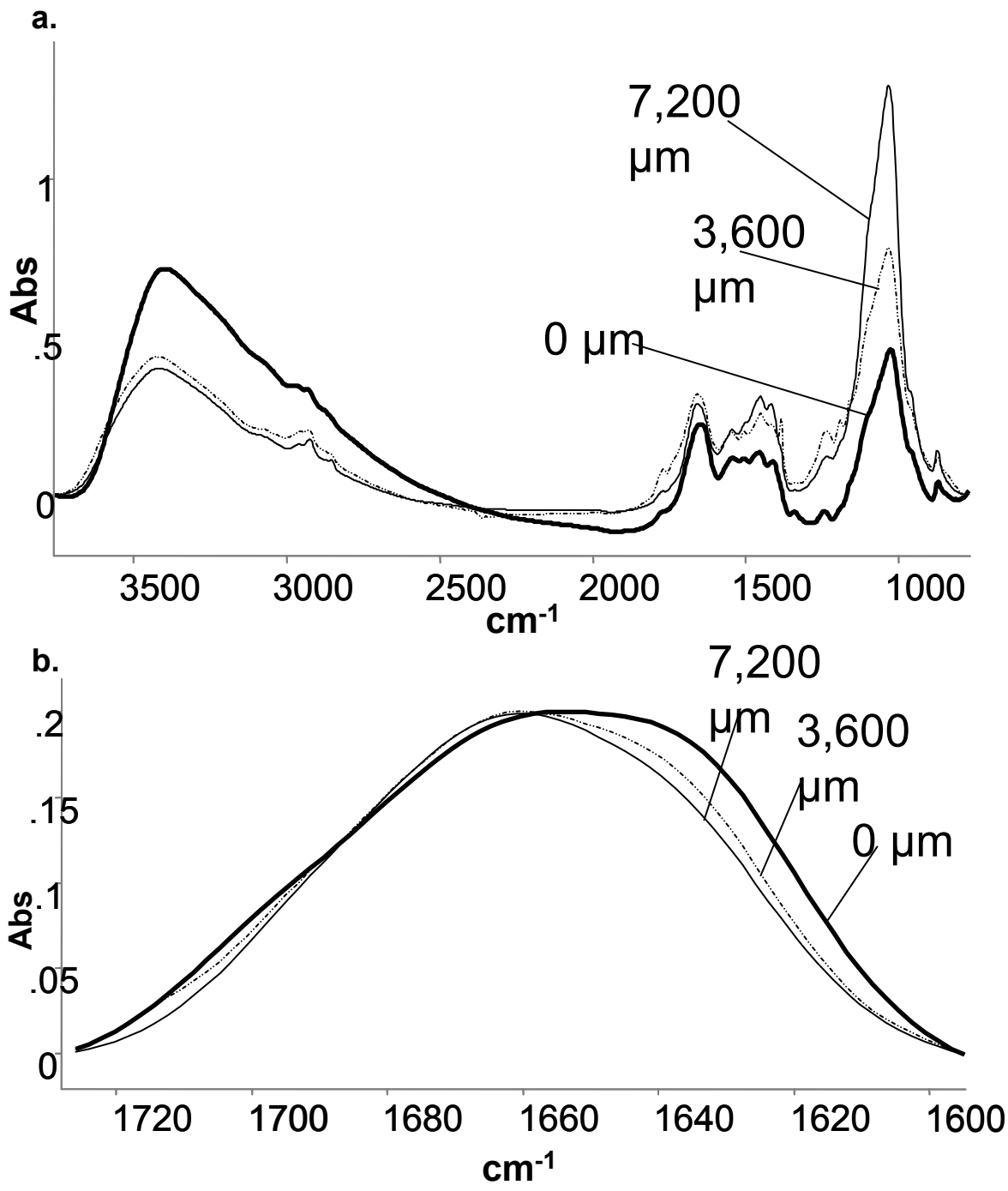

Fig. 3-10: Superimposed spectra from mantle dentin specimens dissected at distances from the cervix indicated. Scale for every spectrum adjusted for normalization of the total marix (Amide I) areas. (a): Total spectral range (b): Amide I areas of spectra shown in A. Peak heights have been normalized to enable comparison.

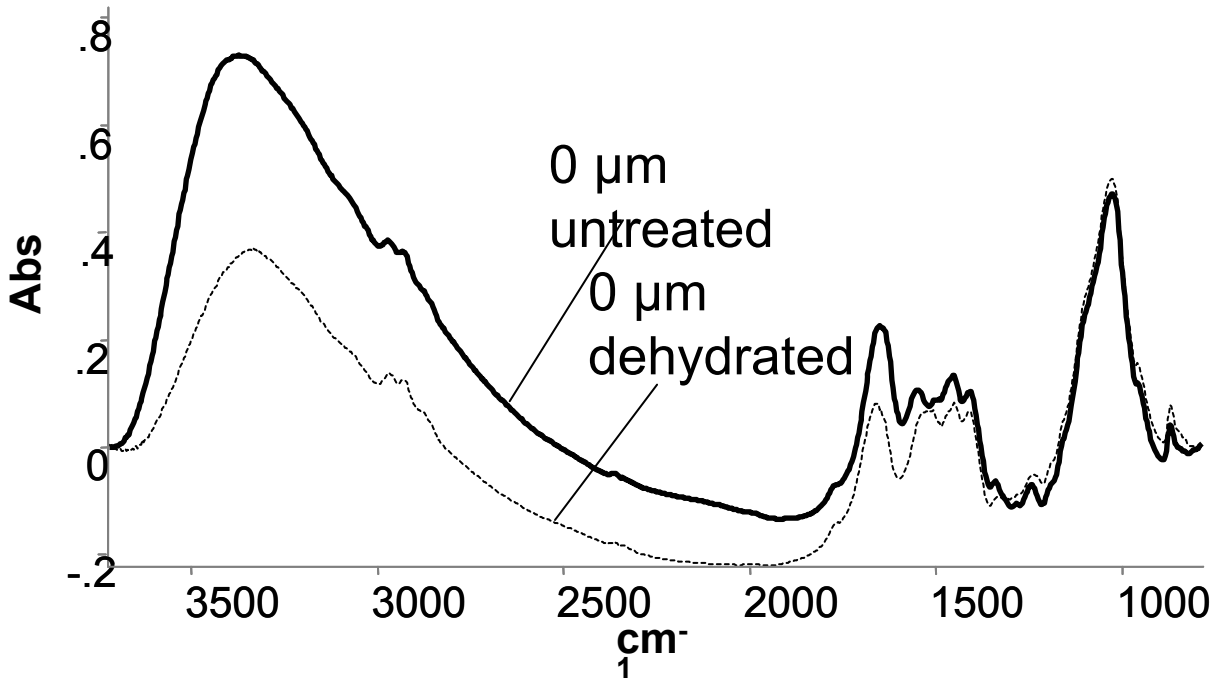

Fig. 3-11: Spectra from mantle dentin specimen at 0um shown in fig. 4-8a undehydrated and after dehydration. Thick line=unprocessed specimen. Dotted line=specimen after dehydration by heating at 105° C.

CHAPTER IV

ANALYSIS OF MATRIX PHOSPHOPROTEIN TURNOVER AND OF MATRIX PHOSPHORYLATION DURING DENTIN DEVELOPMENT

INTRODUCTION

As discussed already in Chapter I, noncollagenous proteins are believed to play a critical role in the mineralization of hard tissue matrices. The dentin organic matrix is rich in characteristic highly acidic phosphorylated proteins, the function of which depends on phosphorylation. Contradictory reports on changes in the concentration and/or extent of phosphorylation of highly acidic phosphorylated proteins in dentin have been published (Veis et al, 1979; Masters PM, 1985; Lee et al, 1983; Fujisawa and Kuboki, 1988). As the issue of dentin matrix phosphorylation appears to be of great importance to dentin biomineralization, changes in the relative content of dentin matrix phosphorylated protein content and in the relative matrix phosphate content during maturation of the tissue was examined in this section. The analysis was carried out separately for mantle and circumpulpal dentin specimens.

A description for each of the highly phosphorylated dentin matrix proteins was provided in Chapter I. As there still appears to be some confusion in the literature about whether these particular proteins are expressed in the same way in different species (such as mice, rats and humans), for the purposes of the present part we will be referring to this group as phosphoproteins.

MATERIALS AND METHODS

Specimen preparation: I3 and I4 lateral incisors from 6 different 3rd trimester fetal bovine animals were used in these studies. I3 and I4 incisors were chosen for sampling because of their similar stage of eruption, in the same animal, and their similar lengths. The methodology used for preparation of the teeth and serial sectioning was that described in Chapter III (preparation of samples for microdissection section). Briefly, thick transverse to the long axis of the teeth sections from these incisors were cut and the mantle and circumpulpal dentin areas were marked for microdissection on these thick sections. The transverse sections were 1mm thick for the samples that were amino acid analyzed (conducted earlier in the experiment) and 800μm apart for samples analyzed for organic phosphate. For both amino acid and organic phosphate analyses, approximately 80μm-wide strips of fetal bovine dentin were dissected out of mantle and the part of circumpulpal dentin immediately adjacent to mantle dentin, with a typical yield of 8-10 mantle and 6-8 circumpulpal dentin samples of progressive tissue age from cervical and incisal locations. Four incisors were used for total amino acid analysis and seven for determination of total matrix phosphate and hydroxyproline content (for normalization of matrix phosphate content). Mantle and circumpulpal dentin specimens were microdissected out of the mesial and distal, respectively, halves of the same incisors. The final number of sample series analyzed was 7 for mantle dentin and 6 for circumpulpal dentin. Additionally, one I1 (central) and one I2 (first lateral) incisors were analyzed for matrix phosphate and hydroxyproline, in order to

examine the effect of tooth type on the changes in matrix phosphorylation under analysis.

Amino acid analysis: Specimens for amino acid analysis were desiccated and weighed. Each sample was transferred with 200µL of 6N HCL in a glass tube sealed in vacuum with nitrogen purging and hydrolyzed at 110°C for 20 hs, after which tubes were opened and residual HCL dried by a Speed-Vac system. Complete amino acid analysis was performed by a custom-built cation exchange HPLC, configured as an amino acid analyzer, as described elsewhere (Yamauchi et al, 1986).

Organic Phosphate and hydroxyproline determination: Samples were initially demineralized individually in 6 well-tissue culture plates by continuous stirring in several changes of 3mL of 0.5N HCL for 48 hs. In a preliminary part, the removal of PO_4^{3-} ions was monitored and the number of changes/amount of time needed for complete decalcification determined. Serial extracts and demineralized dentin pieces were stored. Extracts from each specimen were combined at the end of decalcification, neutralized with the theoretically required amount of 6N NaOH and lyophilized to reduce their volume. After lyophilization, 2mL of distilled water was added to each extract, transferred into a 3.5KDa molecular weight cut-off dialysis cassettes (Slide-A-Lyzer, Pierce, Rockford, IL) and dialyzed against several changes of 4L volumes of .05N HCL (to prevent reprecipitation of dissolved in extract solution PO_4^{3-} ions from hydroxyapatite) to remove all inorganic phosphate from mineral. Again, this part was monitored in a pilot study for complete removal of PO_4^{3-} ions and the conditions described were found to be adequate for our purposes. After the

completion of dialysis, extracts were relyophilized, dialyzed in 500μL 1M NaOH, transferred into 2mL heat -resistant, screw-capped Teflon tubes and combined with the demineralized dentin samples from which they originated. NaOH dialyzed extracts and demineralized pieces in the tubes were subsequently subjected to alkaline hydrolysis at 110°C for release of organic phosphate from phosphorylated proteins and of hydroxyproline from collagen. A 300μL aliquot was taken from each tube at 12 hs for the organic phosphate analysis and a 150μL aliquot at 18hs for hydroxyproline determination. These time spans were found to be optimal for organic phosphate release (determined phosphate levels are lower after that time point, due to β-elimination) and complete (for Hyp release) collagen hydrolysis, in pilot experiments. Aliquots for both the organic phosphate and the Hyp analysis were first neutralized by addition of the required amount of 6N HCl.

Colorimetric determination of phosphate from phosphorylated protein residues was performed using a modified malachite green method, as described by Baykov et al (Baykov et al, 1988). For normalization of phosphate results, the total collagen content in samples was estimated through hydroxyproline determination, for which a colorimetric method (Neuman and Logan, 1949). The particular analytical method for phosphate determination was chosen because of the very high sensitivity that it provides, as the organic phosphate levels in our samples were relatively low. The colorimetric method for Hyp analysis was chosen because its sensitivity is well within the range of Hyp concentration in our samples and is also essentially not affected by small variations of the sample pH, as other methods based on complexation of the

analyte with p-aminobenzaldehyde are. Results in this part were reported as nmols phosphate/nmol collagen.

Pilot experiment for determination of inorganic phosphate reprecipitation: To exclude the possibility of re-precipitation of inorganic phosphate from the HCl solution on the decalcifying collagen, during the decalcification part, the following experiment was performed: dentin was dissected clean of enamel and predentin from a 3rd trimester fetal I3 incisor and pulverized using a Spex-Mill apparatus, yielding a total of 16 mgs. 8 aliquots of approximately 2mgs of pulverized dentin were decalcified as described above for analysis of matrix phosphorylation and decalcified aliquots were divided in two groups of 4 aliquots each, $D_1$1-4 and $D_2$1-4. After decalcification D_1 samples were stored at 4°C, while D_2 samples were further stirred for 4 hours in 3ml of .5N HCl into which 8 mgs of synthetically produced apatite were added, to simulate a maximum concentration of mineral that could be dissolved in the decalcifying solution of a developing mantle or circumpulpal dentin piece. The D_2 samples were then washed off twice by stirring in 3ml .5N HCl for 4 hours. All D_1 and D_2 aliquots were analyzed for phosphate and hydroxyproline.

RESULTS

The results for aspartic acid (Asp), serine (Ser) and tyrosine (Tyr) from microdissected mantle and circumpulpal dentin specimens of the four developing incisors examined are given on Figure 4-1 a-b for Asp, c-d for Thr and e-f for Ser (separate charts for mantle and circumpulpal dentin). Results are expressed as mM of each amino acid per mM of collagen (assuming 300 mmols Hyp/mol collagen).

Despite some fluctuations around the baseline value, there are no changes observed in the relative content of these 3 amino acids in the dentin matrix. Bivariate correlation statistical tests performed separately for each of the examined amino acids, as well as partial correlation tests with correction for the tooth of origin, failed to show any statistical trend of correlation between location of dentin specimen and relative amount of Asp, Thr or Ser. Similar statistical results were repeated when the mantle and circumpulpal dentin specimens were analyzed in common in order to increase the number of observations each time.

Figure 4-2 presents the results for assessment of possible re-precipitation of dissolved apatite phosphate on the dentin matrix experiment. Comparable levels of organic phosphate/ hydroxyproline were found for all but one samples in the D_1 control group and the D_2, re-precipitation of apatite phosphate on matrix group. From these results, no significant likelihood is demonstrated for such a re-precipitation of phosphate from dissolved apatite on proteins of the matrix, as also assessed by an independent samples t-test performed.

The results for microdissected mantle dentin specimens from the I3 and I4 fetal incisors analyzed in the matrix phosphorylation analysis part are presented in Figures 4-3 a and b, respectively. I3 and I4 mantle dentin results are combined in Figure 4-4 c, where a linear regression based on least squares has been added. Figures 4-4 a- b-c present similar results for circumpulpal dentin from the same teeth. All the graphs show a gradual increase of the relative amount of the matrix phosphate which is still present at the maximum distance of dentin specimens from the cervix (late stages of maturation). The overall levels of matrix phosphate vary

considerably (up to twofold) between different teeth, even of the same type, but within any given incisor these levels steadily show a gradient from the cervix to the incisal edge. Figures 4-5 and 4-6 present mantle and circumpulpal dentin, respectively, results for the I1 and I2 fetal incisors analyzed. These results also show an increase of the matrix phosphate with distance of dentin specimen from tooth cervix and, hence, tissue age. As there is not enough data from the two teeth, it cannot be stated with certainty how the organic phosphate levels in these incisors compare to the levels from I3 and I4 incisors. The statistical analysis for the I3 and I4 incisor data is displayed on tables 4-1 a-b and 4-2 a-b. Both simple and partial correlation tests showed a statistically significant ($p<0.01$) positive correlation of matrix phosphorylation with specimen location considered as distance from the incisor cervix. The Pearson's correlation coefficient, on the other hand, shows an only fair correlation ($R=.348$ for mantle and $R=.471$ in circumpulpal specimens), most likely because of the scattering that data points show within a certain series (a certain tooth of origin) and between different incisor series, as well as between I3 and I4 incisors. That last fact also becomes obvious from the increase in Pearson's coefficients in partial correlation, after correction for tooth of origin (Tables 4-2 a-b). These results indicated a substantial increase of matrix protein residues that are phosphorylated occurring during dentin maturation. This increase occurs to a similar extent in mantle and circumpulpal dentin (as estimated by the linear regression).

DISCUSSION

.Depending on the species, aspartic acid and serine or phosphoserine have been reported to constitute from 75% up to 90% of all the amino acid residues of dentin highly phosphorylated proteins (Qin et al, 2004), which is the reason for their highly anionic character. The levels of the same amino acids in dentin collagen are up to ten times lower (Linde, 1984). Since hydroxyproline is an essentially unique amino acid to collagen (hydroxylation of proline residues in the dentin matrix only occurs in collagen) accounting for approximately 100 amino acid residues per 1,000, any changes in the concentration of phosphoproteins relative to that of collagen in the matrix is likely to be reflected in a similar change in the ratio of Asp or Ser/ Hyp residues of the total matrix amino acid composition. In the present results, the relative Asp, Ser and Thr (being the other amino acid that is most commonly phosphorylated) to Hyp concentration did not show significant changes from the mantle or circumpulpal dentin specimens of newly formed tissue to the more mature counterparts (cervical to incisal regions). These values rather fluctuated around an average, perhaps as a result of some variability in localization of the specimens during specimen acquisition. This amino acid analysis data indicate that there are no significant changes in the amount of phosphoproteins in the developing bovine dentin. That fact allowed interpretation of the changes in the levels of organic phosphate of the matrix.

The increase in organic phosphate, observed with dentin development, was statistically highly significant. Exactly, though, how big this increase is cannot be estimated with certainty from the present results. That is probably because the many

steps in the analytical procedure and the very different levels between different types of teeth introduce some variability. The increase in matrix phosphate seems to be extensive, about threefold between youngest and oldest specimens in most of the samples analyzed. For the same maturation point (defined by the distance of specimen location from the cervix), the organic phosphate/collagen values seem to also depended on the particular tooth of origin. This was indicated by the higher significance of partial correlation after controlling for tooth of origin and this might reflect differences in maturation stage for these teeth between different animals. Although the analysis was focused on two tooth groups, lateral incisors I3 and I4, this increase was also observed in the I1 and I2 incisors examined (Figure 4-4 a-b). Some outlier data points present in the distribution of organic phosphate with tissue age are most likely a result of some contamination in one of the steps of the analytical procedure, or some accidental inclusion of enamel during microdissection of dentin specimens. Both amino acid analysis and matrix phosphate results were reported as a function of distance of specimens from the incisor apex, as the latter was shown to correlate well with tissue maturity from the results described in Chapter II. Relative mineral density of the specimen, that would have been an alternative, was difficult to determine in the same samples due to the limited amount that could be obtained for each sample. Whereas an age-dependent degradation (evident as multiple protein fragments of lower molecular weights) of phosphorylated proteins in the dentin matrix has been well documented (Butler et al, 1981; Jontell , 1982; Lee et al, 1983), there are few existing reports on changes in the extent of matrix phosphorylation with maturation. In one study where human teeth (3-45

years-old) were used (Masters PM, 1985), an up to fourfold decrease was observed in the levels of organic phosphate of the dentin matrix –in contrast with the present data. In the same study, serine was also found to be partially eliminated (by ~60%) as a result of dehydration and aldol cleavage. However, these changes were described to be chemically, not enzymatically, induced and the starting point for the observations used was at 3 years after beginning of formation, at which point dentin is likely to be fully mineralized. Therefore, the observed changes were unlikely to be associated with a tightly controlled process such as mineralization. In another study, EDTA soluble and insoluble matrix protein fractions from fetal calf and young adult bovine dentin were analyzed by chromatography and amino acid analysis (Lee et al, 1983). The levels of aspartic acid, serine and phosphoserine were found to be 30-50% lower in the soluble phosphoprotein pool for older dentin and comparable between the two groups in the respective insoluble pool. On the other hand, as demonstrated in the results of Chapter II, there is a wide range in mineral, and possibly matrix, properties within the crown dentin, independent of tissue age. An additional concern is the use of partial collagen hydrolysis method for phosphoserine determination in both the studies in question. Partial hydrolysis of the matrix is sensitive to the particular conditions used and the extent of hydrolysis needed for a complete release of phosphoserine is arguably dependent on the association of phosphoproteins examined with the mineral and the rest of the matrix. Two other reports on changes of phosphorylated proteins or phosphoserine concentration in the dentin matrix related to dentin age have been made using chromatography and amino acid analysis methodology. In these reports, dentin tissue from the whole

crown of deciduous and permanent bovine molars (Veis et al, 1979) or crowns and root at different stage of formation from 2 year-old cows (Fujisawa and Kuboki, 1988) were compared. While the conclusions reached are generally similar to the present study's, variability in histology of dentin examined (a wide range of locations in the crown, different tooth types, crown vs. root dentin, mantle and circumpulpal dentin examined together) in both of the studies does not allow a direct comparison with our data. Also, in both studies the protein amount is not examined separately from protein phosphorylation in the dentin matrix, as done here, and phosphoserine content is instead assumed to fully reflect phosphoprotein concentration. In the Fujisawa and Kuboki study, the difference in phosphoserine levels observed (an approximately threefold increase from early to later formation stages) was attributed to mantle dentin making a bigger part of the earlier formation stage crowns and roots at 2 years of age. Given, though, the small fraction of the total dentin volume relatively that mantle dentin represents (see Chapter II-mature 1yr-old calf results), this explanation is unlikely to hold true. Additionally to the bovine dentin, in the Fujisawa and Kuboki study, rabbit incisor (continuously erupting) dentin from different eruption stages was examined. An approximately twofold increase in phosphoserine and organic phosphate content was found, giving evidence for an increase in matrix phosphorylation with maturation of dentin across species.

The results in this section did not show any significant differences in the matrix phosphate levels between mantle and circumpulpal dentin specimens for any given stage of maturation. From the early to the latest stages, these levels were found to be very similar between the two dentin compartments. This finding is in contrast with

existing reports on phosphoprotein distribution in dentin, made on fetal bovine molars (Nakamura et al, 1985), rat incisors (Rahima et al, 1988) and human premolars (Takagi and Sasaki, 1986). In these reports, phosphophoryn, as the major dentin phosphoprotein, or highly phosphorylated proteins as a group were described to be absent from mantle dentin. Nevertheless, the lack of sound criteria for defining mantle dentin in the studies mentioned makes the direct comparison between the present and the existing data difficult. Indeed, from this study's FTIR imaging results (described in Chapter II), mantle dentin as a zone that presents different mineral properties from the rest of dentin occupies 80-100μm next to DEJ. In the report on fetal calf molars (Nakamura et al, 1985), where a monoclonal antibody raised against bovine phosphophoryn was used for immunolocalization, the results indicate absence of immunostaining in the ~10μm next to the DEJ, a fraction of the mantle dentin identified in the present study. Other unique properties of mantle dentin, such as the presence of matrix vesicles (Katchburian, 1973) have been described to characterize only the most proximal to the DEJ part of mantle dentin. On the other hand, in a study of phosphophoryn distribution in rat incisor (Rahima et al, 1988) using a polyclonal antibody, the dentin part next to DEJ described as mantle dentin that was shown to be scarce in phosphophoryn was also 10μm wide, which is a very wide zone in a rat incisor and would correspond to an area largely consisting of circumpulpal dentin in a fetal bovine incisor. Technical issues, such as limited accessibility of the epitopes on the nondecalcified sections used in the immunohistochemistry studies or lack of specificity through use of a stain that has an affinity also for other anionic matrix proteins (Takagi and Sasaki, 1986),

are also a concern when it comes to comparing the present and existing data. Under the present study's conditions, virtually all the matrix phosphate from the microdissected specimens was recovered after demineralization and analyzed without interference from the mineral or other matrix groups. The total matrix phosphate was analyzed, while only one protein was targeted in the studies that used immunolocalization. A certain part of the mantle dentin matrix phosphate described in this section may have also originated in phospholipids that are present in matrix vesicles (and released by the alkaline hydrolysis performed) and that would not be detected in the immunohistochemical and histochemical studies of phosphoprotein distribution discussed.

As discussed in Chapter I (see "Composition of Dentin- b)Matrix"), there has been speculation that acidic matrix proteins –especially phosphoproteins in dentin- determine where initial deposition of mineral takes place and regulate mineral nucleation. Furthermore, it has been proposed that the same proteins may regulate crystal growth and determine crystal size and shape. The possibility of a dual role has been shown in vitro for PP through experiments of mineral nucleation in different states and concentrations (Boskey et al, 1990) and the importance of phosphorylation for their function has been demonstrated, as well (Saito et al, 1997; Tartaix et al, 2004; Gericke et al, 2005; He et al, 2005). In the present study, the present amino acid analysis results the indicated no significant changes in the relative amount of dentin phosphoprotein during maturation. On the other hand, a 3 to 4-fold increase (from very early to latest stages of maturation) in the relative amount of organic phosphate of the phosphoproteins was found. Taken together,

these results indicate a continued *in vivo* phosphorylation of the dentin phosphoproteins, after their apposition at the mineralization front. The mechanism of dentin matrix phosphorylation has been discussed elsewhere. The enzymes responsible for phosphorylation of noncollagenous proteins were identified as casein kinase I (CKI) and casein kinase II (CKII)-like kinases (Veis et al, 1997; Mikuni-Takagaki and Glimcher, 1990). Most of the phosphorylation takes place at Ser or Thr residues located within acidic sequences of the target protein. ATP and GTP are phosphate donors for the phosphorylation reactions, which appear to be tightly regulated in mineralized tissues, as shown by studies of activity of CKI and CKII and by the fact that residues that are phosphorylated are specifically determined by the proteins' conformation (Veis et al, 1998; He et al, 2005). In the present study, we were able to report an increase with tissue age of the dentin matrix phosphorylation for both mantle and circumpulpal dentin. For the particular formation stages of the teeth that were studied (mainly the I3 and I4 lateral incisors), this increase is still present at late maturation, when the dentin mineral density (for the mantle and the proximal to the DEJ circumpulpal dentin part examined) has almost reached its final levels. It follows that this increase indicates a significance of phosphoproteins in dentin in the later parts of mineralization, rather than a function only in initial mineral nucleation. A likely function for the newly –after initial mineral deposition- introduced matrix phosphate groups would be in the mineral crystal growth regulation. It has been determined that "At the less specific end of recognition, a charged protein polyelectrolyte can be adsorbed on crystal surfaces by virtue of multiple electrostatic interactions" (Adadi et al, 1992), which would result in modification of the direction or

altogether inhibition of crystal growth. Something that remains difficult to interpret is the activity of serine kinases I and II in the fully mineralized tissue and the origin of the ATP or GTP that has been described to be the donor of phosphate groups in phosphorylation of dentin phosphoproteins. Extracellular casein kinase activity has to be taking place in dentin, in a way similar to bone as it has been described (Mikuni-Takagaki and Glimcher, 1990) in a study where periosteal bone strips were isolated from homogenized bone through centrifugation and presented protein kinase activity levels equal to these of cytosolic proteins. The ATP or GTP that provides the phosphate groups for the phosphorylation reaction can only reach the tissue through the cytoplasmic process of the odontoblast. One other possible factor creating variation of the matrix during maturation could be the relative amount of peritubular dentin. It has been described (Weiner et al, 1999) that there are many more anionic phosphoproteins in peritubular dentin than intertubular dentin, so that with accumulation of more peritubular dentin in the aging dentin a higher overall level of matrix phosphorylation would be the final result. This possibility, though, is not supported by the present study's amino acid analysis results which showed no changes in the amount of dentin matrix phosphoproteins themselves during maturation.

In conclusion, the results of the present section supported a significant increase in phosphorylation of bovine dentin matrix phosphoproteins during maturation of the tissue, which was continuous through later stages of dentin maturation. This increase was observed for both mantle and circumpulpal dentin. The hypothesis is therefore proposed that a significant *in vivo* function of dentin matrix

phosphoproteins is regulation of crystal growth and that this function is mediated by protein domains that are highly phosphorylated..

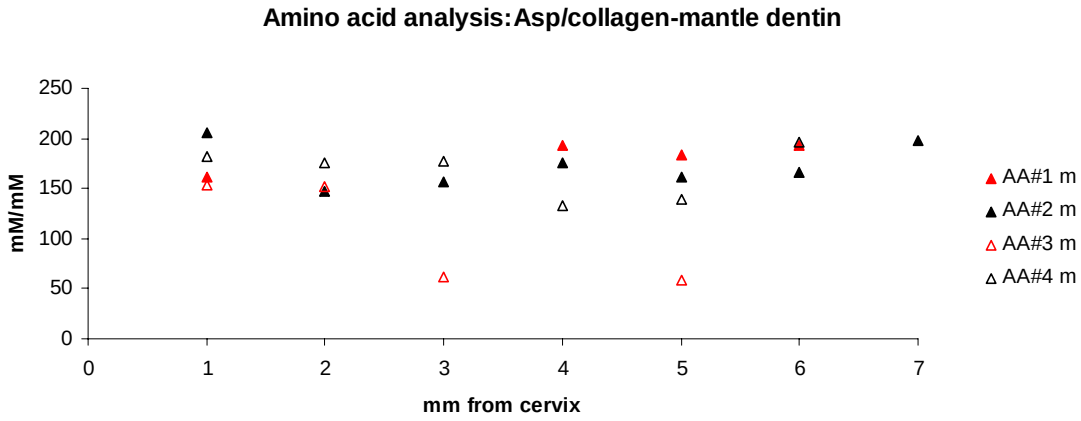
Amino acid analysis: Asp/collagen-mantle dentin
mM/mM
mm from cervix
AA#1 m
AA#2 m
AA#3 m
AA#4 m

4-1 a

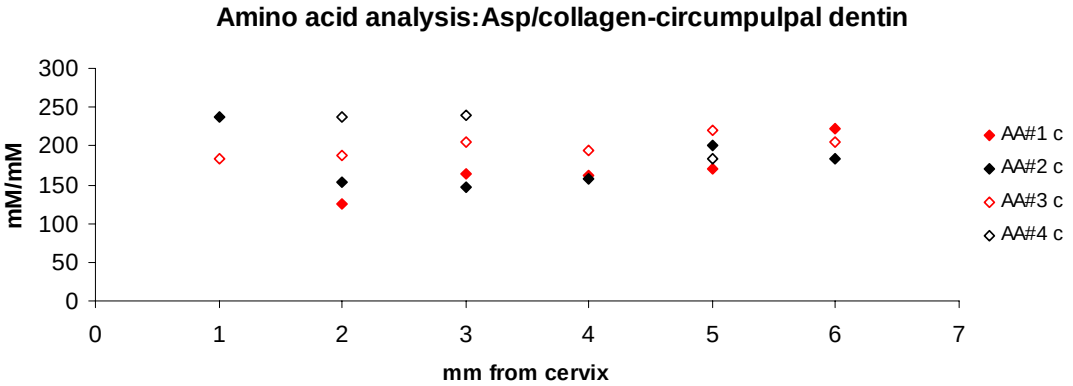
Amino acid analysis: Asp/collagen-circumpulpal dentin
mM/mM
mm from cervix
AA#1 c
AA#2 c
AA#3 c
AA#4 c

4-1 b

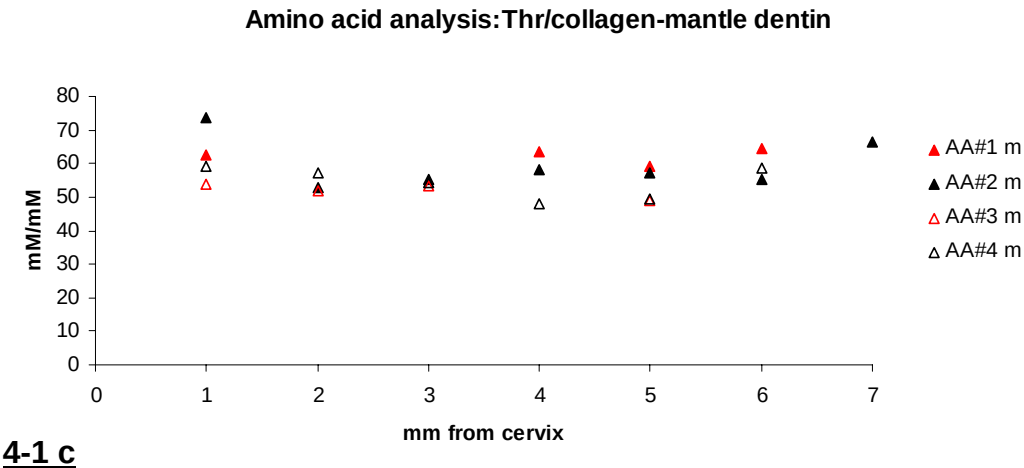
Amino acid analysis: Thr/collagen-mantle dentin
mM/mM
mm from cervix
AA#1 m
AA#2 m
AA#3 m
AA#4 m

4-1 c

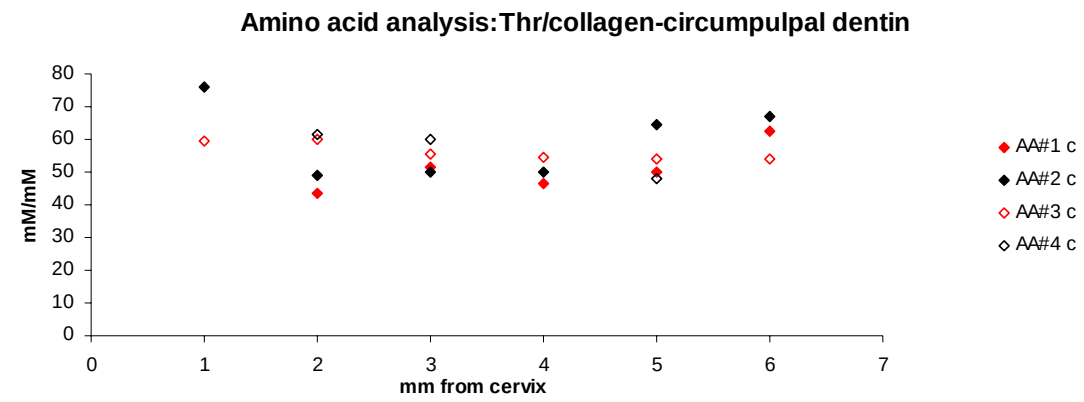

4-1d

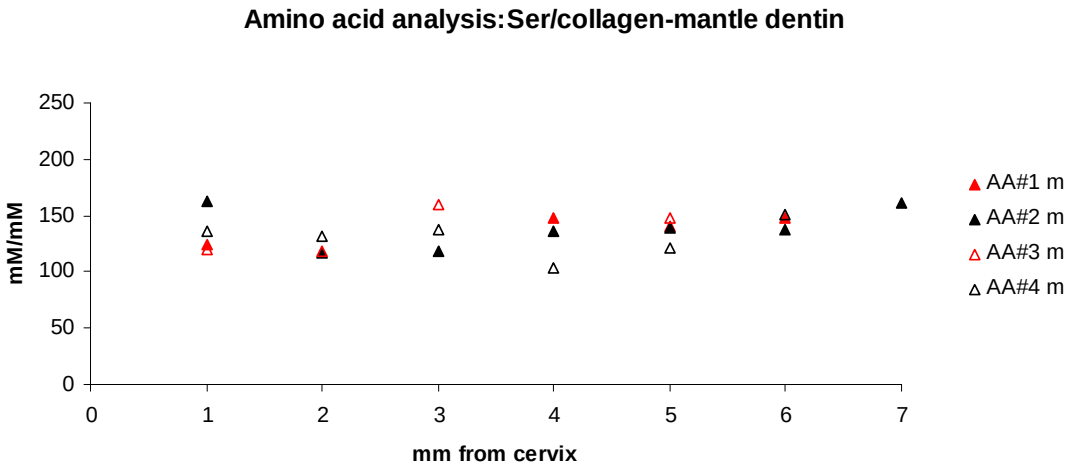

4-1e

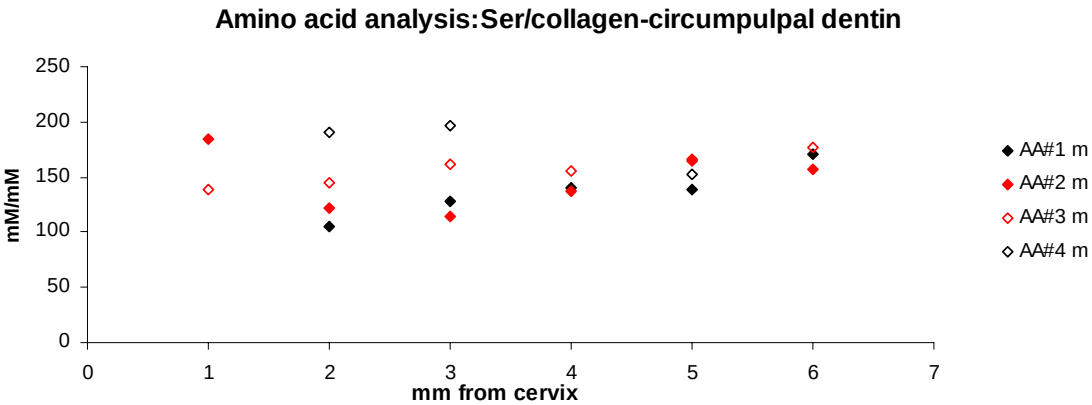

4-1 f

Fig 4-1: Amino acid analysis of microdissected mantle and circumpulpal dentin specimens of successive tissue ages. Mmols of amino acids/ mmol collagen. (a): Mantle dentin-Aspartic acid (b): Circum. dentin-Aspartic acid (c):Mantle dentin-Serine (d): Circum. dentin-Serine (e): Mantle dentin-Threonine (f): Circum. dentin-Threonine. Specimens from same incisor indicated by same color markers.

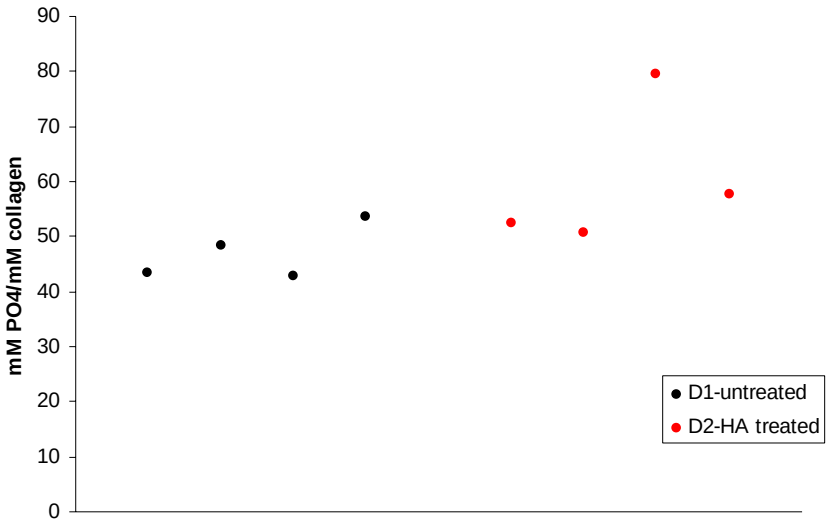

Fig. 4-2: Evaluation of dissolved hydroxyapatite re-precipitation on demineralizing dentin specimens. mM PO4/mM collagen of homogenized dentin samples, untreated (D_1) and treated with an excess of hydroxyapatite (D_2).

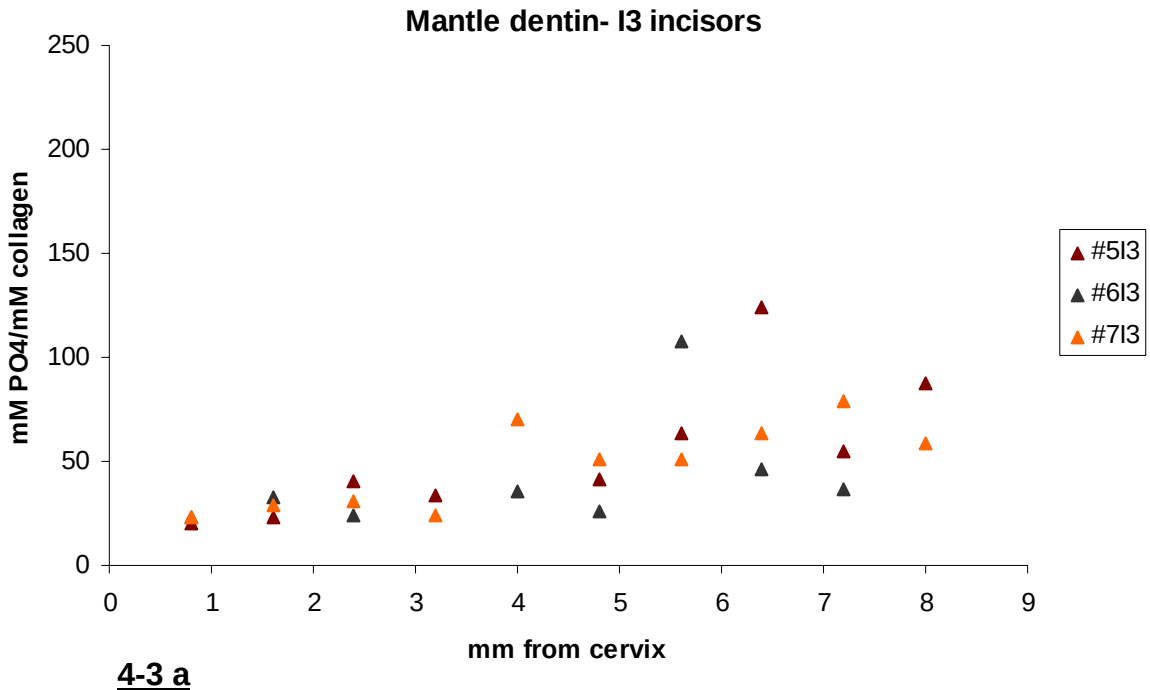
Mantle dentin- I3 incisors
mM PO4/mM collagen
mm from cervix
#5I3
#6I3
#7I3

4-3 a

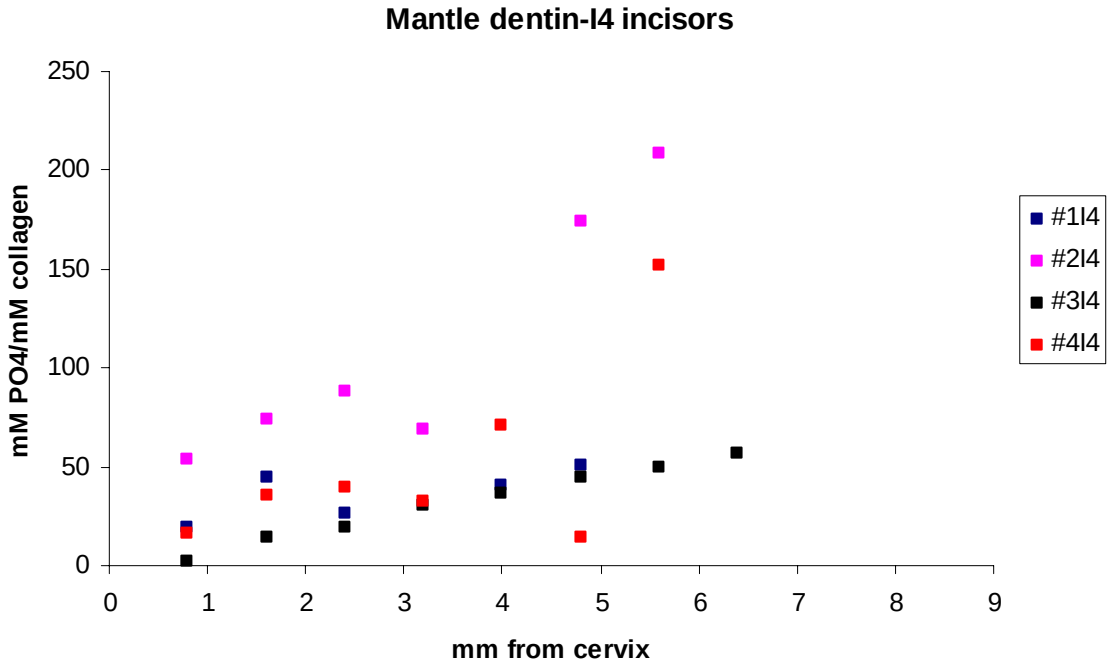
Mantle dentin-I4 incisors
mM PO4/mM collagen
mm from cervix
#1I4
#2I4
#3I4
#4I4

4-3 b

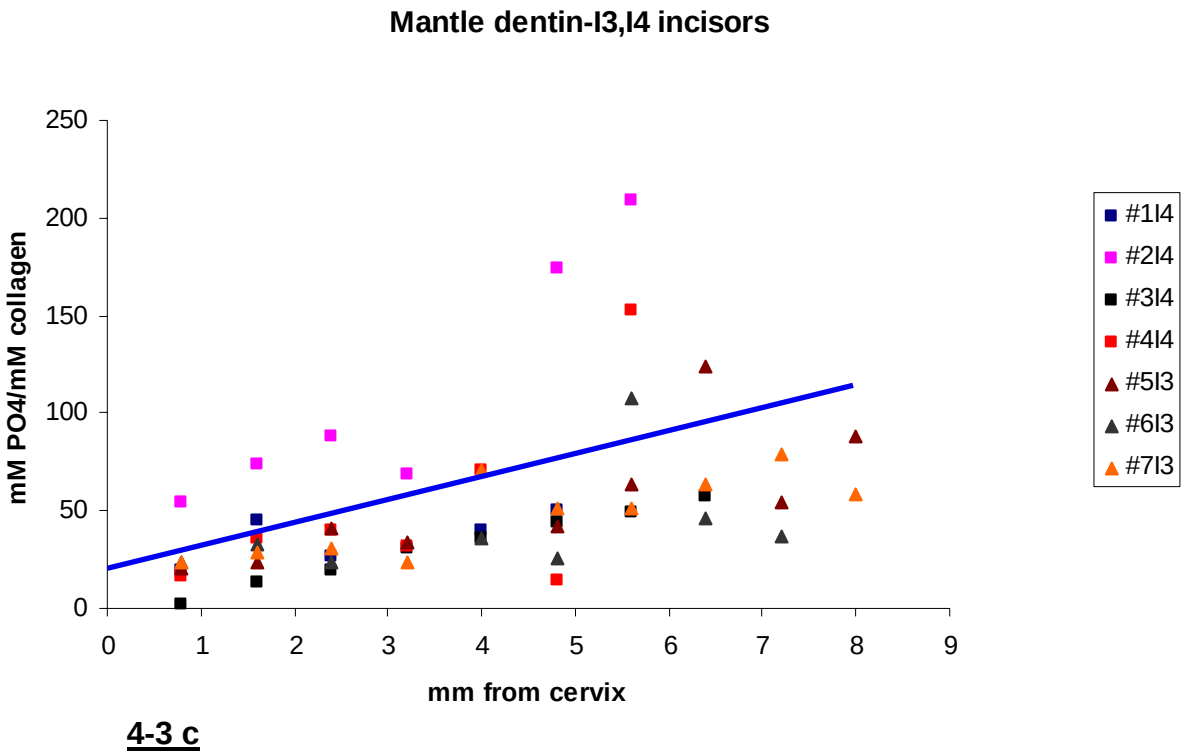

Fig. 4-3. Analysis of matrix phosphate from microdissected mantle dentin specimens as a function of location. (a): I3 incisors (b): I4 incisors (c): I3 and I4 incisors with linear regression.

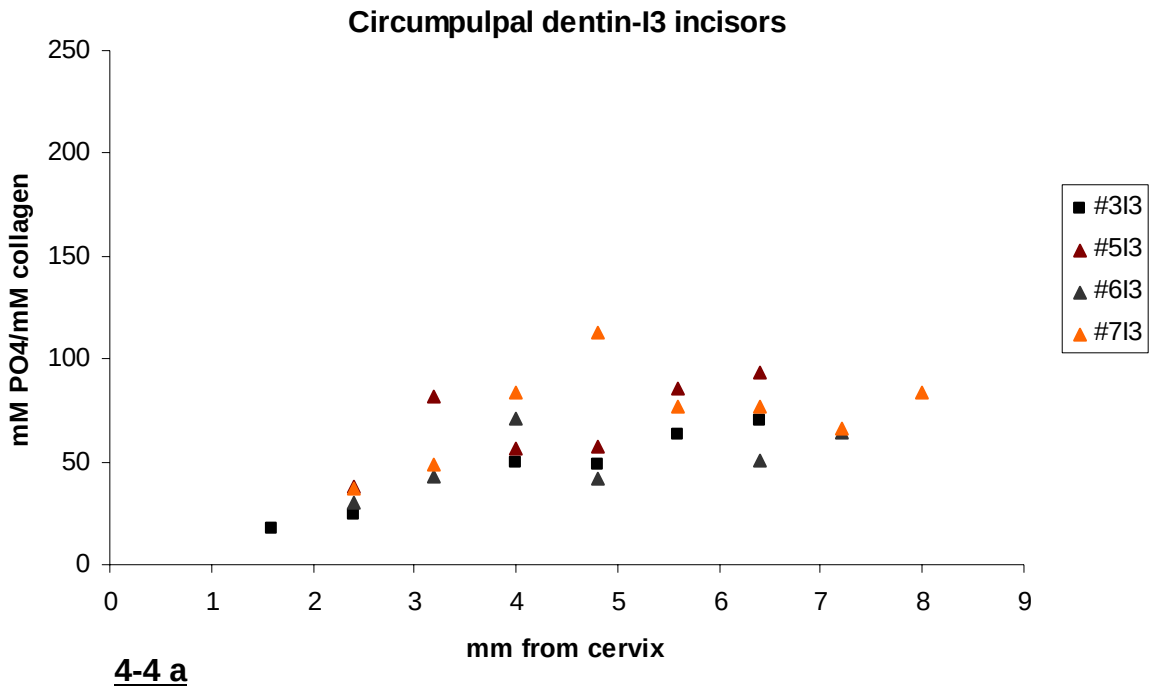
Circumpulpal dentin-I3 incisors
mM PO4/mM collagen
mm from cervix
#3I3
#5I3
#6I3
#7I3

4-4 a

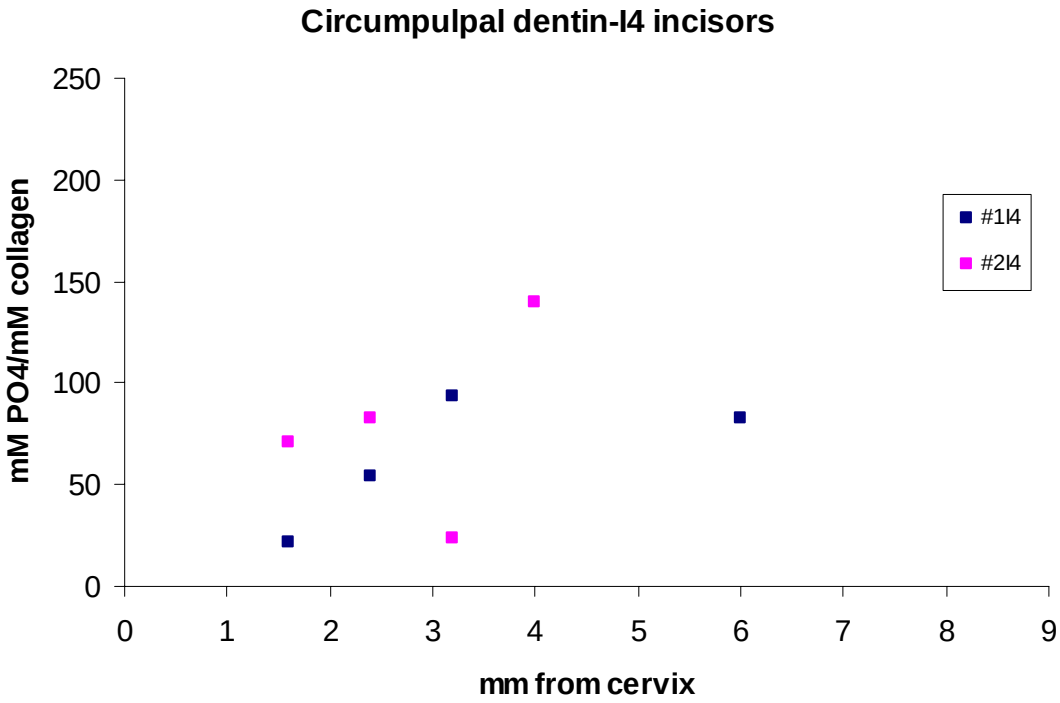
Circumpulpal dentin-I4 incisors
mM PO4/mM collagen
mm from cervix
#1I4
#2I4

4-4 b

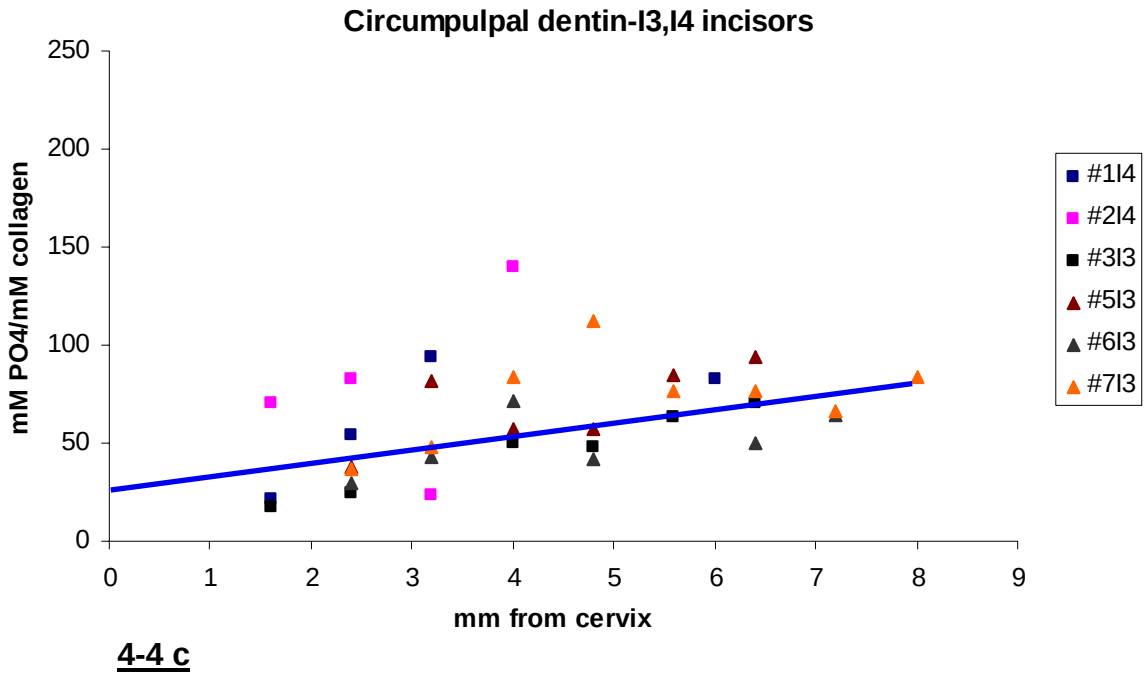

Fig. 4-4. Analysis of matrix phosphate from microdissected circumpulpal dentin specimens as a function of location. (a): I3 incisors (b): I4 incisors (c): I3 and I4 incisors with linear regression.

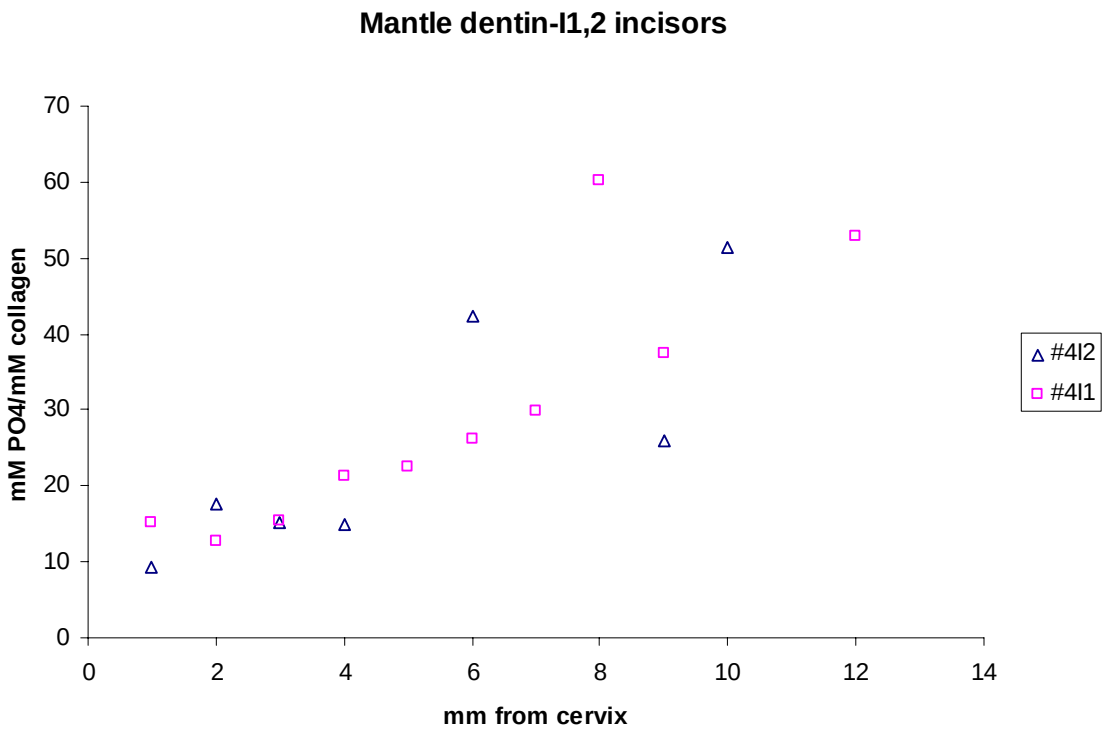

Fig. 4-5. Analysis of matrix phosphate from microdissected mantle dentin specimens as a function of location in I1 and I2 incisors.

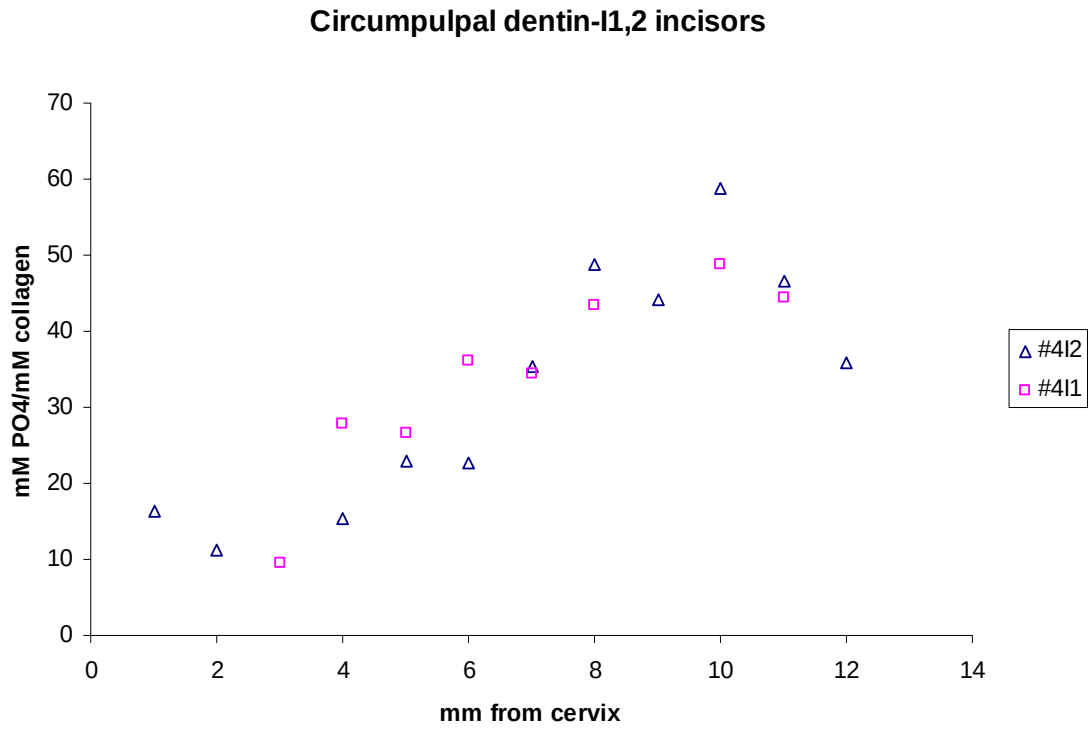

Fig. 4-6. Analysis of matrix phosphate from microdissected circumpulpal dentin specimens as a function of location in I1 and I2 incisors.

		mm from cervix	mmol PO4/mmol collagen
mm from cervix	Pearson Correlation	1	.348**
	Sig. (2-tailed)		.007
	N	64	59
mmol PO4/mmol collagen	Pearson Correlation	.348**	1
	Sig. (2-tailed)	.007	
	N	59	59

**. Correlation is significant at the 0.01 level (2-tailed).

4-1 a

		mm from cervix	mmol PO4/mmol collagen
mm from cervix	Pearson Correlation	1	.471**
	Sig. (2-tailed)		.004
	N	46	35
mmol PO4/mmol collagen	Pearson Correlation	.471**	1
	Sig. (2-tailed)	.004	
	N	35	35

**. Correlation is significant at the 0.01 level (2-tailed).

4-1 b

Table 4-1 Bivariate correlation between mmols phosphate/mmol collagen test results. (a): Mantle dentin specimens from I3-I4 incisors (b): Circumpulpal dentin from I3-I4 incisors.

Correlations

Control Variables			mm from cervix	mmol PO4/mmol collagen
1=#1I4m,2=#2I4m,3=#3I4m,4=#4I4m,5=#5I3m,6=#6I3,7=#7I3,8=#1I4c,9=#2I4c,10=#3I3c,11=#5I3c,12=#6I3c,13=#7I3c	mm from cervix	Correlation	1.000	.425
		Significance (2-tailed)	.	.001
		df	0	56
	mmol PO4/mmol collagen	Correlation	.425	1.000
		Significance (2-tailed)	.001	.
		df	56	0

4-2 a

Correlations

Control Variables			mm from cervix	mmol PO4/mmol collagen
1=#1I4m,2=#2I4m,3=#3I4m,4=#4I4m,5=#5I3m,6=#6I3,7=#7I3,8=#1I4c,9=#2I4c,10=#3I3c,11=#5I3c,12=#6I3c,13=#7I3c	mm from cervix	Correlation	1.000	.495
		Significance (2-tailed)	.	.003
		df	0	32
	mmol PO4/mmol collagen	Correlation	.495	1.000
		Significance (2-tailed)	.003	.
		df	32	0

4-2 b

Table 4-2: Partial correlation between mmols phosphate/mmol collagen contolling for incisor of origin test results. (a): Mantle dentin specimens from I3-I4 incisors (b): Circumpulpal dentin from I3-I4 incisors.

CHAPTER V

FTIRI ANALYSIS ON DEVELOPING DENTIN IN MOUSE MOLARS

INTRODUCTION

The feasibility of using developing postnatal murine molars for developing dentin studies, along with limitations existing in the particular application and patterns of mineral properties changes in normal animals is investigated in the present study. The basis for performing a study of dentin maturation on fetal bovine incisors was described and spectroscopic imaging results on developing dentin were provided in Chapter II. Results from spectral analysis of fetal bovine incisor sections and of microdissected mantle and circumpulpal dentin from the same teeth were reported in Chapter III.

There has been an increasing interest in dentin studies on mouse models concerning organogenesis and dental tissue formation (D'Souza et al, 1997; Ouyang et al, 2000; Yamashiro et al, 2003; Ye et al, 2004; Hao et al, 2004), that makes an application of the methodology used in Chapters II and III to mice particularly interesting. The purpose of this study was to examine the changes in mineral properties of developing mouse molars, using a methodology similar to that used in Chapters II and III. Aspects of the same methodology have been used on developing rat and mouse molar dentin in other studies (Engel and Hilding, 1984; Stratmann et

al, 1991; Stratmann et al, 1996; Stratmann et al, 1997; Arnold et al, 1998) although not for quantitative analysis of several dentin mineral properties at the same time, as in the present study.

METHODS AND MATERIALS

Preparation of the samples: Mandibles from eleven 6 postnatal day-old male C3H mice provided by a commercial source (Charles River Laboratories, Wilmington, MA) were used for analysis of dentin on the developing mouse molars. The mandibles were stored at -80° C until the molars were collected. Only second molars, which at this age are unerupted and have approximately ¾ of their crowns formed, were used for the present study. Soft tissue covering the unerupted molars was carefully removed, molars exposed and removed by means of a dental micro-spoon excavator. The samples were subsequently processed for dehydration and PMMA embedding, as described in Chapter II, with the following modification: after the samples were PMMA embedded and PMMA was polymerized, a small PMMA block containing the sample was cut out, using grit 800 silicon carbide paper under water irrigation on a rotating polisher machine (Ecomet 3, Buehler, Germany). This was done to trim one side of the small PMMA blocks as close as possible to the distal surface of the molars that would be sectioned and parallel to the intended sectioning plane. The trimmed block was then re-embedded in PMMA with the oriented side on the surface and polymerized, then sectioned at 4-5 μm using a sliding microtome as described previously. The final plane of sectioning was through the tip of the distal cusps and parallel to the long axis of the crown, as shown in

figure6-1 on the crown of a second permanent molar 3D reconstruction from a microcomputed tomography analysis (a developing molar was not used for the figure, due to the low contrast between the low density-mineralized young molar and background). The molar sections were placed on a BaF_2 window for FTIRI analysis immediately after sectioning.

FTIRI analysis: The experimental conditions for the FTIRI analysis were identical to those described for the fetal bovine dentin spectral analysis in Chapter III. Due to the smaller size of the mouse molars, the whole molar crown was scanned and analyzed. The spectroscopic parameters examined were the same as in Chapter III, namely mineral: matrix, mineral crystallinity, relative acidic phosphate content, carbonate: mineral, typeA:typeB of carbonate substitution in mineral, labile carbonate:typeB carbonate substitution in mineral. Again, the spectroscopic ratio 1660:1650 cm^{-1} in the Amide I (matrix) band, which reflects collagenous vs noncollagen matrix relative density (see Chapter III for details), was used to differentiate between dentin and young enamel pixels, as the mineral: matrix values for dentin and enamel in most of the 6 day-old mouse molars are very similar. In addition to analysis of images for the spectral parameters, areas of dentin next to DEJ were identified and spectra of pixels in these areas were co-added to a single spectrum, in a similar manner to the spectral processing in Chapter III. The areas in question were typically 20-28μm (3-4 pixels) wide and were spanning approximately 35μm (5 pixels) along a cervical-incisal direction. As mantle dentin in the mouse is less than 1μm –that is, a fraction of a pixel- wide, no attempt was made to differentiate between mantle and circumpulpal dentin using FTIRI in mouse molars.

RESULTS

As there were losses of one of the two molars (mostly from excessive trimming during the orientation of the preliminarily embedded molar for final embedding or during the final sectioning) in most of the jaws used, the final total number of second molars analyzed was 15. From those, 7 molars were unpaired and 4 were paired with the contralateral counterparts. As the analysis of the images and the extracted spectra results for all the parameters examined showed, there was no real correlation between the paired molars, at least not a higher one than between any two random samples. Therefore, results from the left and right molars were pooled for the purposes of this experiment.

Figure 5-2 a shows the micrograph of a second molar section. FTIRI images of the 1650:1660 cm^{-1} (noncollagenous:collagenous matrix) ratio and mineral: matrix from this section are presented respectively in figures 5-2 b and c. The low mineral density of enamel in the 6 day-old mice second molars is notable, as it appears that even the most occlusal (equivalent to cervical for the incisors) enamel parts show a lower density than dentin formed in adjacent areas. The range of mineral: matrix ratios observed in developing dentin is lower than the respective one from the fetal bovine dentin analysis. Individual spectra from pixels of analyzed young dentin seemed to have a low signal/noise (S/N), even in the 4-5 μm-thick sections analyzed, while older parts of dentin gave satisfactory S/N spectra. While young dentin spectra S/N was not high enough from individual pixels, though, it was satisfactory even in the extracted spectra from the youngest areas (figure 5-4 a).

Figures 5-3 a-f present the mineral data for the same spectroscopic parameters examined in Chapter III. The total number of observations (spectra extracted across the developing crown of all the molars analyzed) was 79. With the possible exception of mineral: matrix and crystallinity, no reproducible pattern of changes was found for these spectroscopic parameters based on results from all the molars analyzed. Mineral: matrix (5-3 a) presents a gradual increase, with a final plateau, or even a slight decrease in the occlusal parts of the crown (>300μm from the cervix). Crystallinity (5-3 b) paradoxically shows a small decrease with maturation, while the acidic phosphate content of the mineral (5-3 c) shows an increase after an initial decrease. Carbonate substitution in the mineral (5-3 d), as well as relative type A or labile carbonate substitution, did not give a reproducible patterns of change. Nevertheless, higher such reproducibility in the pattern of mineral changes was observed in molars that were actually cut at a sectioning plane close to the one intended and at a greater (4-5μm) thickness. One such molar was the one shown in figure 5-2 a. Spectra extracted from successive locations on the crown of the molar are shown in figure 5-4 a. A gradual decrease in the acidic phosphate content of the mineral was observed (5-3 b), as well as for other molars that were sectioned at a close to optimal orientation and thickness. Similarly, a decrease during maturation in type A: type B carbonate substitution (879:871 cm^{-1} relative peak height ratio) and the presence of labile carbonate (shoulder in the 866 cm^{-1} area) could be observed (figure 5-4 c) in the molars that were optimally cut.

DISCUSSION

In this study, the feasibility of applying the methodology used in Chapters II and III to analysis of dentin from mouse molars was investigated. Molars were used rather than incisors, as they have been studied more extensively from an organogenesis and development point of view also because incisors in rodents have a complex anatomy (a crown-analogue and a root-analogue aspects of crown) and are continuously erupting, making post natal comparisons difficult. The present results did not conclusively support specific patterns in changes of mineral properties that could be shown from all of the molars analyzed. Contrary to what was shown in Chapter III, in this study patterns of changes in mineral properties varied widely between the samples analyzed. From analysis of the imaging results, it was concluded that spatial variability within the mouse molar dentin is an especially critical factor in similar dentin studies. As cusps develop from a growth center outwards and down the cusp slope, a concentric pattern of development arises. This renders the exact positioning of sectioning plane through the centers of the cusps and parallel to the long axis of the crown central to the outcome of the analysis. It has also been described (Gaunt, 1955) that the posterior aspect of the crown develops at a greater rate than the anterior, making precise orientation even more important. Another limiting factor in the present methodology was the resolution provided by FTIRI as the analytical method. This level of resolution appears to be too low to analyze the thin young dentin areas, the width of which in most of the samples was a total of approx. 20μm (3 pixel rows). This probably did not represent adequate tissue for acquiring reproducible results from this particular area. Finally, the failure to recognize in the results patterns of mineral properties changes similar

to the ones described for fetal bovine dentin in Chapters II and III might be due to different maturation mechanisms between the two species. In enamel, such differences have been reported to exist between human and porcine teeth (Kirkham et al, 1988), as porcine mature enamel has a much lower mineral density and a much higher matrix content than human enamel. Optimizing the methodology for future studies on developing mouse molar dentin would involve using samples from an older stage, probably 10 day-old animals, and using 2 different thicknesses of section to carry out analysis on strong and weak IR bands. Also, modifying the embedding and sectioning technique for consistently orienting and sectioning the specimens along the intended plane on the crown appear essential. Raman microprobe analysis might also prove a valuable alternative, as it provides adequate spatial resolution (down to 1μm) and does not require sectioning of the samples. Dentin studies have been conducted using Raman vibrational spectroscopy (Tsuda et al, 1996) and successful applications of the Raman microprobe method have been described in biological samples (Diem et al, 2004).

The concept of a line analysis along the tooth crown for study of the dentin mineral ultrastructure (Plate et al, 1994), histologic (Kagayama et al, 1997) and elemental composition (Steinfort et al, 1991) changes has been applied on rat incisors and molars. All of the above studies employed high resolution analytical methods. In the study on rat molars (Kagayama et al, 1997), the development of interglobular dentin (which was the subject of the study) on the molar was concluded to be “time- and position- specific”, implying that some inherent spatial variability of dentin histology is involved on mouse molars. Elemental composition changes in

developing enamel (Lundgren et al, 1998) have been studied using a line analysis along the crown principle. Elemental analysis data on developing dentin and enamel from mouse molars has also been reported in one study (Engel and Hilding, 1984). In that study, analysis for Ca and P was conducted on molars from 5, 8 and 14 day-old animals, at predetermined points at different distances from DEJ in dentin and enamel. While a substantial increase (up to 20fold) was shown for enamel for equidistant from the DEJ locations between 5 and 14 day-molars, from both Ca and P concentrations, the equivalent concentrations in dentin did not differ more than 50% in dentin. It is possible that this study focused on a location in the developing crown, where dentin was already close to maturity even from day 5. Enamel mineral, at the same location, was relatively immature at day 5 and attained much higher density levels through day 14. The same pattern was shown in our results, where enamel presented on an average much lower mineral density for the same location on the crown molar than dentin at day 6.

In conclusion, studies on the developing mineral of mouse molar dentin appear to require thicker sections or a denser tissue for successful analysis. For denser tissue, 1st molars from the same age (6 day-old) or older 2nd molar samples should be used and the mineral change results they provide should be evaluated. Use of different techniques providing similar information, such as Raman microprobe analysis, may be needed.

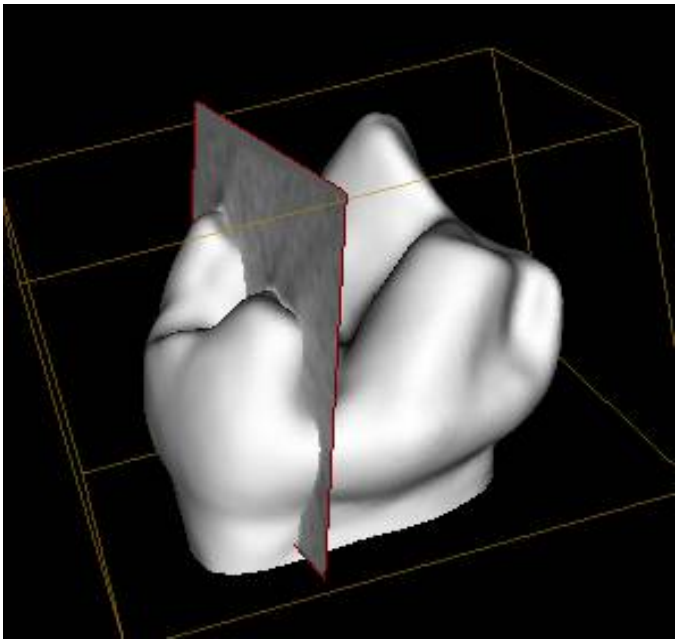

Fig. 5-1 : Plane of sectioning used on 6 day- developing second molars demonstrated on a mature second molar from a 3D microcomputed tomography reconstruction.

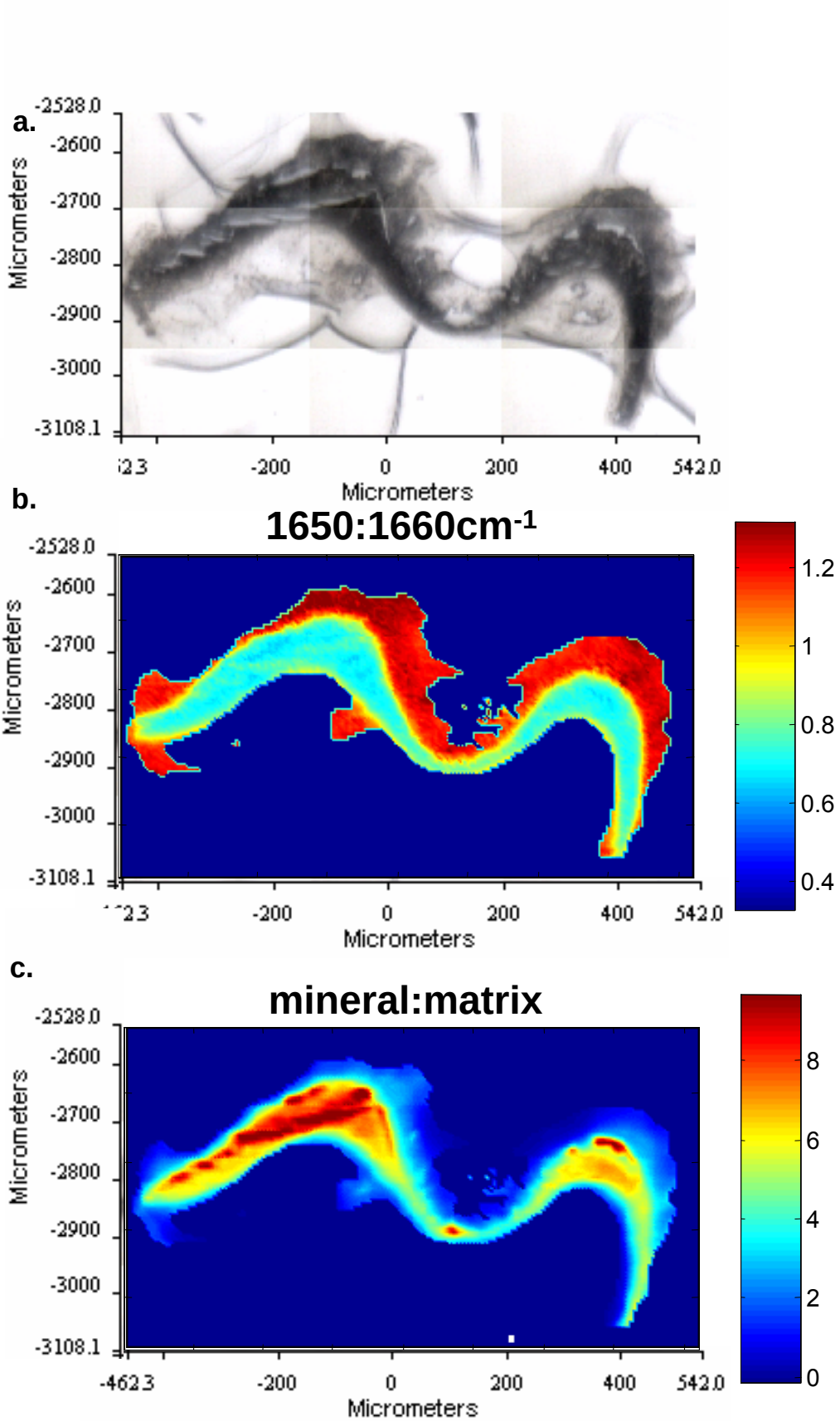

Fig. 5-2 : FTIRI analyzed 6 day-old 2nd mouse molar. (a): Optical micrograph (b):1650:1660cm^{-1} (noncollagenous:collagenous matrix) image (c):Mineral:matrix image

(Next 2 pages) **Fig. 5-3**: Spectral data from FTIRI of all mouse molars. (a): Mineral/matrix (b): Crystallinity of the mineral (c): Relative acidic phosphate content of the mineral (d): Relative carbonate content in the mineral (e): Relative type A carbonate subsitution in the mineral (f): Relative labile carbonate content in the mineral.

5-3 a

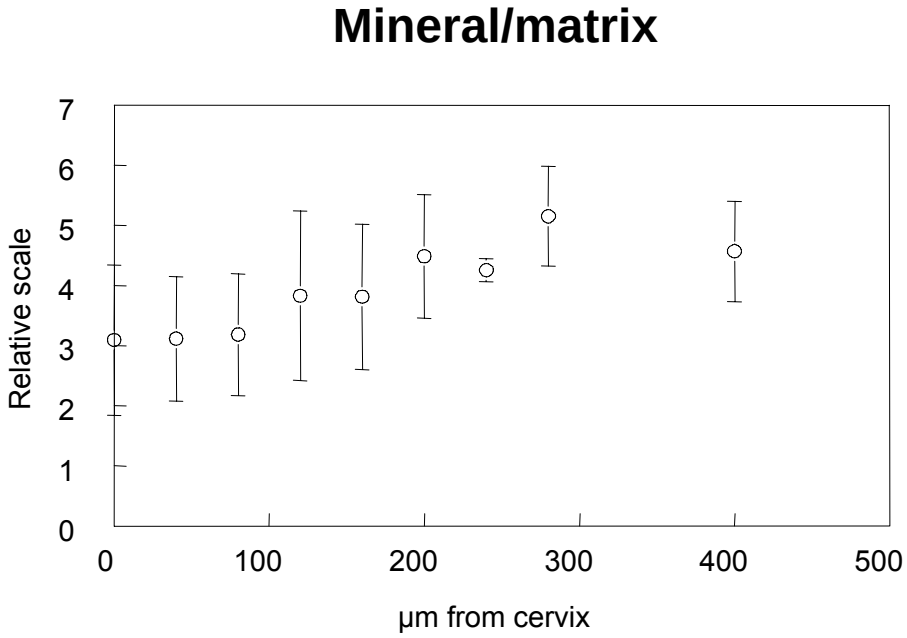
Mineral/matrix
Relative scale
0
1
2
3
4
5
6
7
0
100
200
300
400
500
µm from cervix

5-3 b

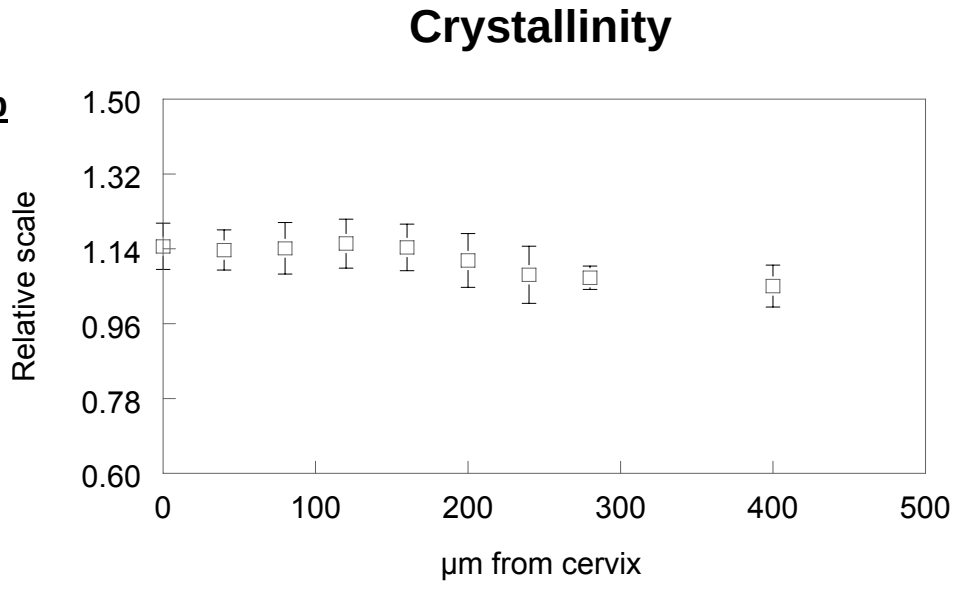
Crystallinity
Relative scale
0.60
0.78
0.96
1.14
1.32
1.50
0
100
200
300
400
500
µm from cervix

Relative acidic phosphate content

5-3 c

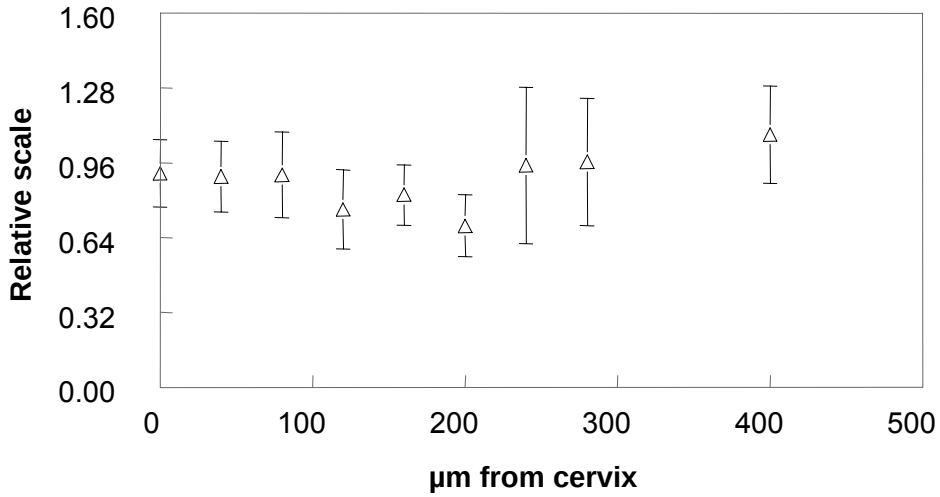

Carbonate/mineral

5-3 d

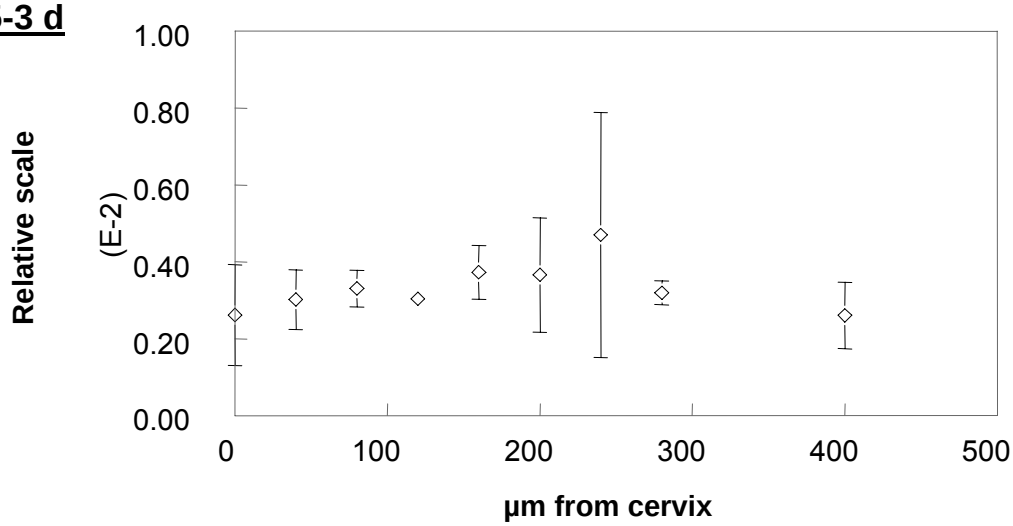

5-3 e

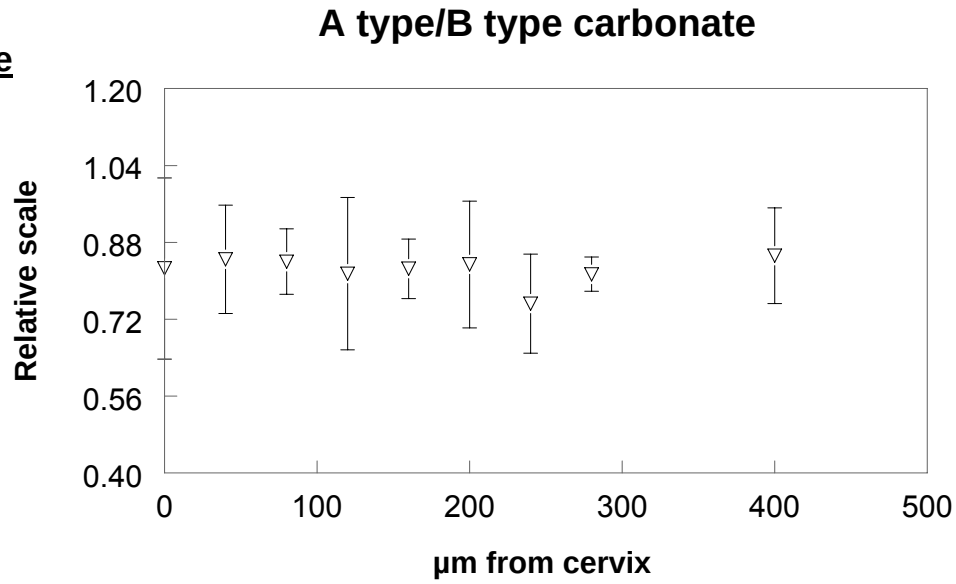
A type/B type carbonate
Relative scale
1.20
1.04
0.88
0.72
0.56
0.40
0
100
200
300
400
500
µm from cervix

5-3 f

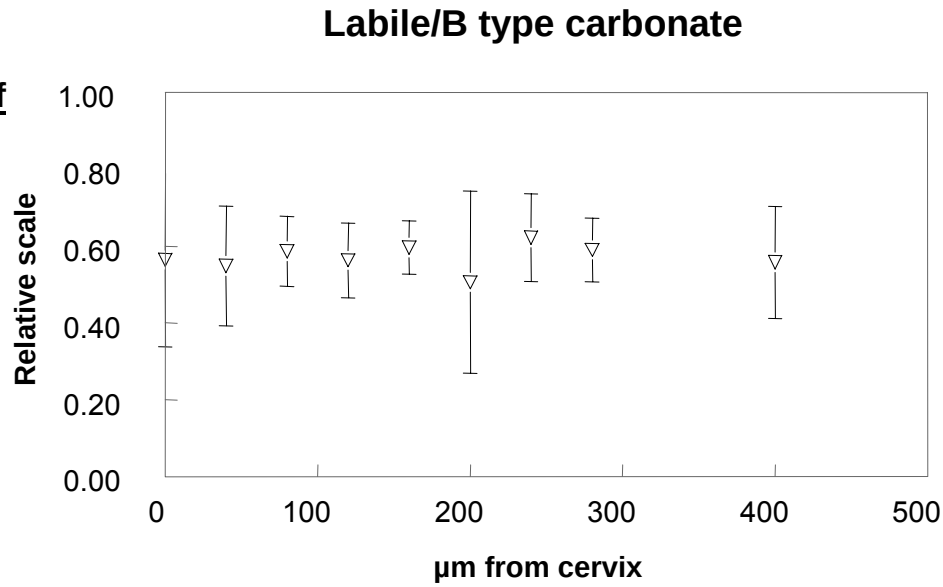
Labile/B type carbonate
Relative scale
1.00
0.80
0.60
0.40
0.20
0.00
0
100
200
300
400
500
µm from cervix

(Next 2 pages) **Fig. 5-4**: Superimposed spectra extracted from FTIRI analysis of molar shown in 5-2a. (a): The whole spectral range. Scale for every spectrum adjusted after normalization of the total marix (Amide I) areas (b) v_1v_3 PO43- bands of spectra shown in a. Peak heights have been normalized to enable comparison. (c):v_2 carbonate bands. Peak heights have been normalized to enable comparison.

5-4 a

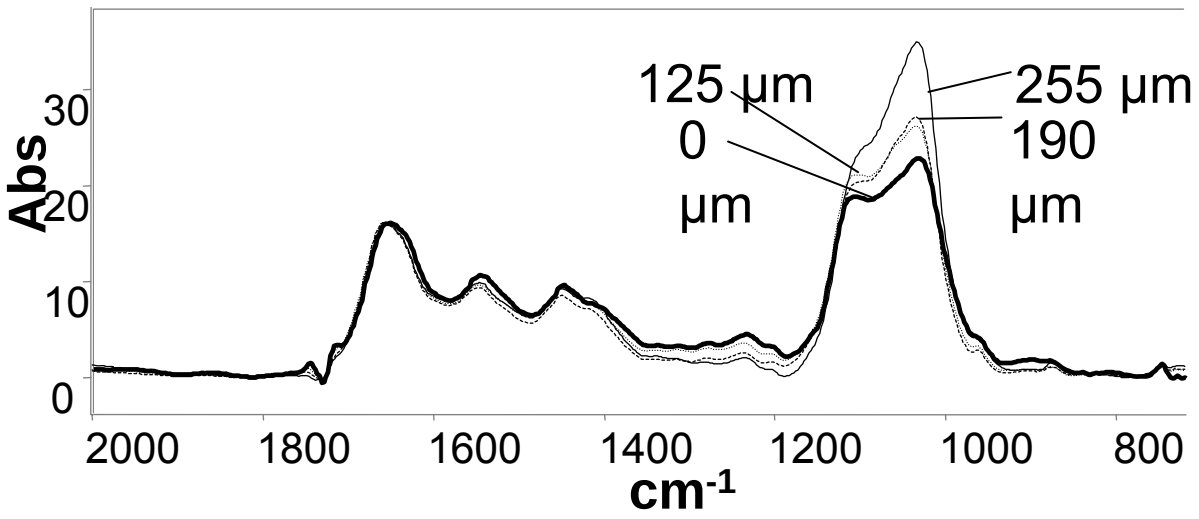
125 µm
255 µm
0
µm
190
µm
Abs
30
20
10
0
2000
1800
1600
1400
1200
1000
800
cm-1

5-4 b

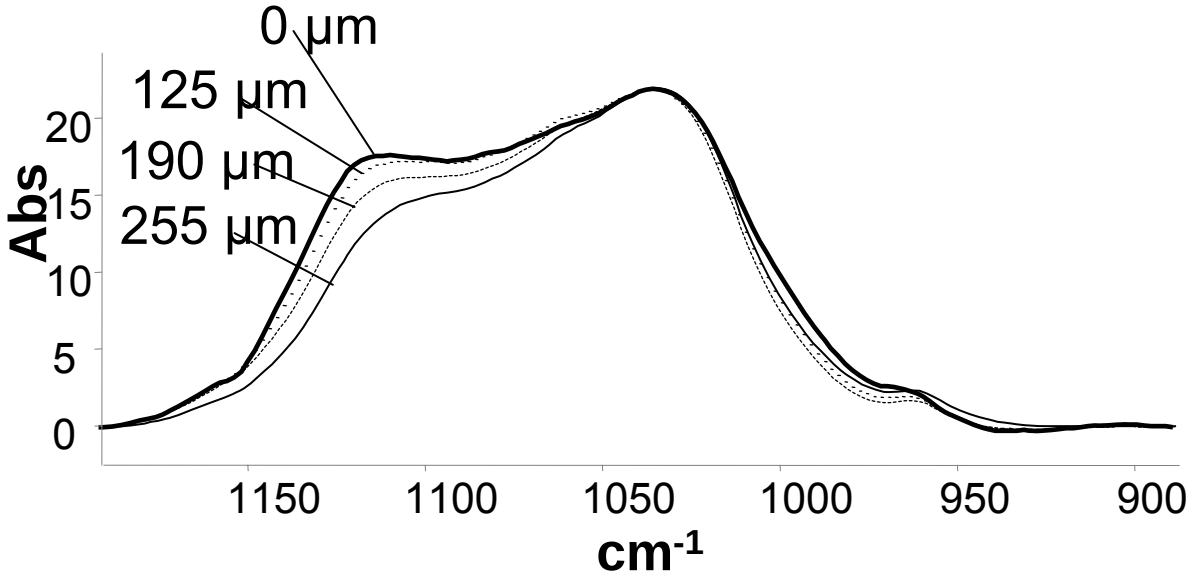
0 µm
125 µm
190 µm
255 µm
Abs
20
15
10
5
0
1150
1100
1050
1000
950
900
cm-1

5-4 c

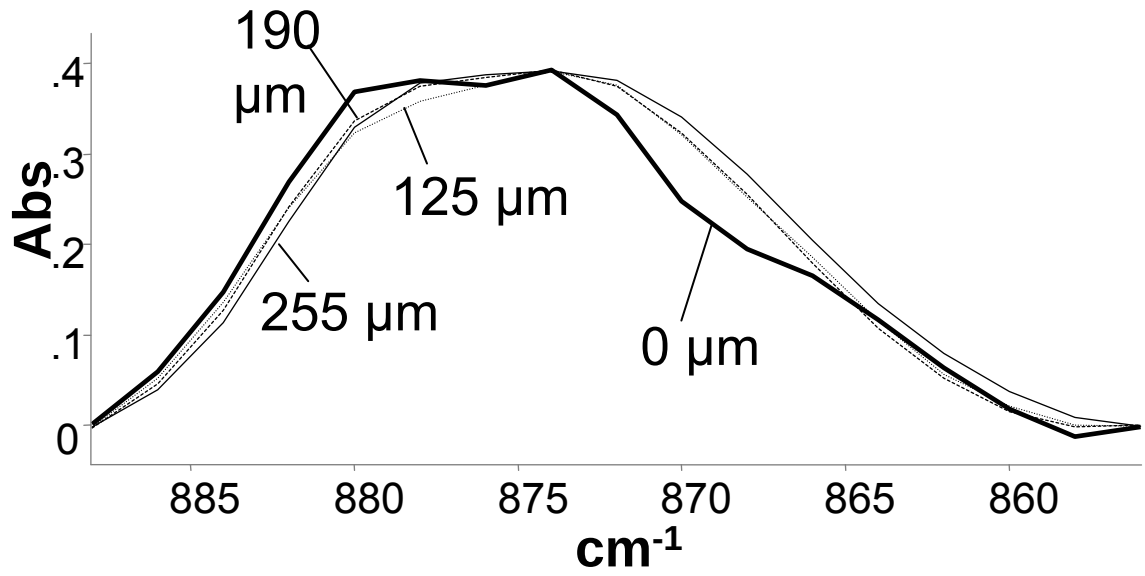

CHAPTER VI

SUMMARY AND CONCLUSIONS

In the studies of this dissertation, the use of a fetal bovine incisor model analyzed by FTIRI for the study of mineral changes during dentin maturation was evaluated, the evolution in maturation of mantle and circumpulpal dentin as two dentin compartments distinct in mineral properties was established and changes in these mineral properties during maturation in mantle and circumpulpal dentin were described. Changes in properties of the dentin matrix during maturation were also analyzed by FTIR spectroscopy, organic phosphate and amino acid analyses. Finally, the application of the same analytical method in 6 day-mouse molars was evaluated.

In Chapters II and III, imaging analysis for mineral properties and spectral analysis of mantle and circumpulpal dentin areas of successive tissue ages for the same mineral properties was performed on dentin of fetal bovine incisors. It was shown that during dentin maturation there is an increase in mineral:matrix and crystallinity of the mineral, while the relative content of mineral in acidic phosphate decreases. This pattern holds true for both mantle and circumpulpal dentin and the biggest part of the changes described mainly occurs in early stages of maturation, while in later stages the levels for the same mineral properties reach a plateau or continue changing very gradually. Based its lower levels of mineral:matrix and

crystallinity, a mantle dentin zone could be differentiated from circumpulpal dentin early in maturation and continued to represent an approximately 80-100μm wide dentin strip next to DEJ (for lateral I3 and I4 incisors) through final maturation stages, as also evidenced in analyzed 1 year-old incisors. No significant changes were found to occur in the levels of carbonate substitution in dentin, with the exception of a small increase in mantle dentin at later maturation stages. The relative type of carbonate substitution (substitution for phosphate or hydroxyl ions or presence of labile carbonate) was also not found to vary significantly during maturation, again with the exception of a decrease in the relative A type carbonate (substitution for hydroxyl ions) in mantle dentin at later stages. When compared to the existing data on bone maturation, these results show a higher and steeper mineral:matrix increase, but lower crystallinity increase and no changes in carbonate substitution, whereas in bone the carbonate content has been described to increase or decrease, depending on the model used. While the same tissue age-dependent variations in mineral properties were observed on the left and right incisors as groups of samples, there was not a 1:1 correspondence in the distribution of these properties values between individual left incisors and their right counterparts. This suggested that factors such as reproducibility in the sectioning plane orientation may contribute to similar studies' outcomes. Additionally, the presence of functional interfaces around the mineralization front and the dentinoenamel junction was shown by the distribution of mineral:matrix and crystallinity at the respective sites for all maturational stages.

Based on the FTIR imaging results approximately 80μm wide dentin areas of mantle dentin and of circumpulpal dentin immediately adjacent to mantle at successive maturational stages were identified on fetal bovine incisors and specimens from these areas were microdissected. Matrix properties (Chapter III), matrix relative content in phosphoproteins and overall phosphorylation (Chapter IV) were subsequently analyzed in these dentin specimens. The relative water content of the matrix was found to be greatly decreased during dentin maturation, again mainly during the initial maturational stages, by roughly the same amount for mantle and for circumpulpal dentin. A significant shift of the peak of the matrix main vibrational mode (Amide I) from early to later maturational stages that was identified suggested a change in the matrix secondary structure that is probably associated with the changes in the matrix hydration. The relative total matrix phosphate content of similar microdissected specimens presented a significant increase, while the amino acid analysis of the same specimens did not support any significant difference in phosphoprotein content of the matrix during dentin maturation. These results gave evidence for a continued phosphorylation of phosphoproteins in mineralizing dentin, which implied an involvement of phosphoproteins in later maturational stages.

When the same FTIRI analysis was applied to developing dentin of 6 day-old mouse molars (Chapter V), a continuous change in the mineral:matrix was shown occuring in a range much lower than in fetal bovine incisors. Crystallinity did not show a steady increase as in the fetal bovine incisors. Reproducibility in the mineral

changes results was found to be highly dependent on the specimen orientation during sectioning.

These studies provided a refined model for analysis and a description of mineral and matrix changes separately for mantle and circumpulpal dentin at true successive maturational stages and without any superimposed histological variability. It also provided a baseline for studying changes in developing dentin in other species (human, rodents) and in the presence of disease, where the relevant studies would provide a better understanding of pathogenesis in dental tissues. The present data will equally complement data on mineralization in reparative dentin, with a view to maximizing the reparative dentin mineral and biomechanical properties in future studies. The described matrix properties findings supported a pronounced decrease in the dentin water content that had not been clearly described for mantle and circumpulpal dentin, which can be quantitatively estimated by weight determination in future studies. These studies also provided evidence of a continued matrix phosphorylation in mineralizing dentin, a fact that merits further investigation by analysis of casein kinase activity in dentin or of post-translational modifications of matrix proteins from different tissue age dentin specimens. The possibilities and limitations of general methodology based on FTIRI analysis application on developing mouse dentin were also investigated for the first time. If that methodology is optimized, probably by using higher resolution analytic techniques and a highly reproducible specimen preparation method, for the purpose, the transfer of all the mentioned kinds of studies to animals genetically targeted for one or more matrix proteins will be possible.

ACKNOWLEDGMENTS

The author is thankful to the advisors (A.L. Boskey and J. Timothy Wright) and the other members of the thesis committee (P. Flood, R. Arnold, R. Murray, W. Duarte) for their guidance and support. He is also very thankful to L. Lukashova for the great effort she contributed to this thesis. Without their support this thesis would not have been realized. The studies described were supported by NIH grants K08 00467 and DEO 4141..

BIBLIOGRAPHY

About, I., Bottero, M.J., de Denato, P., Camps, J., Franquin, J.C., Mitsiadis, T.A. (2000). Human dentin production in vitro. Experimental Cell Research, 258(1), 33-41.

About, I., Mitsiadis, T.A. (2001). Molecular aspects of tooth pathogenesis and repair: in vivo and in vitro models. Advances in Dental Research, 15, 59-62.

About, I., Camps, J., Mitsiadis, T.A., Bottero, M.J., Butler, W., Franquin, J.C. (2002).Influence of resinous monomers on the differentiation in vitro on human pulp cells into odontoblasts. Journal of Biomedical Materials Research , 63(4), 418-423.

Addadi, L., Weiner, S. (1985). Interactions between acidic proteins and crystals: Stereochemical requirements in biomineralization. Proceedings of the National Academy of Sciences of the United States of America, 82(12), 4110-4114.

Addadi, L., Moradian-Oldak, J., Furedi-Milhofer, H., Weiner, S., Veis, A. (1992). Stereochemical aspects of crystal regulation in calcium phosphate-associated mineralized tissues. In: Slavkin, H.C., Price, P.A. Chemistry and Biology of mineralized tissues. New York: Elsevier, p 153-176.

Ameye, L., Aria, D., Jepsen, K., Oldberg, A., Xu, T., Young, M.F. (2002). Abnormal collagen fibrils in tendons of biglycan/fibromodulin-deficient mice lead to gait impairment, ectopic ossification, and osteoarthritis. The Federation of American Societies for Experimental Biology journal, 16, 673-680.

Aoba, T., Moreno, E.C. (1990). Changes in the nature and composition of enamel during porcine amelogenesis. Calcified Tissue International, 47(6), 356-364.

Aparicio, S., Doty, S.B., Camacho, N.P., Paschalis, E.P., Spevak, L., Mendelsohn, R., Boskey, A.L. (2002). Optimal methods for processing mineralized tissues for Fourier transform infrared microspectroscopy. Calcified Tissue International, 70(5), 422-429.

Arnold, S., Plate, U., Wiesmann, H.P., Stratmann, U., Kohl, H., Höhling, H.J. (1999). Quantitative electron spectroscopic diffraction analyses of the crystal formation in dentine. Journal of Microscopy, 195, 58-63.

Arsenault, A.L. (1989). A comparative electron microscopic study of apatite crystals in collagen fibrils of rat bone, dentin and calcified turkey leg tendon. Bone and Mineral, 6(2), 165-77.

Atti, E., Gomez, S., Wahl, S.M., Mendelsohn, R., Paschalis, E.P., Boskey, A.L. (2002). Effects of transforming growth factor-beta deficiency on bone development: a Fourier transform-infrared imaging analysis. Bone, 31(6), 675-684.

Bailey, R., Holt, C. (1989). In: Calcified Tissues. Hukins D.W., (eds) Houndmills, Basingstoke, Great Britain: Mc Millan Press.

Banes, A.J., Yamauchi, M., Mechanic, G.J. (1983). Nonmineralized and mineralized compartments of bone. The role of pyridinoline in nonmineralized collagens. Biochemical and Biophysical Research Communications, 113, 975-981.

Baykov, A.A., Evtushenko, O.A., Avaeva, S.M. (1988). A malachite green procedure for orthophosphate determination and its use in alkaline phosphatase-based enzyme immunoassays. Analytical Biochemistry, 171, 266-270.

Bernard, G.W. (1972). Ultrastructural observations of initial calcification in dentin and enamel. Journal of Ultrastructure Research, 41, 1-17.

Bhargava, R., Levin, I.W. (2001). Fourier Transform Infrared Imaging: theory and practice. Analytical Chemistry, 73(21), 5157-5167.

Bodier-Houllé, P., Steuer, P., Meyer, J.M., Bigeard, L., Cuisinier, F.J.G. (2001). High-resolution electron-microscopic study of the relationship between human enamel and dentin crystals at the dentinoenamel junction. Cell and Tissue Research, 301, 389-395.

Bohic, S., Heyman, J.A., Pouezat, J.A., Guathier, O., Daculci, G. (1998). Transmission FT-IR microspectroscopy of mineral phases in calcified tissues. Comptes rendus de l'Academie des sciences. Serie III, Sciences de la vie, 321(10), 865-876.

Bonar, L.C., Roufosse, A.H., Sabine, W.K., Grynpas, M.D., Glimcher, M.J. (1983). X-ray diffraction studies of the crystallinity of bone mineral in newly synthesized and density fractionated bone. Calcified Tissue International, 35(2), 202-209.

Bonar, L.C., Shimizu, M., Roberts, J.E., Griffin, R.G., Glimcher, M.J. (1991). Structural and composition studies on the mineral of newly formed enamel: a chemical, x-ray diffraction and 31P proton nuclear magnetic resonance study. Journal of Bone and Mineral Research, 6(11), 1167-1176.

Boskey, A.L., Posner, A.S. (1976). In vitro nucleation of hydroxyapatite by a bone calcium-phospholipid-phosphate complex. Calcified Tissue Research, 22(S), 197.

Boskey, A.L., Goldberg, M.R., Posner, A.S. (1978). Calcium-phospholipid-phosphate complexes in mineralizing tissue. Proceedings of the Society for Experimental Biology and Medicine, 157, 590.

Boskey, A.L. (1989). Phospholipids and Calcification. In: The Connective Tissue Matrix. Vol. III. Hukins D.W.L. , editor. Ch. 9, 284-381.

Boskey, A.L., Maresca, M., Doty, S., Sabsay, B., Veis, A. (1990). Concentration-dependent effects of dentin phosphophoryn in the regulation of in vitro hydroxyapatite formation and growth. Bone and Mineral, 11(1), 55-65.

Boskey, A.L., Maresca, M., Wikstrom, B., Hjerpe, A. (1991). Hydroxyapatite formation in the presence of proteoglycans of reduced sulfate content: studies in the brachymorphic mouse. Calcified Tissue International, 49(6), 389-393.

Boskey, A.L., Maresca, M., Ullrich, W., Doty, S.B., Butler, W.T., Prince, C.W. (1993). Osteopontin-hydroxyapatite interactions in vitro: inhibition of hydroxyapatite formation and growth in a gelatin-gel. Bone and Mineral, 22(2), 147-159.

Boskey, A.L., Goldberg, M. (1996). Biomineralization and lipids. Progress in Histochemistry and Cytochemistry, 31(2), 1-187.

Boskey, A.L., Boyan, B.D., Schwartz, Z. (1997). Matrix vesicles promote mineralization in a gelatin gel. Calcified Tissue International, 60(3), 309-315.

Boskey, A.L., Spevac, M., Doty, S., Rosenberg, L. (1997). Effects of bone proteoglycans decorin and biglycan on hydroxyapatite formation in a gelatin gel. Calcified Tissue International, 61, 298-305.

Boskey, A.L., Gadaleta, S., Gundberg, C., Doty, S., Ducy, P., Karsenty, G. (1998). FTIR microspectroscopic analysis of bones of osteoclastic deficient mice provides insight into the function of osteocalcin. Bone, 23, 187.

Boskey, A.L., Wright, T.M., Blank, R.D. (1999). Collagen and bone strength. Journal of Bone and Mineral Research, 14(3), 350-355.

Boskey, A.L., Stiner, D., Binderman, I., Doty, S.B. (2000). Type I collagen influences cartilage calcification: an immunoblocking study in differentiating chick limb-bud mesenchymal cell cultures. Journal of Cellular Biochemistry, 79(1), 89-102.

Boskey, A.L. (2001). Bone mineralization. In: Bone Mechanics Handbook. Boca Raton, Florida: S.C. Cowin (Ed) CRC Press.

Boskey, A.L., Paschalis, E.P., Binderman, I., Doty, S.B. (2002). BMP-6 accelerates both chondrogenesis and mineral maturation in differentiating chick limb-bud mesenchymal cell cultures. Journal of Cellular Biochemistry, 84(3), 509-519.

Boskey, A.L., Spevak, L., Paschalis, E., Doty, S.B., McKee, M.D. (2002). Osteopontin deficiency increases mineral content and mineral crystallinity in mouse bone. Calcified Tissue International, 71(2), 145-1,54.

Boskey, A.L. (2003). Bone mineral crystal size. Osteoporosis international, 14(S 5), 16-21.

Boskey, A.L., Moore, D..J, Amling, M., Canalis, E., Delany, A.M. (2003). Infrared analysis of the mineral and matrix in bones of osteonectin-null mice and their wildtype controls. Journal of Bone and Mineral Research, 18(6), 1005-1011.

Boskey, A.L., Mendelsohn, R. (2005). Infrared spectroscopic characterization of mineralized tissues. Vibrational Spectroscopy, 38, 107-114.

Bronckers, A.L., Lyaruu, D.M., Woltgens, J.H.M. (1989). Immunohistochemistry of extracellular matrix proteins during various stages of dentinogenesis. Connective Tissue Research, 22, 65-70.

Butler, W.T., Brown, M., Dimuzio, M.T., Linde, A. (1981). Noncollagenous proteins of dentin. Isolation and partial characterization of rat dentin proteins and proteoglycans by a three-step preparation method. Collagen and Related Research, 1, 187-199.

Butler, W.T. (1984). Dentin collagen: chemical structure and role in mineralization. In: Dentin and Dentinogenesis. Vol. II. A. Linde, Ed. Boca Raton, Florida: CRC Press.

Butler, W.T. (1995). Dentin Matrix Proteins and Dentinogenesis. Connective Tissue Research, 33(nos 1-3), 59-65.

Butler, W.T., Richie, H.H., Bronckers, A.L. (1997). Extracellular matrix proteins of dentine. In Dental Enamel. Wiley, Chichester, Ciba Foundation Symposium 205. p 107-117.

Butler, W.T. (1998). Dentin matrix proteins. European Journal of Oral Sciences, 106 Suppl (1), 204-210.

Camacho, N.P., Landis, W.J., Boskey, A.L. (1996). Mineral changes in a mouse model of osteogenesis imperfecta detected by Fourier transform infrared microscopy. Connective Tissue Research, 35(1-4), 259-265.

Camacho, N.P., West, P., Torzilli, P.A., Mendelsohn, R. (2001). FTIR microscopic imaging of collagen and proteoglycans in bovine cartilage. Biopolymers, 62(1), 1-8.

Camarda, A.J., Butler, W.T., Finkelman, R.D., Nanci, A. (1987). Immunochemical localization of γ-carboxyglutamic acid-containing proteins (osteocalcin) in rat bone and dentin. Calcified Tissue International, 40, 349-355.

Caterson, B., Griffin, J., Mahmoodian, F., Sorrell, J.M. (1990). Monoclonal antibodies against chondroitin sulfate isomers: their use as probes for investigating proteoglycan metabolism. Biochemical Society Transactions, 18(5), 820-823.

Chenu, C, Ibaraki, K, Gehron, Robey, P, Delmas, PD, Young, MF. (1994) Cloning and sequence analysis of bovine bone sialoprotein cDNA: conservation of acidic domains, tyrosine sulfation consensus repeats, and RGD cell attachment domain. Journal of Bone and Mineral Research 9(3), 417-21.

Chiou, J.S., Krishna, P.R., Kamaya, H., Ueda, I. (1992). Alcohols dehydrate lipid membranes: an infrared study on hydrogen bonding. Biochimica et Biophysica Acta, 1110(2), 225-33.

Coclica, V., Brudevold, F., Amdur, B.H. (1969). The distribution and composition of density fractions from human crown dentine. Archives of Oral Biology, 14, 451-460.

D'Souza, R.N., Cavende, A., Sunavala, G., Alvarz, J,. Ohshima, T., Kulkarni, A.B., MacDougall, M. (1997). Gene expression patterns of murine dentin matrix protein 1 (DMP 1) and dentin sialophosphoprotein (DSPP) suggest distinct developmental functions in vivo. Journal of Bone and Mineral Research 12(12), 2040-2049.

DeJong, W.F. (1926). La substance minerale dans les os. Recueil des Travaux Chimiques des Pays-Bas, 45, 445-448.

Deutsch, D. (1989). Structure and function of enamel gene products. The Anatomical Record, 224, 189-210.

Diem, M., Romeo M., Boydston-White S., Miljkovic M., Matthaus C. (2004) A decade of vibrational micro-spectroscopy of human cells and tissue (1994-2004). Analyst 129(10), 880-5.

Dimuzio, M.T., Veis, A. (1978). Phosphophoryns-Major noncollagenous proteins of rat incisor dentin. Calcified Tissue International, 25, 169-178.

Dimuzio, M.T., Veis, A. (1978). The biosynthesis of phosphophoryns and dentin collagen in the continuously erupting rat incisor. Journal of Biological Chemistry, 253, 6845-6852.

Doyle, B.B. (1975). Infrared spectroscopy of collagen and collagen-like polypeptides. Biopolymers, 14, 937-957.

Eisenmann, D.R., Glick, P.L. (1972). Ultrastructure of initial crystal formation in dentin. Journal of Ultrastructure Research, 41, 18.

Embery, G., Hall, R., Waddington, R., Septier, D., Goldberg, M. (2001). Proteoglycans in dentinogenesis. Critical Reviews in Oral Biology and Medicine,12(4), 331-349.

Endo, A. (1987). Potential role of phosphoprotein in collagen mineralization- an experimental study in vitro. Nippon Seikeigeka Gakkai Zasshi, 61, 563-69.

Erben, R.G. (1997). Embedding of bone samples in methylmethacryalate: an improved method suitable for bone histomorphometry, histochemistry and immunohistochemistry. The Journal of Histochemistry and Cytochemistry, 45(2), 307-313.

Faibish, D., Gomes, A., Boivin, G., Boskey, A.L. (2005). Infrared imaging of calcified tissues in bone biopsies from adults with osteomalacia. Bone 36, 6-12.

Fanchon, S., Bourd, K., Septier, D., Everts, V., Beertsen, W., Menashi, S., Goldberg, M. (2004). Involvement of matrix metalloproteinases in the onset of dentin mineralization. European Journal of Oral Sciences, 112(2), 171-176.

Fernandez, D.C., Bhargava, R., Hewitt, S.M., Levin, I.W. (2005). Infrared spectroscopic imaging for histopathologic recognition. Nature Biotechnology, 23(4), 469-467.

Fisher, L.W., Termine, J.D., Dejter, S.W., Whitson, S.W., Yanagishita, M., Kimura, J.H., Hascall, V.C., Kleimann, H.K., Hassel, J.R., Nilsson, B. (1983). Proteoglycans of the developing bone. The Journal of Biological Chemistry, 258, 6588-6594.

Fisher, L.W., Torchia, D.A., Fohr, B., Young, M.F., Fedargo, N.S. (2001). Flexible structures of SIBLING proteins, bone sialoprotein and osteopontin. Biochemical and Biophysical Research Communications, 280, 460-465.

Fratzl, P., Groschner, M., Vogl, G., Plenk, H., Eschlberger, J., Klaushofer, K. (1992). Mineral crystals in calcified tissues: A comparative study by SAXS. Journal of Bone and Mineral Research, 7, 329-334.

Fratzl, P., Fratzl, N., Klaushofer, K. (1993). Collagen packing and mineralization. An x-ray investigation of turkey leg tendon. Biophysical journal, 64(1), 260-266.

Fujisawa, R., Nodasaka, Y., Kuboki, Y. (1995). Further characterization of interaction between bone sialoprotein (BSP) and collagen. Calcified Tissue International, 56(2), 140-144.

Fujisawa, R., Kuboki, Y. (1998). Conformation of dentin phosphophoryn adsorbed on hydroxyapatite crystals. European Journal of Oral Sciences, 106, 249-253.

Hunter, G., Szigety, S.K. (1992). Effects of proteoglycan on hydroxyapatite formation under non steady-state and pseudosteady-state conditions. Matrix, 12, 362-68.

Gadaleta, S.J., Camacho, N.P., Mendelsohn, R., Boskey, A.L. (1996). Fourier Transform Infrared microscopy of calcified turkey leg tendon. Calcified Tissue International, 58(1), 17-23.

Gadaleta, S.J., Landis, W.J., Boskey, A.L., Mendelsohn, R. (1996). Polarized FT-IR microscopy of calcified turkey leg tendon. Connective Tissue Research, 34(3), 203-211.

Genge, B.R., Wu, L.N., Adkinsson, H.D., Wuthier, R.E. (1991). Matrix vesicle annexins exhibit proteolipid-like properties : selective partitioning into lipophilic solvents under acidic conditions. The Journal of Biological Chemistry, 226, 10678-10685.

George, A., Sabsay, B., Simonian, P.A.L., Veis, A. (1993). Characterization of a novel dentin matrix acidic phosphoprotein. The Journal of biological chemistry, 268, 12624-12630.

George, A., Bannon, L., Sabsay, B., Dillon, J.W., Malone, J., Veis, A., Jenkins, N.A., Gilbert, D.J., Copeland, N.G. (1996). The carboxyl-terminal domain of phosphophoryn contains unique extended triplet amino acid repeat sequences forming ordered carboxyl-phosphate interaction ridges that may be essential in the biomineralization process. The Journal of Biological Chemistry, 271(51), 32869-32873.

Gericke, A, Qin, C, Spevak, L, Fujimoto, Y, Butler, W.T., Sorensen, E.S., Boskey, A.L. Importance of phosphorylation for osteopontin regulation of biomineralization. Calcified Tissue International, in press.

Gilkey, J.C., Staehelin, L.A. (1986). Advances in ultrarapid freezing for the preservation of cellular ultrastructure. Journal of Electron Microscopy Technique, 3, 177-210.

Glimcher, M.J. (1989). Mechanism of calcification: role of collagen fibrils and collagen-phosphoprotein complexes in vitro and in vivo. The Anatomical Record , 224, 139-153.

Glimcher, M.J. (1998). The Nature of the Mineral Phase in Bone: Biological and Clinical Implications. In: Metabolic Bone Disease. LV Avioli, SM Krane (eds). San Diego,CA: Academic Press.

Gokhale, J.A., Boskey, A.L., Robey, P.G. (2001). The Biochemistry of Bone. In: Osteoporosis. Vol 1. San Diego, CA: Academic Press.

Goldberg, M., Takagi, M. (1993). Dentin proteoglycans: composition, ultrastructure and functions. The Histochemical Journal, 25(11), 781-806.

Goldberg, M., Septier, D., Lecolle, S., Chardin, H., Quintana, M.A., Acevedo, A.C., Gafni, G., Dillonya, D., Vermelin, L., Thonemann, B. (1995). Dental Mineralization. The International Journal of Developmental Biology, 39(1), 93-110.

Goldberg, M., Boskey, A.L. (1996). Lipids and biomineralization. The Journal of Histochemistry and Cytochemistry, 31(2), 1-187.

Goldberg, M., Septier, D., Torres-Quintana, M., Lecolle, S., Hall, R., Gafni, G., Menachi, S., Embery, G. (1998). New insights on the dynamics of dentin formation. Proceedings of the 6th International Conference on Chemistry and Biology of Mineralized Tissues. Vittel, France.

Gorter de Vries, I., Quartier, E., Boute, P., Wisse, E., Coomans, D. (1987). Immunocytochemical localization of osteocalcin in developing rat teeth. Journal of Dental Research, 66(3), 784-790.

Grynpas, M.D., Hunter, G.K. (1988). Bone mineral and glycosaminoglycans in newborn and mature rabbits. Journal of Bone and Mineral Research, 3(2), 159-164.

Hall, R., Septier, D., Embery, G., Goldberg, M. (1999). Stromelysin-1 (MMP-3) in forming enamel and predentin in rat incisor-coordinated distribution with proteoglycans suggests a functional role. Histochemical Journal, 31(12), 761-770.

Hao, J., Zou, B., Narayanan, K., George, A. (2004). Differential expression patterns of the dentin matrix proteins during mineralized tissue formation. Bone, 34(6), 921-932.

Haris, P.I., Chapman, D. (1995). The conformational analysis of peptides using Fourier Transform IR Spectroscopy. Biopolymers, 37, 251-263.

He, G., Ramachandran, A., Dahl, T., George, S., Schultz, D., Cookson, D., Veis, A., George, A. (2005) Phosphorylation of phosphophoryn is crucial for its function as a mediator of biomineralization. Journal of Biological Chemistry, 280(39), 33109-14.

Herr, P., Holz, J., Baume, L.J. (1986). Mantle dentin in man- a quantitative microradiographic study. Journal de Biologie Buccale, 14, 139-146.

Heywood, B.R., Sparks, N.H., Shellis, R.P., Weiner, S., Mann, S. (1990). Ultrastructure, morphology and crystal growth of biogenic and synthetic apatites. Connective Tissue Research, 25(2), 103-119.

Holm, I.A., Huang, X., Kunkel, L.M. (1997). Mutational analysis of the PHEX gene in patients with X-linked hypophosphatemic rickets. American Journal of Human Genetics, 60(4), 790-797.

Hopwood, D. (1985). Cell and tissue fixation, 1972-1982. Histochemistry Journal, 17, 389-442.

Hu, B., Nadiri, A., Bopp-Kuchler, S., Perrin-Schmitt, F., Lesot H. (2005). Dental Epithelial Histomorphogenesis in vitro**.** Journal of Dental Research. 84(6), 521-5.

Hunter, G.K., Goldberg, H.A. (1994). Modulation of crystal formation by bone phosphoproteins: role of glutamic acid-rich sequences in the nucleation of hydroxyapatite by bone sialoprotein. The Biochemical Journal, 302 (Pt 1), 175-179.

Hunter, G.K., Kyle, C.L., Goldberg, H.A. (1994). Modulation of crystal formation by bone phosphoproteins: structural specificity of the osteopontin-mediated inhibition of hydroxyapatite formation. The Biochemical Journal, 300 (Pt 3), 723-728.

Hunter, G.K., Haushka, P.V., Poole, A.R., Rosenberg, L.C., Goldberg, H.A. (1996). Nucleation and inhibition of hydroxyapatite formation by mineralized tissue proteins. The Biochemical Journal, 317(Pt 1), 59-64.

Ingram, F.D., Ingram, M.J. (1980). Freeze-dried, plastic-embedded tissue preparation: a review. Scanning Electron Microscopy, (4), 147-160.

Irving, J.T. (1958). A histological stain for newly calcified tissues. Nature, 181, 704.

Johnson and Boyde A. (1984). Dentin and Dentinogenesis. A. Linde ed., CRC Press, Bocca Raton,

Jontell, M., Pertoft, H., Linde, A. (1982). Disagreement in molecular weight determination of dentin phosphoproteins. Biochimica et Biophysica Acta, 705, 315.

Katchburian, E. (1973). Membrane-bound bodies as initiators of mineralization of dentine. Journal of Anatomy, 116(2), 285-302.

Katz, E.P., Wachtel, E.J., Maroudas, A. (1986). Extrafibrillar proteoglycans osmotically regulate the molecular packing of collagen in cartilage. Biochimica et Biophysica Acta, 882(1), 136-139.

Keene, D.R., San Antonio, J.D., Mayne, R., McQuillan, D.J., Sarris, G., Santoro, S.A., Iozzo, R.V. (2000). Decorin binds near the C terminus of type I collagen. Journal of Biological Chemistry, 275, 21801-21804.

Kellenberger, E., Johansen, R., Maeder, M., Borhmann, B., Stauffer, E., Villiger, W. (1992). Artefacts and morphological changes during chemical fixation. Journal of Microscopy, 168, 181-201.

Kinney, J.H., Balooch, M., Marshall, S.J., Marshall, G.W., Weihs, T.P. (1996). Hardness and Young's modulus of human peritubular and intertubular dentine. Archives of Oral Biology, 41(1), 9-13.

Kinney, J.H., Pople, J.A., Marshall, G.W., Marshall, S.J. (2001). Collagen orientation and crystallite size in human dentin: a small angle X-ray scattering study. Calcified Tissue International, 69(1), 31-37.

Krishnaraju, R.K., Hart, T.C., Schleyer, T.K. (2003). Comparative genomics and structure prediction of dental matrix proteins. Advances in Dental Research, 17(Dec), 100-103.

Kuboki, Y., Fujisawa, R., Aoyama, K., Sask,i S. (1979).Calcium specific precipitation of dentin-specific phosphoproteins: a new method for purification and the significance for the mechanism of calcification. Journal of Dental Research, 58, 1926-1932.

Kuhn, L.T., Wu, Y., Rey, C., Gerstenfeld, L.C., Grynpas, M.D., Ackerman, J.L., Kim, H.M., Glimcher, M.J. (2000). Structure, composition and maturation of newly deposited calcium-phosphate crystals in chicken osteoblast cell cultures. Journal of Bone and Mineral Research, 15(7), 1301-1309.

Landis, W.J., Song, M.J. (1991). Early mineral deposition in calcifying tendon characterized by high voltage electron microscopy and three-dimesional graphic imaging. Journal of Structural Biology, 107(2), 116-127.

Landis, W.J., Hodgens, K.J., Arena, J., Song, M.J., McEwen, B.F. (1996). Structural relations between collagen and mineral in bone as determined by high voltage electron microscopic tomography. Microscopy Research and Technique, 33, 192-202.

Lazarev, Y.A., Grishnkovsky, B.A., Khromova, T.B., Lazareva, A.V., Grechishko, V.S. (1992). Bound water in the collagen-like triple helical structure. Biopolymers, 32(2), 189-195.

Lee, S., Kossiva, D., Glimcher, M.J. (1983). Phosphoproteins of bovine dentin: evidence for polydispersity during tooth maturation. Biochemistry, 22, 2596-2601.

Lees, S., Mook, H.A. (1986). Equatorial diffraction spacing as a function of water content in fully mineralized cow bone determined by neutron diffraction. Calcified Tissue International, 39(4), 291-292.

LeGeros, R.Z., Trautz, O., LGeros, J.P., Klein, E. (1968). Carbonate substitution in the apatite structure. Bulletin de la Societé de Chimie Biologique, No 1712.

Levine, R.S. (1971). The distribution of hydroxyproline in sound human coronal dentin. Archives of Oral Biology, 16, 473-476.

Linde, A. (1984). Noncollagenous proteins and proteoglycans in dentinogenesis. Dentin and Dentinogenesis, Vol II. Linde A, Ed. CRC Press, Boca Raton, FLA

Linde, A., Lussi, A., Crenshaw, M.A. (1989). Mineral induction by immobilized polyanionic proteins. Calcified Tissue International, 44, 286-295.

Linde, A., Goldberg, M. (1993). Dentinogenesis. CRC Critical Reviews in Oral Biology and Medicine, 4, 679-728.

Ling, Y, Feng, J.Q, Myers, E, Boskey, A.L. Characterization of mineral properties in the bones of DMP1 knockout mice. Journal of Bone and Mineral Research, in press.

Litwin, J.A. (1985). Light microscopic histochemistry on plastic sections. Progress in Histochemistry and Cytochemistry, 16(2), 1-84.

Longas, M.O., Breitweiser, K.O. (1991). Sulfate composition of glycosaminoglycans determined by infrared spectroscopy. Analytical Biochemistry, 192(1), 193-196.

Lormée, P., Lecolle, S., Septier, D., Le Denmat, D., Goldberg, M. (1989). Autometallography for histochemical visualization of rat incisor polyanions with cuprolinic blue. Journal of Histochemistry and Cytochemistry, 37, 203-208.

Magne, D., Pilet, P., Weiss, P., Daculci, G. (2001). Fourier transform infrared microspectroscopic investigation of the maturation of nonstoichiometric apatites in mineralized tissues: a horse dentin study. Bone, 29(6), 547-552.

Magne, D., Weiss, P., Bouler, J.M., Laboux, O., Daculci, G. (2001). Study of the maturation of the organic (type I collagen) and mineral (nonstoihiometric apatite) constituents of a calcified tissue (dentin) as a function of location: a Fourier Transform Infrared Microspectroscopic investigation. Journal of Bone and Mineral Research, 16(4), 750-757.

Magne, D., Bluteau, G., Faucheux, C., Palmer, G., Vignes-Colombeix, C., Pilet, P., Rouillon, T., Carvezasio, J., Weiss, P., Daculsi, G., Guicheux, J. (2003). Phosphate is a specific signal for ATDC5 chondrocyte maturation and apoptosis-associated mineralization: possible implication of apoptosis in the regulation of endochondral ossification. Journal of Bone and Mineral Research, 18(8), 1430-1442.

Maier, G.D., Lechner, J.H., Veis, A. (1983). The dynamics of formation of a collagen-phosphophoryn conjugate in relation to the passage of the mineralization front in rat incisor dentin. J Biological Chemistry, 258, 1450-1455.

Malone, J.D., Teitelbaum, S.L., Griffin, G.L., Senior, R.M., Kahn, A.J. (1982). Recruitment of osteoclast precursors by purified bone matrix constituents. Journal of Cell Biology, 92, 227.

Marcott, C., Reeder, R.C., Paschalis, E.P., Boskey, A.L., Mendelsohn, R. (1999). Infrared microspectroscopic imaging of biomineralized tissues using a Mercury-Cadmium-Telluride focal plane array detector. Phosphorus, Sulfur, Silicon & Related Elements, 146, 417-420.

Marsh, M.E. (1989). Binding of calcium and phosphate ions to dentin phosphophoryn. Biochemistry, 28, 346-352.

Marshall, G.W. Jr., Ballooch, M., Gallagher, R.R., Gasky, S.A., Marshall, S.J. (2001). Mechanical properties of the dentinoenamel junction: AFM studies of nanohardness, elastic modulus and fracture. Journal of Biomedical Materials Research, 54, 87-95.

Masters, P.M. (1985). In vivo decomposition of phosphoserine and serine in noncollagenous proteins from human dentin. Calcified Tissue International, 37, 236-241.

Mayer, I., Schneider, S., Sydney-Zax, M., Deutch, D. Thermal decomposition of developing enamel. Calcified Tissue International, 46, 254-257.

McKee, M.D., Nanci, A. (1995). Postembedding colloidal-gold immunocytochemistry of noncollagenous extarcellular matrix proteins in mineralized tissues. Microscopy Research and Technique, 31, 44-62.

McKee, M.D., Zalzal, S., Nanci, A. (1996). Extracellular matrix in tooth cementum and mantle dentin: localization of osteopontin and other noncollagenous proteins, plasma proteins and glycoconjugates by electron microscopy. The Anatomical Record, 245(2), 293-312.

Mechanic, G.L., Katz, E.P., Henmi, M., Noyes, C., Yamauchi, M. (1987). Locus of a histidine-based, stable tri-functional, helix to helix collagen cross-link: stereospecific collagen structure of type I skin fibrils. Biochemistry, 26, 3500-3509.

Mendelsohn, R., Camacho, N.P., Boskey, A.L. (in press). Infrared Microscopy and Imaging of Hard and Soft Tissues: Applications to Bone, Skin, and Cartilage. Biospectroscopy. …: Blackwell Press.

Mendelsohn, R., Hassankhani, A., DiCarlo, E., Boskey, A.L. (1989). FT-IR microscopy of endochondral ossification at 20 mu spatial resolution. Calcified Tissue International, 44(1), 20-24.

Mendelsohn, R., Paschalis, E.P., Boskey, A.L. (1999). Infrared spectroscopy, microscopy and microscopic imaging of biomineralizing tissues. Spectra-structure correlations from human iliac crest biopsies. Journal of Biomedical Optics, 4, 14-21.

Mendelsohn, R., Paschalis, E.P., Sherman, P.J., Boskey, A.L. (2000). IR microscopic imaging of pathological states and fracture healing of bone. Applied Spectroscopy, 54, 1183-1191.

Mikuni-Takagaki, Y., Glimcher, J. (1990). Post-translational processing of chicken bone phosphoprotein. Identification of bone (phosphor)protein kinase. The Biochemical Journal, 268(3), 593-597.

Miller, L.M., Novatt, J.T., Hamerman, D., Carlson, C.S. (2004). Alterations in mineral composition observed in osteoarthritic joints of cynomolgus monkeys. Bone, 35(2), 498-506.

Mjor, I.A. (1972). Human coronal dentin: structure and reactions. Journal of Oral Surgury, 33, 810-823.

Moradian-Oldak, J., Frolow, F., Addadi, L., Weiner, S. (1992). Interactions between acidic matrix macromolecules and calcium phosphate ester crystals: Relevance to carbonate apatite formation in biomineralization. Proceedings of the Royal Society of London, Series B, 247, 47-55.

Moss, M.L. (1974). Studies on dentin. I. Mantle dentin. Acta Anatomica, 87(194), 481-507.

Nakamura, O., Gohda, E., Ozawa, M., Senba, I., Miyazaki, H., Murakami, T., Daikura, Y. (1985). Immunohistochemical studies with a monoclonal antibody on the distribution of phosphophoryn in predentin and dentin. Calcified Tissue International, 37, 491-500.

Nanci, A. (1999). Content and distribution of noncollagenous matrix proteins in bone and cementum: relationship to speed of formation and collagen packing density. Journal of Structural Biology, 126, 256-269.

Narayanan, K., Srinivas, R., Ramachandran, A., Hao, J., Quinn, B., George, A. (2001). Differentiation of embryonic mesenchymal cells to odontoblast-like cells by overexpression of dentin matrix protein 1. Proceedings of the National Academy of Sciences of the United States of America, 98, 4516-4521.

Neame, P.J., Kay, C.J., McQuillan, D.J., Beales, M.P., Hassell, J.R. (2000). Independent modulation of collagen fibrillogenesis by decorin and lumican. Cellular and molecular life sciences : CMLS, 57, 859-863.

Nefussi, J.R., Septier, D., Sautier, J.M., Goldberg, M. (1992). Localization of malachite green positive lipids in the matrix of bone nodule formed in vitro. Calcified Tissue International, 50(3), 273-282.

Neuman, R.E., Logan, M.A. (1949). The determination of hydroxyproline. Journal of Biological Chemistry, 299-306.

Nomura, S., Hiltner, A., Lando, J.B., Baer, E. (1977). Interaction of water with native collagen. Biopolymers, 16, 231-246.

Ouyang, H., McCauley, LK., Berry, JE., Saygin, NE., Tokiyasu, Y., Somerman, MJ. (2000). Parathyroid hormone-related protein regulates extracellular matrix gene expression in cementoblasts and inhibits cementoblast-mediated mineralization in vitro. Journal of Bone & Mineral Research. 15(11), 2140-53.

Ou-Yang, H., Paschalis, E.P., Mayo, W.E., Boskey, A.L., Mendelsohn, R. (2001). Infrared microscopic imaging of bone: spatial distribution of $CO_3^{(-2)}$. Journal of Bone and Mineral Research, 16(5), 893-900.

Pampena, D.A., Robertson, K.A., Litvinova, O., Lajoie, G., Goldberg, H.A., Hunter, G.K. (2004). Inhibition of hydroxyapatite formation by osteopontin phosphopeptides. The Biochemical Journal, 378(Pt 3), 1083-1087.

Papagerakis, P., Berdal, A., Mesbah, M., Peuchmaur, M., Malaval, L., Nydegger, J., Simmer, J., MacDougall, M. (2002). Investigation of osteocalcin, osteonectin and dentin sialophosphoprotein in developing human teeth. Bone, 30(2), 377-385.

Paschalis, E.P., Betts, F., Mendelsohn, R., Boskey, A.L. (1996). Fourier transform infrared spectroscopy of the solution-mediated conversion of amorphous calcium phosphate to hydroxyapatite: new correlations between X-ray diffraction and infrared data. Calcified Tissue International, 58(1), 9-16.

Paschalis, E.P., DiCarlo, E., Betts, F., Sherman, P., Mendelsohn, R., Boskey, A.L. (1996). FTIR mocrospectroscopic analysis of human osteonal bone. Calcified Tissue International, 59(6), 480-487.

Paschalis, E.P., Jacenko, O., Olsen, B., Mendelsohn, R., Boskey, A.L. (1996). Fourier transform infrared microspectroscopic analysis identifies alterations in mineral properties in bones from mice transgenic for typr X collagen. Bone, 19(2), 151-156.

Paschalis, E.P., Betts, F., DiCarlo, E., Mendelsohn, R., Boskey, A.L. (1997). FTIR microspectroscopic analysis of normal human cortical and trabecular bone. Calcified Tissue International, 61(6), 480-486.

Paschalis, E.P., Betts, F., DiCarlo, E., Mendelsohn, R., Boskey, A.L. (1997). FTIR mocrospectroscopic analysis of human iliac crest biopsies from untreated osteoporotic bone. Calcified Tissue International, 61, 487-492.

Paschalis, E.P., Recker, R., DiCarlo, E., Doty, S.B., Atti, E., Boskey, A.L. (2003). Distribution of collagen cross-links in normal human trabecular bone. Journal of Bone and Mineral Research, 18(11), 1942-1946.

Pashley, D.H. (1989). Dentin: a dynamic substrate-a review. Scanning Microscopy, 3, 161-176.

Pashley, D.H. (1996). Dynamics of the pulpo-dentin complex. Critical Reviews in Oral Biology and Medicine, 7(2), 104-133.

Payne, K.J., Veis, A. (1988). Fourier Transform IR Spectroscopy of collagen and gelatin solutions: deconvolution of the Amide I band for conformational studies. Biopolymers, 27(11), 1749-1760.

Pienkowski, D., Doers, T.M., Camacho, N.P., Boskey, A.L., Malluche, H.H. (1997). Calcitonin alters bone quality in beagle dogs. Journal of Bone and Mineral Research, 12, 1936-1943.

Pleshko, N.L., Boskey, A.L., Mendelsohn, R. (1991). Novel infrared spectroscopic method for the determination of crystallinity of hydroxyapatite minerals. Biophysical Journal, 60, 786-793.

Posner, A.S. and Tannenbaum, P.J. (1984). The mineral phase of dentin. Dentin and Dentinogenesis. Linde A, Ed. CRC Press, Boca Raton, Fla

Prockop, D.J., Udenfriend, S. (1960). A specific method for the analysis of hydroxyproline in tissues and urine. Analytical Biochemistry, 1, 228-239.

Qin, C., Brunn, J.C., Jones, J., George, A., Ramachandran, A., Gorski, J.P., Butler, W.T. (2001). A comparative study of sialic acid-rich proteins in rat bone and dentin. European Journal of Oral Sciences, 109(2), 133-141.

Qin, C., Baba, O., Butler, W.T. (2004). Post-translational modifications of SIBLING proteins and their roles in osteogenesis and dentinogenesis. Critical Reviews in Oral Biology and Medicine, 15(3), 126-136.

Raggio, C.L., Boyan, B.D., Boskey, A.L. (1986). In vivo hydroxyapatite formation induced by lipids. Journal of Bone and Mineral Research, 1, 409-415.

Rahima, M., Tsay, T.G., Andujar, M., Veis, A. (1988). Localization of phosphophoryn in rat incisor dentin using immunocytochemical techniques. Journal of Histochemistry and Cytochemistry, 36(2), 153-157.

Rey, C., Collins, B., Goehl, T., Dickson, I.R., Glimcher, M.J. (1989). The carbonate environment in bone mineral: a resolution-enhanced Fourier Transform Infrared Spectroscopy study. Calcified Tissue International, 45, 157-164.

Rey, C., Beshah, K., Griffin, R., Glimcher, M.J. (1991). Structural studies of the mineral phase of calcifying cartilage. Journal of Bone and Mineral Research, 6(5), 515-525.

Rey, C., Renugopalakrishnan, V., Collins, B., Collins, B., Glimcher, M.J. (1991a). Fourier transform infrared spectroscopic study of the carbonate ions in bone mineral during aging. Calcified Tissue International, 49, 251-258.

Rey, C., Renugopalakrishnan, V., Collins, B., Shimizu, M., Collins, B., Glimcher, M.J. (1991b). A resolution fourier transform infrared spectroscopic study of the environment of the CO_3^{2-} ion in the mineral phase of enamel during its formation and maturation. Calcified Tissue International, 49, 259-268.

Rey, C., Hina, A., Glimcher, M.J. (1995). Maturation of poorly crystalline apatites: chemical and structural aspects in vivo and in vitro. Cells and Materials, 5(4), 345-356.

Rittling, S.R., Matsumoto, H.N., McKee, M.D., Nanci, A., An, X.R., Novick, K.E., Kowalski, A.J., Noda, M., Denhardt, D.T. (1998). Mice lacking osteopontin show normal development and bone structure but display altered osteoclast formation in vitro. Journal of Bone and Mineral Research, 13, 1101.

Roberts, J.E., Bonar, L.C., Griffin, R.G., Glimcher, M.J. (1992). Characterization of very young mineral phases of bone by solid state 31phosphorus magic angle sample spinning nuclear magnetic resonance and X-ray diffraction. Calcified Tissue International, 50(1), 42-48.

Robey, P.G., Boskey, A.L. (1996). The biochemistry of bone, in Osteoporosis. Marcus R, Feldman D, Kelsey J, editors. Academic Press Inc.

Robinson, C., Kirkham, J. (1985). Dynamics of amelogenesis as revealed by protein compositional studies. In: The Chemistry and Biology of Mineralized Tissues. WT Butler, Ed. Birmingham: Ebsco Media.

Saito, T., Arsenault, A.L., Yamauchi, M., Kuboki, Y., Crenshaw, M.A. (1997). Mineral induction by immobilized phosphoproteins. Bone, 21(4), 305-11.

Sauer, G.N., Wuthier, R.E. (1988). Fourier Transform Infrared characterization of mineral phases formed during induction of mineralization by collagenase-released matrix vesicles in vitro. Journal of Biological Chemistry, 263(27), 13718-13724.

Septier, D., Hall, R.C., Lloyd, D., Embery, G., Goldberg, M. (1998). Quantitative immunohistochemical evidence of a functional gradient of chondroitin 4-sulfate/dermatan sulfate, developmentally regulated in the predentin of rat incisor. The Histochemical Journal, 30(4), 275-284.

Smith, BC. (2001) In: Fundamentals of Fourier Transform Infrared Spectroscopy. Wiley, Chichester, Ciba Foundation Symposium 205. p 107-117.

Sodek, J., Ganss, B., McKee, M.D. (2000). Osteopontin. Critical Reviews in Oral Biology and Medicine, 11(3), 279-303.

Sodek, K.L., Tupy, J.H., Sodek, J., Grynpas, M.D. (2000). Relationships between bone protein and mineral in developing porcine long bone and calvaria. Bone, 26(2), 189-198.

Sreenath, T., Thyagarajan, T., Hall, B., Longenecker, G., D'Souza, R., Hong, S., Wright, J.T., MacDougall, M., Sauk, J., Kulkarni, A.B. (2003). Dentin sialophosphoprotein knockout mouse teeth display widened predentin zone and develop defective dentin mineralization similar to human dentinogenesis imperfecta type III. Journal of Biological Chemistry, 278, 24874-24880.

Stetler-Stevenson, W.G., Veis, A. (1986). Type I collagen shows a specific binding affinity for bovine dentin phosphophoryn. Calcfied Tissue International, 38, 135-141.

Stratmann, U., Barckhaus, R.H., Lyaruu, D.M., Woltgens, J.H., Wessling, G., Baumeister, A. (1991). Electron probe X-ray microanalysis of calcium and phosphorus distribution in developing hamster tooth germs in vitro and in vivo. Acta Anatomica, 140(4), 343-349.

Stratmann, U., Schaarschmidt, K., Wiesmann, H.P., Plate, U., Höhling, H.J. (1996). Mineralization during matrix-vesicle-mediated mantle dentin formation in molars of albino rats: a microanalytical and ultrastructural study. Cell and Tissue Research, 284, 223-230.

Stratmann, U., Schaarschmidt, K., Wiesmann, H.P., Plate, U., Hohling, H.J., Szuwart, T. (1997). The mineralization of mantle dentin and of circumpulpal dentin in the rat: an ultrastructural and elemental-analytical study. Anatomy and Embryology, 195, 289-297.

Sydney-Zax, M., Mayer, I., Deutsch, D. (1991). Carbonate content in developing human and bovine enamel. Journal of Dental Research, 70(5), 913-916.

Takagi, Y., Veis, A. (1984). Isolation of phosphophoryn from human dentin organic matrix. Calcified Tissue International, 36, 259-265.

Tagaki, Y., Sasaki, S. (1986). Histological distribution of phosphophoryn in normal and pathological human dentins. Journal of Oral Pathology, 15, 463-467.

Tagaki, Y., Nagai, H., Sasaki, S. (1988). Difference in concollagenous matrix composition between crown and root dentin of bovine incisor. Calcified Tissue International, 42(2), 97-103.

Takano, Y., Sakai, H., Baba, O., Sakamoto, Y., Terashima, T., Ohya, K., Kurosaki, N. (1998). Demonstration of putative Ca-binding domains in dentin matrix of rat incisors after daily injections of 1-hydroxyethylidene-1,1-bisphosphonate (HEBP). European Journal of Oral Sciences, 106 Suppl 1, 274-281.

Tarnowski, C.P., Ignelzi Jr., M.A., Morris, M.D. (2002). Mineralization of developing mouse calvaria as revealed by Raman microspectroscopy. Journal of Bone and Mineral Research, 17(6), 1118-1126.

Tartaix, P.H., Doulaverakis, M., George, A., Fisher, L.W., Butler, W.T., Qin, C., Salih, E., Tan, M., Fujimoto, Y., Spevak., L, Boskey, A.L. (2004). In vitro effects of dentin matrix protein-1 on hydroxyapatite formation provide insights into in vivo functions. The Journal of Biological Chemistry, 279(18), 18115-18120.

Ten Cate, A.R. (1994). Oral Histology. Mosby Year Book, St. Louis.

Ten Cate, A.R., Ed. (1994). Oral Histology: Development, Structure and Function. 4th edition. St. Louis: Mosby.

Termine, J.D., Belcourt, A.B., Miyamoto, M.S., Conn, K.M. (1980). Properties of dissociatively extracted fetal tooth matrix proteins. II. Separation and purification of fetal bovine dentin phosphoprotein. The Journal of Biological Chemistry, 255, 9769-9772.

Termine, J.D., Eanes, E.D., Conn, K.M. (1980). Phosphoprotein modulation of apatite crystallization. Calcified Tissue International, 31, 247-251.

Termine, J.D., Kleinman, H.K., Whitson, S.W., Conn, K.M., McGarvey, M.L., Martin, G.R. (1981). Osteonectin, a one-specific protein linking mineral to collagen. Cell, 26, 99.

Tjaderhane, L., Hietala, E.L., Larmas, M. (1995). Mineral element analysis of carious and sound rat dentin by electron probe microanalyzer combined with back-scattered image. Journal of Dental Research, 74(11), 1770-1774.

Tomazic, B.B., Brown, W.E., Schoen, F.J. (1994). Physicochemical properties of calcific deposits isolated from porcine bioprosthetic heart valves removed from patients following 2-13 years function. Journal of Biomedical Materials Research , 28(1), 35-47.

Traub, W., Jodaikin, A., Arad, T., Veis, A., Sabsay, B. (1992). Dentin phosphophoryn binding to collagen fibrils. Matrix, 12, 197-201.

Tsuda, H., Ruben, J., Arends, J. (1996) Raman spectra of human dentin mineral. European Journal of Oral Sciences, 104, 123-31.

Tung, P.S., Domenicucci, C., Wasi, S., Sodek, J. (1985). Specific immunohistochemical localization of osteonectin and collagen types I and III in fetal and porcine dental tissues. The Journal of Histochemistry and Cytochemistry, 33, 531-540.

Turley, E.A., Erikson, C.A., Tucker, R.P. (1985). The retention and ultrastructural appearances of various matrix molecules incorporated into three-dimensional hydrated collagen lattices. Developmental Biology, 109(2), 347-369.

Veis, A., Spector, A.R., Zamoscianyk, H. (1972). The isolation of an EDTA-soluble phosphoprotein from mineralizing bovine dentin. Biochimica et Biophysica Acta, 257, 404.

Veis, A., Sharkey, M., Dickson, I. (1979). Noncollagenous proteins of bone and dentin extracellular matrix and their role in organized mineral deposition. In: Calcium Binding Proteins and Calcium Function. Wasserman RH, Corradino, R.A., Crafoli, E., Kretsinger, R.H., McLennan, D.H., Siegel, F.L., Eds. North-Holland, New York

Veis, A. (1993). Mineral-matrix Interactions in bone and dentin. Journal of Bone and Mineral Research, 8(S2), 493-497.

Veis, A., Sfeir, C., Wu, C.B. (1997). Phosphorylation of the proteins of the extracellular matrix of mineralized tissues by casein kinase-like activity. Critical Reviews in Oral Biology and Medicine, 8(4), 360-379.

Veis, A., Wei, K., Sfeir, C., George, A., Malone, J. (1998) Properties of the (DSS)n triplet repeat domain of rat dentin phosphophoryn. European Journal of Oral Sciences, 106(S1), 234-8.

Vogel, J.J., Boyan, B.D. (1976). Acidic lipids associated with the local mechanism of calcification. Clinical orthopaedics, 118, 230-241.

Vogel, V.G., Trotter, J.A. (1987). The effect of proteoglycans on the morphology of collagen fibrils formed in vitro. Collagen and related research, 7, 105-114.

Waddington, R.J., Hall, R., Embery, G., Lloyd, D.M. (2003). Changing profiles of proteoglycans in the transition of predentin to dentine. Matrix Biology, 22(2), 153-161.

Walters, C., Eyre, D.R. (1983). Collagen crosslinks inhuman dentin: increasing content of hydroxypyridinium residues with age. Calcified. Tissue International, 35(4-5), 401-405.

Weiner, S., Veis, A., Beniash, E., Arad, T., Dillon, J.W., Sabsay, B., Siddiqui, F. (1999). Peritubular dentin formation: crystal organization and the macromolecular constituents in human teeth. Journal of Structural Biology, 126, 27-41.

Weinstock, M., Leblond, C.P. (1973). Radioautographic visualization of the deposition of a phosphoprotein at the mineralization front in the rat incisor. The Journal of Cell Biology, 56, 838-845.

West, P.A., Torzilli, P.A., Chen, C., Lin, P., Camacho, N.P. (2005). Fourier transform infrared imaging spectroscopy analysis of collagenase-induced cartilage degradation. Journal of Biomedical Optics, 10(1), 140-115.

Wetherell, J.A., Robinson, C. (1973). The inorganic composition of teeth. In: Biological Mineralization. Zipkin, I., (ed.) New York: John Wiley & Sons.

White, S.W., Hulmes, D.J.S., Miller, A., Timmins, P.A. (1977). Collagen-mineral axial relationship in calcified turkey leg tendon by x-ray and neutron diffraction. Nature, 266, 421-425.

Wu, L.N., Genge, B.R., Dunkelberger, D.G., LeGeros, R.Z., Concannon, B., Wuthier, R.E. (1997). Physicochemical characterization of the nucleational core of matrix vesicles. Journal of Biological Chemistry, 272(7), 4404-4411.

Wuthier, R.E. (1984). Lipids in Dentinogenesis. In: Dentin and Dentinogenesis. Linde A, Ed. Boca Raton, Florida: CRC Press.

Xiao, S., Yu, C., Chou, X., Yuan, W., Wang, Y., Bu, L., Fu, G., Qian, M., Yang, J., Shi, Y., Hu, L., Han, B., Wang, Z., Huang, W., Liu, J., Chen, Z. Zhao, G., Kong, X. (2001). Dentinogenesis imperfecta 1 with or without progressive hearing loss is associated with distinct mutations in DSPP. Nature Genetics, 27(2), 201-204.

Xu, T., Fisher, L., Bianco, P., Longnecker, G., Boskey, A.L., Smith, E., Bonadio, J., Goldsteins, S., Zhao, C., Dominguez, P., Heergard, A., Satomura, K., Gehron Robey, P., Kulkarni, A., Sommer, B., Young, M. (1998). Targeted disruption of the biglycan gene leads to osteoporosis in mice. Nature Genetics, 20, 78.

Yamashiro, T., Tummers, M., Thesleff, I. (2003). Expression of bone morphogenetic proteins and Msx genes during root formation**.** Journal of Dental Research. 82(3), 172-6

Ye, L., McDougall, M., Zhang, S., Xie, Y., Zhang, J., Li, Z., Lu, Y., Mishina, Y., Feng, JQ. (2004). Deletion of dentin matrix protein-1 leads to a partial failure of maturation of predentin into dentin, hypomineralization and expanded cavities of pulp and root canal during postnatal tooth development. Journal of Biological Chemistry, 279(18), 19141-19148.

Young, R.A., Holcomb, D.W. (1984). Role of acid phosphate in hydroxyapatite lattice expansion. Calcified Tissue International, 36, 60-63.

.